KONINKLIJK NEDERLANDSCH METEOROLOGISCH INSTITUUT

DE BILT (NEDERLAND)

No. 125

MEDEDEELINGEN EN VERHANDELINGEN

SERIE B

DEEL I, No. 7

*

W. F. SCHALKWIJK

A CONTRIBUTION TO THE STUDY OF STORM SURGES ON THE DUTCH COAST

INDEX DECIMALIS 551.579.4

*

TE VERKRIJGEN BIJ DE: TO BE PURCHASED FROM:

RIJKSUITGEVERIJ / 'S-GRAVENHAGE

1947

CONTENTS

CHAPTER I. HISTORICAL SURVEY

INTRODUCTION

It is known from history, that already before the beginning of our era the North Sea shores of Holland and Germany were badly damaged by floods, of which many are said to have been accompanied by heavy storms. It was indeed soon realized, that they were caused by the wind. These floods were therefore called „*Storm surges*" (one must distinguish between the actual *storm surges* and those caused by waterswollen rivers !). One of the best-known storm surges occurred on November 18th of 1421, when 10 000 persons perished and 72 villages were completely swept away by the sea. Other well-known surges are those of November 1st of 1570, December 25th of 1717, November 14th of 1775 and February 4th of 1825.

The last storm surge that caused considerable damage occurred on 13—14 January 1916. After this flood a "Warning-service for storm surges" was built up in Holland. This service gives warnings when dangerously high levels of the sea at the coast are to be expected. As, however, in practice it turned out, that the method, used for calculating the waterlevels, was not wholly satisfactory, an attempt is made to improve the method of prediction. The results are contained in the present publication. After a survey of the most important investigations concerning this problem, theoretical considerations follow. These are applied to the working up of the collected data. The results of this application are in their turn discussed, likewise with the help of the theoretical considerations mentioned.

1. Investigations of storm surges on the Dutch coast

In the preceding century it was already discovered that a satisfactory study of the influence of the wind on the sealevel could only be carried out after elimination of the astronomical tides. One of the first to do this was ENGELENBURG (1, 2). He calculated for the years 1887 and 1888 the average value of the sealevel at Flushing for each day of this period, simply by averaging the values of high tide and low tide. These averages were correlated with the wind and air-pressure prevailing on the same day. Considering the values of the height of the sealevel as a function of the direction of the wind it was found, that the sealevel was higher than normal when a *seawind* was blowing, especially with *Westerly* wind. Southerly and Northerly winds increased also the height of the sealevel, but much less than the Westerly winds. An Easterly wind, however, *diminished* the height of the sealevel.

But not only the effect of the direction of the wind was considered, ENGELENBURG studied also the effect of the pressure of the air. He found, that an increase in air-pressure of 1 mm mercury caused a *lowering* of the sealevel by 6 mm when an Easterly wind prevailed, and by 8 mm when a seawind was blowing.

ENGELENBURG had not yet the pre-computed heights of the astronomical tides at his disposal. But ORTT had, who in 1897 published (3, 4, 5) very valuable researches on the effect of wind and barometric pressure on the height of the sealevel. He compared the heights of the tides given in the tide-tables (calculated for Hook of Holland and IJmuiden, and later also for Helder) with the actually observed ones. The difference between calculated and observed values must be caused by wind and by changes in the air pressure. As a first result of his study, and a very valuable one, ORTT found, that the meteorological and astronomical effects can be *superposed* upon each other as they disturb each other only very slightly. Though the sealevel is indeed slightly more affected by the wind at low tide than at high tide, ORTT could safely neglect this small difference in his final formula. The difference between calculated and observed

height of sealevel is called *meteorological effect.* This effect is caused by the combined action of wind and atmospheric pressure. When we consider exclusively the effect of the *wind,* we use the term "*windeffect*".

A second result of ORTT's investigation was the introduction of a "*time-lag*". Already other investigators had noticed (see § 2), that a certain time is needed for the wind to reach its full effect. When a storm breaks suddenly, the sea reaches its maximum height only after a certain lapse of time. ORTT found, that for the Dutch North Sea-coast the time-lag amounts to *6 hours.* For that reason he related in his further investigations all values of the height of the sealevel to the data of wind and atmospheric pressure prevailing *6 hours earlier.*

In this way the relation between height of the sealevel and meteorological conditions was studied. His results can be summarized in the following formula:

$$\zeta = K \,.\, R + R_b\,(76 - B), \tag{1}$$

where:

ζ = meteorological effect;
K = factor, indicating the influence of the force of the wind;
R = „ „ „ „ „ „ „ direction of the wind;
R_b = „ „ „ „ „ „ „ atmospheric pressure;
B = atmospheric pressure in cm mercury.

The relation between the velocity of the wind and the magnitude of the factor K is given in table 1.

TABLE 1 *Value of K as a function of the velocity of the wind*

Windvelocity (m/sec)	1.5	3.5	6.0	8.0	10.0	12.5	15.0	18.0	21.5	25.0	29.0
K	0.4	2	6	10	16	25	36	50	70	90	110
0,14 V^2	0.3	2	5	9	14	22	32	45	65	88	118

In table 2 the relation between the factors R and R_b and the direction of the wind is given.

TABLE 2. *Value of R and R_b as a function of the direction of the wind*

Direction of the wind	N	NNE	NE	ENE	E	ESE	SE	SSE	S	SSW	SW	WSW	W	WNW	NW	NNW
R.	0.6	0.0	— 0.7	— 1.0	— 1.3	— 1.2	— 0.8	— 0.1	0.4	0.6	0.9	1.2	1.6	1.5	1.3	0.9
R_b	12	11	10	9	7	6	7	8	8	6	6	8	10	12	14	13

If we study table 1 more closely, it turns out, that the influence of the wind is nearly proportional to the *square* of its *velocity.* To show this, the value of 0,14 V^2 has been entered also in table 1 (V = velocity of the wind in m/sec.). It is clear, that we may put with sufficient accuracy: $K = 0{,}14\ V^2$.

We may say therefore, that for any direction of the wind the windeffect is proportional to the square of the velocity of the wind. The same result was obtained by other investigators (see § 2).

The influence of the *direction* of the wind can be inferred from table 2. The maximum *positive* value of the windeffect occurs, when the wind has a direction

between W and WNW. The maximum *negative* windeffect is found, when the direction of the wind is between E and ESE, which differs exactly 180° from the former direction! It is also evident that an on-shore-wind has a greater effect than an off-shore-wind (maximum positive value of $R = 1{,}6$, maximum negative value of $R = -1.3$). Analogous results were obtained by other investigators. The explanation is the fact, that in the case of an off-shore-wind part of the sea is more or less sheltered from the wind by the coast.

The influence of the atmospheric pressure is indicated by the second term in the right hand side of equation (1). This term makes it clear, that the level of the sea rises when the atmospheric pressure decreases and vice versa. Now, when on our coast the atmospheric pressure decreases, it might be expected, that the sea would rise proportionally to the fall in pressure, the proportionality factor (R_b) having the value: density of mercury/density of seawater = 13,2, as the hydrostatic equilibrium must be maintained. But ORTT found, that R_b is not constant and equal to 13,2, but a function of the direction of the wind. The theoretical value is reached only for the direction NW ($R_b = 14$). For all other directions we have: $R_b < 13{,}2$. ORTT attributes these differences to the influence of differences in the field of wind at greater distances from the coast. The first term in the right hand side of equation (1) ($K\ R$) is supposed to represent more or less the influence of the *local* field of wind, contrary to the second term, in which, according to the above-mentioned explanation, the influence of the field of wind on the whole North Sea (*distant effect*) plays a role. A more quantitative separation of the two effects was tried by ORTT in a later investigation (5), but the results were far from satisfactory.

As a last result ORTT found, that the effect of meteorological conditions was practically the same at Hook of Holland and IJmuiden. The same formula was therefore given (equation (1)!) for both places.

ORTT's investigation is very important, as he treated the problem of the influence of wind and atmospheric pressure on the level of the sea very thoroughly. We summarize his results therefore as follows:

a. Elimination of the astronomical tides (ORTT: simple superposition).

b. Inertia of the sea (ORTT: the height of the sea lags 6 hours behind the meteorological causes).

c. Relation between the windeffect and the *velocity* of the wind (ORTT: quadratic).

d. Relation between the windeffect and the *direction* of the wind (ORTT: maximum when wind is WNW).

e. Relation between the height of the sea and atmospheric pressure (ORTT: depends on the direction of the wind, $R_b \leqq 13{,}2$).

f. Influence of *distant* parts of the windfield (ORTT: some influence is present).

g. Difference in meteorological effect along the coasts (ORTT: no difference between Hook of Holland and IJmuiden).

The next investigator to be mentioned here, is GALLÉ (6). ORTT obtained only four values for the meteorological effect on each day, by comparing the calculated and actually observed values of high tide and low tide. GALLÉ, however, obtained a complete elimination of the tides for a whole day (every hour of the day!) by introducing the "harmonic analysis" of the tides (see e.g. VAN DER STOK, 7*a* and 7*b*). The tides were represented in the well-known way as a superposition of a set of partial, simply harmonic tides:

$$S = \sum_n S_n \cos(\omega_n t - A_n). \qquad (2)$$

S_n, ω_n and A_n are characteristic constants for each partial tide, which are known for many places on the Dutch coast. With the aid of formula (2) the height of the

astronomical tide can be calculated for any moment. Assuming a simple superposition, the meteorological effect is found afterwards by subtracting the calculated value of the astronomical tide from the actually observed height of the sealevel.

According to this method GALLÉ calculated the meteorological effect for specially selected days, on which storm surges occurred, for some places on the North Sea and Zuiderzee coasts. Qualitatively a close relation between wind and meteorological effect was found (GALLÉ neglected the influence of the atmospheric pressure). More important were his investigations concerning the influence of distant and local effects. He computed for 42 storm surges the *average barometric field* and the average meteorological effect on our coasts present two days before, one day before and on the day itself of the storm surge. The average barometric field shows a deepening depression, moving from Iceland to South-Scandinavia. By the friction between the wind and the surface of the sea a current is set up, which is deflected to the right of the direction of the wind. According to GALLÉ, therefore, the windfield will, already before the day of the storm surge in question, cause an accumulation of water in the North Sea, mainly due to the wind on the Atlantic Ocean: "*effect of distant causes*". Upon this effect the local wind will superpose its own effect on the day of the storm surge considered because the water, already entered into the North Sea through the Channel and the "Norwegian Sea", cannot flow away during the actual storm. In this way the considerations of ORTT were completed by GALLÉ.

A thorough investigation of a number of storm surges was carried out by the Government committee for the "Rotterdamsche Waterweg" (8). This committee was established as a consequence of floods, caused by the storm surge of 13—14 January of 1916. The results, obtained by this body have been used up to the present for the prediction of the height of storm surges. The investigations of this committee were likewise based on the assumption of the simple superposition of the meteorological and astronomical effects. For 19 storm surges occurring between 1887 and 1917, covering in all 100 days, the height of the astronomical tide was calculated with the aid of formula (2) for Hook of Holland for each half hour of the selected days. The values computed in this way were subtracted from the actually observed values of the height of the sealevel, and 2562 values of the meteorological effect were obtained. These values were related to the wind, registered at the same time with the apparatus at Hook of Holland. The effects of atmospheric pressure and "time-lag" were neglected. For each direction of the wind (SW, WSW, W, etc.) and each Beaufort degree of windforce the corresponding values of the meteorological effect were averaged. In this way table 3 was obtained. With the aid of this table figure 1 was drawn.

TABLE 3

Meteorological effect (in cm) at Hook of Holland as a function of the force and the direction of the wind

Direction of the wind \ Windforce (Beaufort)	6	7	8	9	10	11	12
SW	6	8	16	13	32	—	—
WSW	26	29	48	65	101	104	—
W	45	79	84	114	150	153	163
WNW	46	68	118	126	157	213	245
NW	71	82	115	150	178	204	203
NNW	49	64	73	133	150	—	175

An outstanding feature of these curves is that they do not have similar shapes. Evidently, the meteorological effect cannot be represented in this case by formula (1), or by part of it. For then, the curves should nearly conform (as the effect of the

atmospheric pressure is not eliminated, some distortion of the curves will be present). Moreover the quadratic law of the windeffect seems not to hold in this investigation. In figure 1 the windeffect is plotted against the *force* of the wind, measured in degrees Beaufort. For the Beaufort scale, however, the velocity-equivalents are given very nearly (SIMPSON, 9) by: $V = 0{,}75\ B^{1,5}$ (V in m/sec, B in degrees Beaufort).

If the quadratic law were obeyed, we should have:

$$\zeta = a\ V^2 = a\ .\ (0{,}75)^2.\ B^3 = b\ B^3.$$

ζ should therefore be proportional to the cube of the windforce.

As can be seen directly in figure 1, this is certainly not the case. The committee also computed the average meteorological effect existing two days before, one day before and on the day of the actual storm surge. They obtained respectively 22 cm, 39 cm ands 90 cm. The effect for the foregoing days was again attributed to "distant causes". An investigation was carried out concerning the question, where these "distant causes" had to be located. The correlation coefficient was computed for the relation between the "*wind on the North Sea*" (the vectorial mean value of the wind prevailing on the East coast of England, on the Dutch lightships "Schouwenbank" and "Maas" and at Hook of Holland) and the meteorological effect. The direction of the wind was taken into account by using in the correlationformula the WNW-component of the "wind on the North Sea". The value of the correlation coefficient r, computed in this way, was: $r = 0{,}918$.

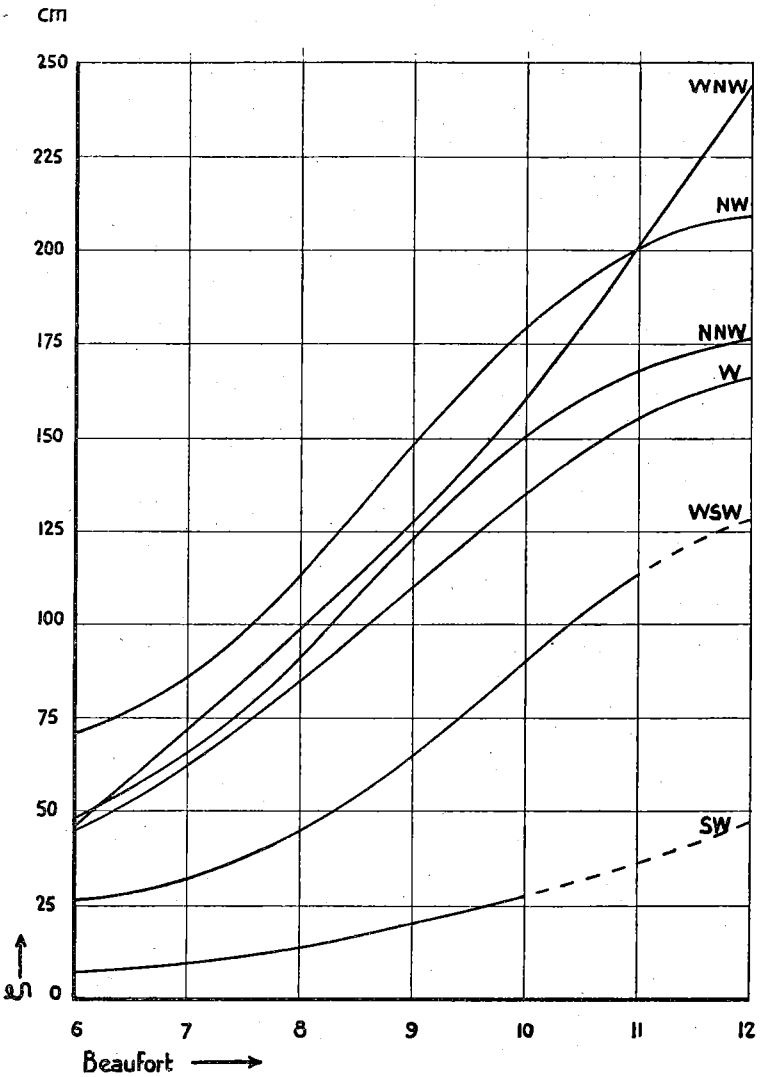

Fig. 1 Meteorological effect (in cm) at Hook of Holland as a function of the force and the direction of the wind

It was found, also with the aid of a graphical method, that the meteorological effect was more strongly connected with the "wind on the North Sea" than with the wind on the coast. This constituted a very valuable result: the effect of distant causes was mainly due to the field of wind present above the whole Southern part of the North Sea. Only a small fraction of the meteorological effect must still be ascribed to wind existing elsewhere.

The change in the meteorological effect along the coast was also investigated. On the day of the actual storm surge practically no differences were found for places on the coast between Brouwershaven and Helder. But in Flushing and Vlieland the effect was slightly less (by $\pm$ 8 %).

The results of the "government committee of 1916" were afterwards used by VAN EVERDINGEN (10) for the establishment of a "Service of Warnings for Storm Surges". We are here of course mainly concerned with the prediction of the actual height of

high tide. The direction and force of the wind occurring some hours before the time of high tide were estimated and the corresponding meteorological effect was read from the curves of figure 1. This value had to be added to the predicted value of the height of high tide from the tide-table to obtain the value of the actual height of high tide. Often the value computed in this way had to be corrected for the effect due to distant causes. For in most cases the heights of the tide computed in this way for the period, immediately preceding the actual storm surge, were too low (the actual heights being communicated to the Meteorological Institute, the seat of the Warning Service for Storm Surges). Now according to VAN EVERDINGEN, the difference between the calculated and observed values of the height of the tides was due to distant causes. This effect was assumed to remain constant throughout the whole storm surge, and was therefore used as a correction in the computation of the heights of high tides during the storm. But in practice it was often found, that the heights of high tide, computed in this way, were too high. Evidently the "effect of the distant causes" did not remain constant throughout the whole storm surge. A new investigation was therefore inaugurated to obtain a better insight into this question. The results of this investigation are laid down in the present publication.

Other valuable researches were published by LELY (11, 12), the "government committee for the Zuiderzee" (13) and MAZURE (14), especially concerning the formula derived and used for the windeffect in a closed channel. This formula is:

$$\zeta = \frac{a\, V^2\, L \cos \psi}{H}. \tag{3}$$

ζ = windeffect (in cm);
a = a constant. Mostly values $0{,}035 \leqq a \leqq 0{,}045$ are found;
V = windvelocity (in m/sec);
L = length of the channel (in km);
H = depth of the channel (in m);
ψ = angle between the direction of the wind and the axis of the channel.

In publications (13) and (14) is assumed: $a = 0{,}036$. The windeffect according to (3) is assumed to be quadratic in the windvelocity. Moreover it is inversely proportional to the depth of the channel.

2. Other investigations

In the preceding paragraph the different causes, which influence the development of a storm surge, are indicated in connection with the Dutch researches on this problem. In this paragraph we shall discuss systematically the results of other investigators, arranged according to these different causes. A summary of all the literature on storm surges is not meant. A survey of this literature is given among others by WITTING (15), KRÜMMEL (16) and THORADE (17).

We discuss the different causes in the same order as in § 1.

a. Elimination of the astronomical tide

According to LENTZ (18) the meteorological effect is practically superposed upon the astronomical tides, without affecting the latter. But according to BUBENDEY (19) this is not quite true. The height of the sealevel is more influenced at low tide than at high tide. His explanation of this fact can be summarized as follows: the depth of the sea at low tide is less than at high tide; as the wind influences shallow water more strongly than deep water, the sea is more influenced at low tide than at high tide. The same result was obtained by DOODSON (20) and DINES (21). On the whole these differences are rather small, however, and they can be easily recognized by their purely periodical character with the period of the tides, so that they can be eliminated subsequently.

b. Inertia of the sea

Already BUBENDEY (19) assumed, that the condition of the sea would become stationary, if the wind blows during a sufficiently long time. For each place on the coast this stationary state would be reached after a certain "retardation-time", characteristic for the place in question. For the Belgian coast SCHULZ (23) obtained a "time-lag" of 3 hours, a value which is considerably lower than that found by ORTT (6 hours). DINES (21) however obtained for the windeffect on the English East coast a time-lag of about 6 hours. DOODSON (20, 22) investigated also these time-lags. He found, that a local wind influences the sea immediately, whereas the wind at more distant places exercised its effect only after a certain time-lag. See further *f*.

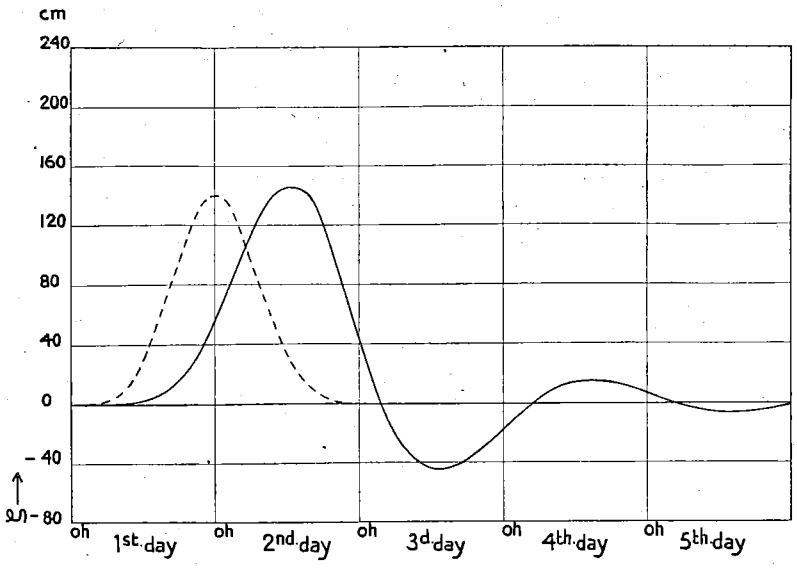

Fig. 2. Oscillations of the sea due to wind.

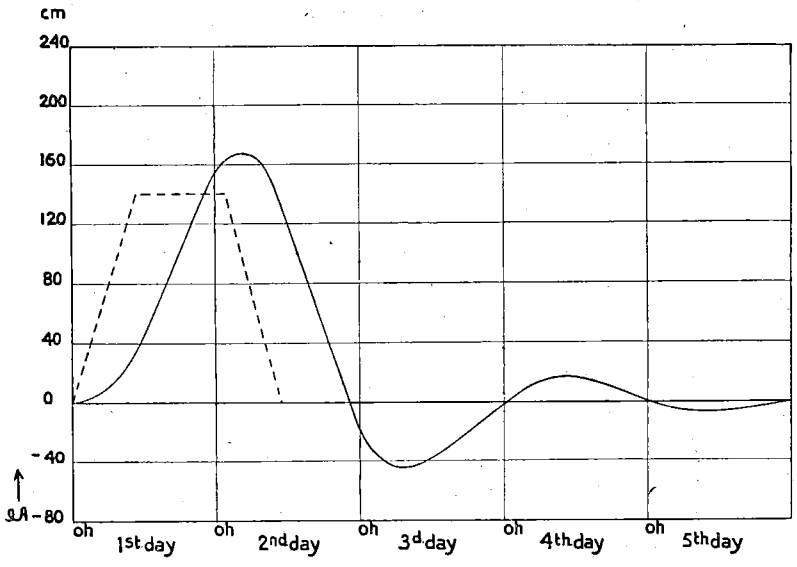

Fig. 3. Oscillations of the sea due to wind.

MÖLLER found already (24), that the sea does not approach its steady state by simply rising asymptotically. According to this investigator oscillations of the sea are created. In approaching its final states the sea oscillates therefore about this stationary values as well in the case of the formation of a windeffect during a storm as in the case of the flowing away of the surplus of water after a storm. The amplitude of these oscillations is the greater the quicker the changes in the direction or force of the wind. According to MÖLLER therefore, a storm which breaks suddenly is more dangerous than a storm which develops gradually, because in the former case the fluctuations of the sea will exceed the stationary level to a much larger extent, thereby causing the maximum meteorological effect to be abnormally great. Oscillations of this type have been discovered also by other investigators. LA COUR (25) found an oscillation of the Southern part of the Baltic during the storm surge of 15—16 January 1916. According to THORADE (26) analogous oscillations were generated in the Sont.

But also oscillations in which the whole North Sea participated were found by THORADE (17). The period amounted approximately to two days, which is rather long for the North Sea. (Longest "eigen periode" of the North Sea according to THORADE is $1\frac{1}{2}$ day).

Waves, travelling from the North around the whole North Sea, have been described by DOODSON (20).

The theoretical explanation of this phenomenon was first given by PROUDMAN and

DOODSON (27). They calculated the variations of the height of the sealevel at the coast caused by a suddenly or gradually varying field of wind or atmospheric pressure. The results of their calculations for two types of variation of a windfield are shown in figures 2 and 3.

In both figures the broken lines indicate the height of the sealevel if at each moment the sea would be in the stationary state corresponding to the field of wind, present at that moment. In both figures the oscillations are clearly present. It is also evident, that the normal state, after the storm has ceased, is reached by asymptotically decreasing oscillations. In both figures a time-lag can also clearly be seen.

In these calculations the rotation of the earth was neglected and other simplifying assumptions were introduced. Nevertheless, it may be said, that this investigation gives a rather complete theoretical account of the phenomena connected with the inertia of the sea. Analogous calculations were performed by HORROCKS (28), the earth's rotation being taken into account. His computations are extremely complicated and their use for numerical work is therefore difficult. HORROCKS, too, was compelled to introduce simplifying assumptions (no wind present at the coast!).

HIDAKA (29, 30, 31, 32) does not assume, that the wind is zero at the coast, but neglects the earth's rotation. He finds, that, when the wind starts, the level of the sea at the coast begins immediately to slant to an extent adjusted to the wind.

The most complete calculations have been carried out by NOMITSU (33, 34, 35, 36, 37, 38, 39). The Coriolis-force is taken into account, and he calculated the height of the sealevel for the case in which the wind at the coast is zero, as well as for the case in which the wind is uniform above the whole sea or channel. In the first case according to his computations oscillations are generated. In the second case he finds, as did HIDAKA, that the level of the sea begins immediately to slant at the coast, which state is then propagated seaward off the coast. The velocity of propagation is nearly the same as for the propagation of a "long wave" (tidal wave, etc.).

c. *Relation between windeffect and velocity of the wind*

LENTZ pointed out already in 1879 (18), that the windeffect is proportional to the square of the windvelocity. A thorough investigation was carried out by COLDING (40, 41). He obtained a formula, which we write (for comparison with formula (3)) in the following form:

$$\zeta = \frac{0{,}048\ L V^2 \cos^2 \psi}{H}.$$

In this formula ζ, L, V, ψ and H have the same meaning as in formula (3). The two formulas are immediately seen to be nearly identical, only in the formula of COLDING the second power of $\cos \psi$ is used. COLDING takes therefore the square of the *component* of the wind in the direction of the channel into account.

COLDING used for the verification of his formula the differences in height of the sealevel, caused by the storm of 12—14 November 1872 in the Danish waters and the Baltic. The formula was found to be fairly satisfactory.

WITTING (15) investigated the relation between the mean value of the height of the sealevel and the *gradient* of the *atmospheric pressure* (means over a month!). This method of correlation had certain advantages, viz. that the effect of the "time-lags" is practically absent in these monthly means. As, moreover, the gradient causes both the wind (and therefore the *windeffect*!) and the effect of the atmospheric pressure on the sea, the relation between gradient and total meteorological effect may be expected to be simple. As both the absolute magnitude and the direction of the gradient should be taken into account, the gradient is decomposed into its North and East component: $\triangle N$ and $\triangle E$ respectively. For the relation between the difference in height of the sealevel between

two places $\triangle V$ and the values of the two components of the gradient WITTING obtained the following general formula:

$$\triangle V = p \,.\, \triangle N + q \,.\, \triangle E.$$

p and q are constants, having their characteristic value for each pair of places on the coast of the Baltic. It is possible to eliminate from this formula the effect of the atmospheric pressure and to connect the windeffect, found in this way, with the vector of the wind, as the windvector can be easily deduced from the vector of the gradient. On doing this, it turns out that a *linear* law holds for the relation between the velocity of the wind and the value of the windeffect. WITTING himself, however, points out, that this relation is not entirely reliable, the water in the Baltic being strongly stratified, which may be the cause of this different behaviour of the relation between the velocity of the wind and the windeffect. These results, too, were obtained with the aid of monthly *means*, which may cause some confusion in the results.

LEVERKINCK (42) assumed for the relation between windeffect and velocities of the wind:

$$\zeta = k\, V^2.$$

In this formula k was not a constant, but was in its turn a function of V. This resulted in the fact, that up to nearly 20 m/sec, ζ was proportional to a power of V much less than 2. But for velocities well above 20 m/sec k was practically a constant.

SCHULZ (23) found in his investigations on the effect of the wind on the level of the sea at the Belgian coast a quadratic law. But his formulas have been derived only for velocities between 1 and 6 degrees Beaufort, that means for rather small values of the velocity of the wind.

HAYFORD (43) investigated the windeffect on the great American lakes. He obtained:

$$\zeta = k\, V^{2.4}.$$

Here the power of V is even *greater* than 2.

PALMÉN (44, 45, 46, 47) investigated the windeffect on the Baltic. The effect of the atmospheric pressure was carefully eliminated. In the beginning he found a linear law for small values of the windvelocity (45). But the observations in cases with strong winds could better be represented by a quadratic law (45, 46). He found for the windeffect at a distance of 100 km:

$$\zeta = 0{,}063\ V^2.$$

This formula only holds for a certain part of the sea, for which PALMÉN estimates a depth of ca. 50 m. He shows theoretically, that the windeffect should be approximately inversely proportional to the depth of the sea. If we introduce this into his formula, and write the latter in a form similar to formula (1), we obtain:

$$\zeta = \frac{0{,}032\ L\ V^2 \cos \psi}{H}.$$

HELLSTRÖM (48) derives from observations, made on the American lake Okeechobee during hurricanes, in which very high wind velocities occurred, the following relation:

$$\zeta = k \,.\, V^{1.6}.$$

The power of V is in this formula less than 2.

d. Relation between windeffect and direction of the wind

SCHULZ (23) found, that the relation between the value of the windeffect and the direction ψ of the wind, could be represented fairly well by a cosine function. The maximum value of the windeffect was reached for the direction WNW. According to SCHULZ the positive and negative values of the windeffect were distributed nearly symmetrically.

LENTZ (18) found, however, that the negative effect is smaller than the positive effect, if we consider the same windforce in both cases. He attributes this phenomenon to the fact, that an off-shore-wind is only able to produce sufficiently high waves after having travelled some distance over the water, so that the part of the sea on which the wind can exert its influence is smaller in the case of an off-shore-wind than in the case of an on-shore-wind, which results in a difference in windeffect between the two cases.

According to LEVERKINCK (42), the greatest effect is caused by a wind, which blows parallel to the longitudinal axis of the North Sea. See below *f*. This is also the opinion of PRÜGEL (49). DINES (21) found, that the greatest values of the windeffect on the East coast of England were caused by Northwesterly wind on the whole North Sea. DOODSON (20) obtained similar results (see however below *f*).

The results we discussed so far in this section were, however, concerned only with the coasts of the North Sea. But we may mention here also some investigation of the windeffect in lakes or inland seas which are more or less enclosed, like the Baltic. Many theoretical researches on this problem have also been published. In this case one is mainly interested in the direction of the slope of the watersurface relative to the direction of the wind, when the equilibrium state of the surface under the influence of the wind has been reached. When we have found this more general relation, the angular distribution of the windeffect can be easily calculated for any place on the coast of the lake or sea (HELLSTRÖM, 48). Investigation showed, that on the European and American lakes the slope of the water surface assumes the same direction as the direction of the wind. On greater inland seas, however, the direction of this slope is not exactly the same as the direction of the wind. This originates in the influence of the rotation of the earth, which causes a deflection of the slope to the right of the direction of the wind; this deflection though small is clearly perceptible. This has been found by many investigators. COLDING (41) constructed for various times the lines of equal height of sealevel of the Baltic and the Danish waters during the storm of 12—14 Nov. 1872. On his splendid charts he also indicated the position of the isobars and the trajectories of the wind. From these charts it is easily derived that indeed the direction of the slope of the sealevel approaches gradually the direction of the wind. If we take the effect of the atmospheric pressure into account it turns out, however, that the direction of the slope is slightly deflected to the right of the direction of the wind. But this difference is small and amounts only from 5° to 10°.

From these charts still an other fact may be derived: the islands in the sea and the *form* of the coasts do not influence at all the position of the isohypses of the waterlevel. This position is fixed by the direction of the wind and the *depth* of the sea only.

WITTING (15) too found, that in the Baltic the slope of the water is deflected only from 0° to 5° to the right of the direction of the wind. For the North Sea, too, WITTING tried to find the relation between the gradient of the atmospheric pressure and the meteorological effect. His results are not very reliable, as sufficient observations were lacking. Nevertheless we may conclude from his work (correcting for the effect of the atmospheric pressure !), that also in the Southern part of the North Sea the slope of the water has nearly the same direction as the wind. The greatest values of the slope occur in the most Southerly part of the North Sea (between Holland and England, in the Helgoland Bight). This can be explained easily: here the sea is shallowest.

PALMÉN, too, (44, 46) studied the angle between the direction of the slope and the direction of the wind in the Baltic, after correcting for the effect of the atmospheric pressure. He found in general a deflection to the right (44). But when the velocity of the wind is small, large individual deviations may occur, the magnitude of the slope then being small, so that other effects have a relatively large influence. During the storm of 3—7 October 1936, however, the whole Baltic reached finally a state of equilibrium. He found, in connection with the high wind-velocities then prevailing, (46) a rather constant deflection to the right, average value 3°, in good agreement with the results of WITTING.

The result of all these investigations is very satisfactorily confirmed by theory. The theory was founded by EKMAN (50, 51, 52). He obtained, that in enclosed seas, in which the force of Coriolis can not be neglected, the slope of the water is deflected to the right of the direction of the wind. The windeffect should be inversely proportional to the depth of the sea. Analogous calculations, based on more general assumptions, were carried out, among others, by JEFFREYS (53, 54) and NOMITSU and TAKEGAMI (38). They assumed a quaratic law of friction for the water along the bottom of the sea (see also chapter II), whereas EKMAN simply assumed the velocity of the water to be zero at the bottom. The latter investigators found also, that the value of the wind-effect is nearly inversely proportional to the depth of the sea, but that the angle between the slope of the surface and the direction of the wind changes slightly with the velocity of the wind and the depth of the sea. From their computations one can, however, deduce that this angle for the case of the Baltic amounts from 1° to 5°, in perfect agreement with the results of PALMÉN and WITTING.

e. Influence of the atmospheric pressure

On this subject, too, many researches have been carried out. For an enclosed sea theory yields the result, that the sea is simply in hydrostatic equilibrium (see, among others, (37)). The slope of the surface of the sea should, therefore, be directed exactly parallel to the gradient of the atmospheric pressure. This result was used by PALMÉN (44, 46) for eliminating the effect of the atmospheric pressure. As the density of the seawater is approximately 1,03, a difference of pressure of 1 cm mercury should cause a difference in height of the sea of 13,2 cm, when perfect hydrostatic equilibrium is reached. This stationary state, however, is very probably never reached under the conditions prevailing during a normal storm surge on the coasts of the North Sea (more or less quickly moving depressions, etc.). Accordingly many different values for the proportionality-factor were found, ranging between 5 and 30 cm of water per cm mercury. This problem will therefore be treated more in particular.

Attention is called here to the work of PROUDMAN (55) on the influence of a moving depression. According to his theory a moving wave is generated under these conditions on the surface of the sea. But the most important result of his considerations is, that in this case higher values of the sealevel may occur, than would follow from the simple hydrostatic law. He derived the following formula for the ratio between the actual variation ζ and the variations according to the simple hydrostatic law $\bar{\zeta}$ in a closed channel:

$$\frac{\zeta}{\bar{\zeta}} = \frac{1}{1 - \frac{v}{c}},$$

v = velocity of the movement of the depression;
c = velocity of propagation of long waves.

If we have approximately: $v = c$, very large disturbances of the watersurface may occur. DOUGLAS (56) is of opinion to have found a confirmation of this theory in practice.

NOMITSU (57) and TAKEGAMI (58, 59) obtain similar results. In this way theory offers an explanation of the occurrence of "waterequivalents" which are larger than the theoretical value deduced from the hydrostatic law.

f. Effects of distant causes

It was already known to LENTZ (18), that the variations of the sealevel near the coast were often more closely connected with the wind in other places than with the local wind. LEVERKINCK (42) assumed, that the height of the sealevel in the Helgoland Bight was principally influenced by the mean value of the wind on the *whole* North Sea. The component of the wind parallel to the longitudinal axis of the sea (approximately perpendicular to the line Skudesnäes-Aberdeen) should in this connection be considered more in particular. Assuming an angle of 16° between the wind on the Sea and the isobars, LEVERKINCK was able to calculate the value of this component from the difference in airpressure between Skudesnäes and Aberdeen. It turned out that the value of this quantity and the meteorological effect in the Helgoland Bight were indeed closely connected. The curves for the two quantities were nearly identical, only one curve lagged a certain time behind the other (see below *b* !). The correlation factor amounted to 0,93.

DINES (21) also correlated in his investigation the meteorological effect with the wind on the *whole* sea. A very important study of this question was carried out by DOODSON (20). He assumed (following WITTING, 15) a linear equation of regression for the relation between the meteorological effect at London Bridge and the North and East components of the gradient of the atmospheric pressure at London Bridge, at 60° N.L., 0° E.L. (a point in the neighbourhood of South-Norway) and at 50° N.L., 10° W.L. (South of Ireland). The local barometric pressure was also taken into account. To connect the direction of the *gradient* with the direction of the *wind* DOODSON assumed an angle of 20° between the wind and the isobars. In this way he was able to obtain the direction of the wind which is most effective in influencing the sealevel at London Bridge, the relative influence of the wind in the three places mentioned and also the time-lag between the wind and its effect. DOODSON finds, that the influence of the wind in these different places is nearly equal. The most effective directions of the wind and the corresponding time-lags are summerized in table 4.

TABLE 4

Most effective directions of the wind for raising the sealevel at London Bridge and corresponding time-lags

Quantity \ Place	London Bridge	North Sea	Irish Sea
Effective direction of wind	NNE	NW	E
Time-lag (hours).	0	12	12

The most important result of this investigation is, that a Northwesterly wind above the North Sea is most effective in raising the sealevel on the coasts of the Southern part of the sea. The effect of the wind in the Irish Sea seems difficult to explain physically. Pronounced time-lags are present.

g. Difference in meteorological effect along the coast

SCHULTZ (23) obtained the result, that the value of the meteorological effect along the Belgian coast varied only little. From other investigations it follows, that the wind-effect in the Helgoland Bight is often larger than on our coasts. This should most probably be attributed to the shallowness of the sea in this place.

3. Scope of the present investigation

The researches mentioned in the preceding paragraphs can be summarized as follows, according to the different aspects:

a. Astronomical and meteorological effects are simply superposed upon each other. After subtraction of the calculated values of the astronomical tides from the actual heights of the sealevel, it is possible that little fluctuations remain, which can however easily be recognized, and removed.

b. Owing to the inertia of the sea oscillations relatively to the equilibrium state occur, in which the whole North Sea eventually partakes, with periods, which may amount to two days. The fluctuations in the field of wind cause fluctuations in the height of the sealevel with a certain time-lag, which on our coasts amounts probably from 3 to 6 hours.

c. The relation between the velocity of the wind and the windeffect obeys approximately a quadratic law.

d. The most effective direction of the wind in raising the level of the sea in the Southern part of the North Sea is approximately NW. This part of the sea behaves nearly as an enclosed sea.

e. The relation between the height of the sealevel and the atmospheric pressure is closely connected with the structure and the movement of the field of pressure. The average value of the "waterequivalent" is however smaller than the theoretical value.

f. The windeffect in the Southern part of the North Sea is closely connected with the mean value of the wind on the *whole* North Sea.

g. The change in the meteorological effect along the Dutch North Sea coast, South of Helder is in most cases negligible.

A great drawback of the methods which hitherto have been used, is, that the results only hold for the *average* of a *great number of cases*. But for the Warning Service for Storm Surges it is of the utmost importance, that *each individual* case could be explained. For that reason a general scheme should be built up to predict the development of every storm surge from the expected development of the field of wind and pressure. In this scheme the wind at *different* places of the sea should be taken into account. In this way the structure of the whole field of wind, even in the case of pronounced inhomogenity, should enter into the computation. To be able to do this in the most simple way, a theoretical investigation into the influence of the wind at different places of the North Sea is first carried out. Also the phenomena of inertia (oscillations, time-lag) are studied. The theoretical considerations serve then to work up the compiled data and finally results are discussed.

CHAPTER II. THEORY OF THE WINDEFFECT IN THE NORTH SEA

In this chapter theoretical considerations are given concerning the various aspects of storm surges, discussed in chapter I. These investigations will guide us in working up the collected data. The problem of the windeffect in an enclosed sea is chosen as the central problem, as this is the most important one for the North Sea. Consequently the following problems are treated: angular distribution of the windeffect, phenomena of inertia, effects of distant causes and inhomogeneity of the field of wind. We shall use throughout this chapter the following symbols:

x, y, z = set of Cartesian coordinates (right hand-system), by which the motion of the water is described. The xy-plane is laid in the undisturbed surface of the sea, the positive direction of the z-axis is pointing downwards.

H = depth of the sea (generally H is a function of x and y).

v_x, v_y = components of the horizontal motion of the water. v_x and v_y are functions of z.

S_x, S_y = components of the total current ($S_x = \int_0^H v_x dz$, $S_y = \int_0^H v_y dz$).

$w = v_x + iv_y$.

$S = S_x + iS_y$.

$\vec{S}$ = vector with components S_x and S_y.

i = imaginary unit of the complex plane.

ζ = deviation of the sealevel from the undisturbed position.

$\gamma_x, \gamma_y = -\frac{\partial \zeta}{\partial x}, -\frac{\partial \zeta}{\partial y}$.

$\gamma = \gamma_x + i\gamma_y$.

$\vec{\gamma}$ = vector with components γ_x and γ_y.

W_x, W_y = shearing stress (frictional force) of the wind along the surface of the sea.

$\vec{W}$ = vector with components W_x and W_y.

$\vec{v}$ = vector with components v_x and v_y.

$\vec{u}$ = vector of the frictional force between two adjacent layers of water (components: u_x and u_y).

ϱ = density of the seawater.

μ = (virtual) coefficient of friction between two adjacent layers of water.

f = coefficient of friction along the bottom of the sea.

ω = angular velocity of the earth.

φ = average geographical latitude of the North Sea.

$l = 2\omega \sin \varphi$.

$a = (1 + i) \sqrt{\frac{\varrho l}{2\mu}}$

g = acceleration of gravity.

m = mixing length.

S_n = component of the total current perpendicular to the coast.

V = velocity of the wind above the sea (measured at a height of 6 m).

$D = \pi \sqrt{\frac{2\mu}{\varrho l}}$ (depth of frictional influence, EKMAN's "Reibungstiefe").

1. The Fundamental equations

The motion of the water, caused by wind and fluctuations of the atmospheric pressure, are governed by the frictional forces which arise, when the various layers of water slide along each other. For our investigations it suffices to consider the forces arising from differences between the horizontal velocities of the various layers. It is true, that also frictional forces are generated when differences of velocity in *horizontal* direction exist

("lateral mixing"), but in our investigation we are allowed to neglect these forces. Moreover, we shall consider exclusively the horizontal motions, neglecting the vertical components of the motion.

According to the theory of turbulence the frictional force (shearing stress) $\vec{u}$, exerted by a layer with a velocity $\vec{v}$ and coordinate z on an adjacent layer with a velocity $(\vec{v} + d\vec{v})$ and coordinate $(z + dz)$ is represented by the formula:

$$\vec{u} = -\mu \frac{\partial \vec{v}}{\partial z}. \tag{1}$$

This is a force per unit of area. μ is a coefficient of friction governed by the turbulence in the water. The particles of water with different velocities are mixed by turbulence; to express the rate of mixing PRANDTL introduced the "*mixing length*" m. With the aid of this quantity μ could be represented in the following way:

$$\mu = \varrho\, m^2 \cdot \left| \frac{\partial \vec{v}}{\partial z} \right|.$$

For the complete description of the motion of the water it is necessary to assume a relation between m and z. m will be closely connected with z. In the neighbourhood of the surface m can never attain large values, as the mixing there is much reduced by the spacial boundary of the water. Downwards the value of m will rapidly increase, as the uppermost water layers will be most strongly disturbed by the wind. After having attained a maximum, m will decrease again, and finally obtain at the bottom a very small value, as here again the mixing of the water is reduced by the fixed boundary of the water.

PRANDTL and v. KÀRMÀN (60, 61) have derived formulas for m. But these formulas are not appropriate for our purpose. It is possible to integrate with these formulas the equations of motion only in those cases, in which it is allowed to neglect the rotation of the earth, as, for example the flow in boundary layers or pipes. But in the case of a sea, in which it is not allowed to neglect the earth's rotation, it is not possible to integrate the equations of motion in closed formulas. For our calculations however we need exactly the solutions for the motion of the water in closed form.

EKMAN (50, 51, 52) calculated the motion of the water assuming m to be a constant. But even in this case it is not possible to express the solution in a closed form. This is due to the factor $|\partial \vec{v}/\partial z|$ which occurs in the formula for μ, causing the formula for $\vec{u}$ to be quadratic in $\partial \vec{v}/\partial z$.

FJELDSTADT (62) gives an other solution. He does not introduce the mixing length, but introduces for μ the formula:

$$\mu = \mu_o \left(1 - \frac{z}{H + \varepsilon}\right)^n, \quad 0 < \frac{\varepsilon}{H} << 1, \quad 0 < n < 1. \tag{2}$$

In this formula ε represents a very small length. According to equation (2) the coefficient of friction has a maximum at the surface of the water, but a very small value at the bottom. Neglecting the rotation of the earth the equations of motion can be integrated in a closed form, on the assumption that the velocity of the water at the bottom is zero, which is physically speaking evident. If, however, the rotation of the earth is taken into account, the integration cannot be performed in closed form. However, PALMÉN has shown (neglecting the earth's rotation) that the decreasing of m towards the bottom results in a motion of the water, which has more or less the nature of a *gliding of the water along the bottom of the sea.* Only in a thin "boundary layer" the velocity of the water decreases rapidly and becomes vigorously zero at the bottom. In order to obtain the integral of the equations of motion, taking the rotation

of the earth into account, we assume therefore, that μ is a constant throughout the water. But gliding of the water along the bottom of the sea is tolerated (cf. a. o. NOMITSU and TAKEGAMI, 38, 39). The condition, that the velocity of flow along the bottom of the sea $= 0$, must then be replaced by a formula governing the "friction" between the water and the bottom of the sea. This "law" of friction can be established in the following way: if we neglect the rotation of the earth the equations of motion can be integrated in closed form in *both* cases (variable μ and constant μ with sliding along the bottom). It turns out, then, that the results of both calculations can be made the same if we assume a linear relation to exist between the frictional force and the velocity at the bottom. This will be shown here in more detail. The formulas (1) and (2) represent the *shearing stress* existing between two adjacent layers of water. But in the equations of motion appears the *force* which acts on a layer of water. For this force $\vec{k}$, acting on a layer of unit area and density ϱ we have (per unit of ~~volume~~ mass):

$$\vec{k} = -\frac{1}{\varrho}\frac{\partial \vec{u}}{\partial z} = \frac{1}{\varrho}\frac{\partial}{\partial z}\left(\mu \frac{\partial \vec{v}}{\partial z}\right).$$

On a layer of water acts also the force caused by the slope of the surface of the water. The components of this force (per unit of ~~volume~~ mass) are:

$$-g\frac{\partial \zeta}{\partial x}, -g\frac{\partial \zeta}{\partial y}.$$

We write this in the condensed form:

$$-g\vec{\gamma}.$$

The equation of motion becomes (neglecting the rotation of the earth, as already mentioned):

$$\frac{\partial \vec{v}}{\partial t} = \frac{1}{\varrho}\frac{\partial}{\partial z}\left(\mu \frac{\partial \vec{v}}{\partial z}\right) + g\vec{\gamma}. \tag{3}$$

Strictly speaking the left hand side of the equation should have the form:

$$\frac{\partial \vec{v}}{\partial t} + v_x\frac{\partial \vec{v}}{\partial x} + v_y\frac{\partial \vec{v}}{\partial y}.$$

In the case of homogeneous fields of wind the terms $v_x\frac{\partial \vec{v}}{\partial x}$ and $v_y\frac{\partial \vec{v}}{\partial y}$ are usually exactly $= 0$. It can be shown by numerical computation that also in the case of inhomogeneous fields of wind their relative influence is so small, that it is allowed to neglect these terms. This is done in all calculations which follow.

Equation (3) can now be integrated, if we introduce the formula for μ and also the boundary conditions. The boundary condition valid for the surface of the water does not depend on the way in which μ varies with z. Here the friction between the layers of water has simply to be in equilibrium with the friction exerted by the wind on the water. This frictional influence of the wind is denoted by $\vec{W}$. In this way we obtain:

$$(\vec{u})_{z=0} = -\left(\mu\frac{\partial \vec{v}}{\partial z}\right)_{z=0} = \vec{W}.$$

But at the bottom of the sea we have different boundary conditions, according as we introduce the formula (2) or a constant μ.

In the first case we obtain:

$$(\vec{v})_{z=H} = 0.$$

In the second case we assume a linear law of friction (see above):

$$(\vec{u})_{z=H} = -\left(\mu \frac{\partial \vec{v}}{\partial z}\right)_{z=H} = \varrho f \cdot (\vec{v})_{z=H}.$$

We shall integrate the equations for the two cases and compare the results.

a. Varable μ.

We assume the fields of wind to be stationary. Then, when the state of equilibrium is reached, no changes with time occur. The equation of motion (3) becomes then:

$$0 = \frac{1}{\varrho} \frac{\partial}{\partial z}\left(\mu \frac{\partial \vec{v}}{\partial z}\right) + g\,\vec{\gamma}.$$

For μ we assume:

$$\mu = \mu_o \left(1 - \frac{z}{H}\right)^n.$$

This is evidently the formula of FJELDSTADT, which we have simplified by putting

$$\varepsilon = 0.$$

The boundary conditions are:

$$-\left(\mu \frac{\partial \vec{v}}{\partial z}\right)_{z=o} = \vec{W}, \quad (\vec{v})_{z=H} = 0.$$

The solution becomes (as can easily be verified):

$$\vec{v} = \frac{\vec{W} H}{\mu_o (1-n)} \cdot \left(1 - \frac{z}{H}\right)^{1-n} + \varrho g \vec{\gamma} H \cdot \left\{ \frac{z\left(1 - \frac{z}{H}\right)^{1-n}}{\mu_o (1-n)} + H \cdot \frac{\left(1 - \frac{z}{H}\right)^{2-n}}{\mu_o (1-n)(2-n)} \right\}.$$

In studying the windeffect we are chiefly interested in the *total current*, which is caused by the wind and the slope of the surface. We compute therefore also:

$$\vec{S} = \int_0^H \vec{v}\, dz = \frac{\vec{W} H^2}{\mu_o (1-n)(2-n)} + \frac{2 g \varrho \vec{\gamma} H^3}{\mu_o (1-n)(2-n)(3-n)}.$$

b. Constant μ.

In this case we assume μ to be a constant, so that the equation of motion becomes:

$$0 = \frac{\mu}{\varrho} \frac{\partial^2 \vec{v}}{\partial z^2} + g\vec{\gamma}.$$

The boundary conditions become:

$$-\left(\mu \frac{\partial \vec{v}}{\partial z}\right)_{z=o} = \vec{W}, \quad -\left(\mu \frac{\partial \vec{v}}{\partial z}\right)_{z=H} = \varrho f \cdot (\vec{v})_{z=H}.$$

The solution is:

$$\vec{v} = \frac{g\varrho\vec{\gamma}}{2\mu} \cdot (H^2 - z^2) + \frac{\vec{W}}{\mu} \cdot (H - z) + \frac{1}{\varrho f}(g\varrho\vec{\gamma}H + \vec{W}).$$

Here, too, we compute $\vec{S}$:

$$\vec{S} = \int_0^H \vec{v}dz = \vec{W}H^2\left\{\frac{1}{2\mu} + \frac{1}{\varrho f H}\right\} + g\varrho\vec{\gamma}H^3\left\{\frac{1}{3\mu} + \frac{1}{\varrho f H}\right\}.$$

Evidently this formula is very much the same as the first formula for $\vec{S}$. Now it is possible to select such values for μ and f, that the coefficients of $\vec{W}$ and $\vec{\gamma}$ in the two formulas become the same. We have attained, then, that in both cases $\vec{S}$ is the same function of $\vec{W}$ and $\vec{\gamma}$, so that conclusions derived from the equation for $\vec{S}$ (a. o. the magnitude of the windeffect !) become also the same. And this is exactly our purpose. To this end we must introduce for μ and f:

$$\mu = {}^1/_6\mu_o(2-n)(3-n),$$

$$f = \frac{\mu_o(1-n)(2-n)(3-n)}{2n\varrho H}.$$

We shall use these formulas in the following calculations.

In order to obtain the value of the windeffect we have to take into account the force of Coriolis. This force, exerted on a particle of unit volume and velocity $\vec{v}$ amounts to:

$$\text{Force of Coriolis} = 2\omega \sin\varphi \,.\, |\vec{v}| = l|\vec{v}|.$$

The direction of this force is perpendicular to the direction of the motion and deflected towards the right. Introducing this in formula (3) and again writing down the boundary conditions, we obtain the following set of equations for the components of the motion of the water:

$$\frac{\partial v_x}{\partial t} = \frac{\mu}{\varrho}\frac{\partial^2 v_x}{\partial z^2} + lv_y + g\gamma_x, \tag{4a}$$

$$\frac{\partial v_y}{\partial t} = \frac{\mu}{\varrho}\frac{\partial^2 v_y}{\partial z^2} - lv_x + g\gamma_y, \tag{4b}$$

$$-\mu\left(\frac{\partial v_x}{\partial z}\right)_{z=o} = W_x, \tag{4c}$$

$$-\mu\left(\frac{\partial v_y}{\partial z}\right)_{z=o} = W_y, \tag{4d}$$

$$-\mu\left(\frac{\partial v_x}{\partial z}\right)_{z=H} = \varrho f \,.\, (v_x)_{z=H}, \tag{4e}$$

$$-\mu\left(\frac{\partial v_y}{\partial z}\right) = \varrho f \,.\, (v_y)_{z=H}, \tag{4f}$$

$$\mu = {}^1/_6\mu_o(2-n)(3-n), \tag{5a}$$

$$f = \frac{\mu_o(1-n)(2-n)(3-n)}{2n\varrho H}. \tag{5b}$$

In the following paragraph we shall use these equations. We compute the windeffect caused by a homogeneous wind in an enclosed sea. It is then allowed to assume

$$\frac{\partial v_x}{\partial t} = \frac{\partial v_y}{\partial t} = 0.$$

2. Windeffect in an enclosed sea

For the integration of equations (4*a*)—(4*f*) and (5*a*)—(5*b*) we introduce the following complex vectors:

$$w = v_x + i\, v_y,$$

$$\gamma = \gamma_x + i\, \gamma_y,$$

$$W = W_x + i\, W_y.$$

The equations can then easily be written as follows:

$$0 = \frac{\mu}{\varrho}\frac{\partial^2 w}{\partial z^2} - i l w + g\gamma, \qquad -\mu\left(\frac{\partial w}{\partial z}\right)_{z=0} = W, \qquad -\mu\left(\frac{\partial w}{\partial z}\right)_{z=H} = \varrho f \cdot (w)_{z=H}.$$

Introducing:

$$\alpha = (1+i)\sqrt{\frac{\varrho l}{2\mu}}$$

and also the well-known abbreviations:

$$\cosh p = \frac{e^p + e^{-p}}{2}, \quad \sinh p = \frac{e^p - e^{-p}}{2},$$

the solution of the last set of equations can be written in the following form:

$$w = \frac{W}{\alpha\mu} \cdot \frac{\frac{f\varrho}{\alpha\mu}\sinh\alpha(H-z) + \cosh\alpha(H-z)}{\sinh\alpha H + \frac{f\varrho}{\alpha\mu}\cosh\alpha H} + \frac{ig\gamma}{l} \cdot \left[\frac{\frac{f\varrho}{\alpha\mu}\cosh\alpha z}{\sinh\alpha H + \frac{f\varrho}{\alpha\mu}\cosh\alpha H} - 1\right]. \tag{6}$$

Now it was already pointed out in paragraph 1, that the *total* current is more important for the following calculations than the *distribution* of the velocities in the water. We compute therefore this total current S:

$$S = S_x + iS_y = \int_0^H v_x dz + i\int_0^H v_y dz = \int_0^H (v_x + iv_y)dz = \int_0^H w dz.$$

We obtain:

$$S = \frac{W}{\alpha^2\mu} \cdot \frac{\frac{f\varrho}{\alpha\mu}(\cosh\alpha H - 1) + \sinh\alpha H}{\frac{f\varrho}{\alpha\mu}\cosh\alpha H + \sinh\alpha H} + \frac{ig\gamma}{l} \cdot \left[\frac{\frac{f\varrho}{\alpha^2\mu}\sinh\alpha H}{\frac{f\varrho}{\alpha\mu}\cosh\alpha H + \sinh\alpha H} - H\right].$$

We introduce the following abbreviations:

$$D = \pi\sqrt{\frac{2\mu}{\varrho l}} \text{ (Ekman's „Reibungstiefe")}, \qquad F = \frac{f\varrho D}{\pi\mu}, \qquad h = \frac{\pi H}{D},$$

$$Na = F \,.\, [\cos h \sinh h + \sin h \cosh h + F \sin h \sinh h],$$
$$Nb = F \,.\, [\cos h \sinh h - \sin h \cosh h + F \cos h \cosh h],$$
$$Nc = \tfrac{1}{2}F \,.\, \big[\cosh 2h - \cos 2h + \tfrac{1}{2}F \,.\, \{\sinh 2h - \sin 2h\}\big],$$
$$Nd = \tfrac{1}{4}F^2 \,.\, [\sinh 2h + \sin 2h],$$
$$N = \cosh 2h - \cos 2h + F \,.\, \{\sinh 2h - \sin 2h\} + \tfrac{1}{2}F^2 \,.\, \{\cosh 2h + \cos 2h\}.$$

Substituting into the equation for S:

$$lS = \frac{W}{\varrho} \,.\, [a - i\,(1-b)] + gH\gamma \,.\, \left[\frac{c}{h} - i\left(1 - \frac{d}{h}\right)\right] \tag{7}$$

Substituting the expressions (5a) and (5b) for f and μ respectively, we can write for F:

$$F = \frac{f\varrho D}{\pi\mu} = \frac{3\,(1-n)\,D}{\pi n H} = \frac{3\,(1-n)}{nh} \tag{8}$$

From the equation for S we can now derive the value of the windeffect, if we introduce the boundary condition for S at the coast. It is clear, that at the coast no component perpendicular to the coast of the *total current* can exist. This current can only be directed parallel to the coast. Introducing this condition, the value of S is fixed for any point in the sea, and, knowing S, we can in its turn calculate γ as a function of W with the aid of equation (7). But this formula holds only, when the vertical distribution of the velocities in the water is represented by equation (6). And this is not fulfilled in the immediate neighbourhood of the coast, because at the coast a vertical interchange of water must exist between the different layers. TAKEGAMI (63) has shown, however, that the disturbance, caused in the vertical distribution of the velocities, extends from the coast only to a distance of the order of 3—5 H. And this distance is completely negligible in comparison with the distances covered by the windeffect in the North Sea. The boundary condition can, therefore, simply be written as follows:

$$S_n = 0.$$

We consider now a sea of constant depth, subjected to a homogeneous field of wind. In the following paragraph it will be shown, that in this case we have for any point in the sea:

$$S = 0, \quad \gamma = \text{const.}$$

The surface of the water remains a plane. The magnitude and direction of its slope is given by γ. From the equation for S the value of γ can be deduced at once:

$$\gamma = -\frac{W}{g\varrho H} \cdot \frac{1 - b + ai}{1 - \dfrac{ic + d}{h}}.$$

$\dfrac{1-b+ai}{1-\dfrac{ic+d}{h}}$ is a complex quantity, so that we canwrite:

$$\frac{1 - b + ai}{1 - \dfrac{ic + d}{h}} = k e^{i\psi},$$

where k is real. Hence:

$$\gamma = -k e^{i\psi} \cdot \frac{W}{g\varrho H}.$$

Taking the absolute value on both sides:

$$|\gamma| = \frac{k}{g\varrho H} \cdot |W|.$$

This formula gives the *magnitude* of the slope. The *direction* of the slope is deflected to the left of the direction of the "windvector" $\vec{W}$ over an angle ψ. Let us now study the values of k and ψ somewhat more closely.

The value of k depends only on the value of h (and through h on the value of H/D) and of n. It can be shown, however, that always:

$$1 \leqq k \leqq {}^3/_2.$$

The slope of the water is therefore inversely proportional to the depth of the water, if we neglect the slight variation of k. To obtain a better insight into this question the value of k for different values of the depth (in terms of the "Reibungstiefe" D) and of n is given in the following table. The values of ψ are also computed.

TABLE 5 *Value of k and ψ*

$H \rightarrow$	$H << \frac{D}{4}$		$H = \frac{D}{4}$		$H = \frac{D}{2}$		$H = D$		$H = 2D$		$H >> 2D$	
$n \downarrow$	k	ψ	k	ψ	k	ψ	k	ψ	k	ψ	k	ψ
0	1.50	0°	1.49	−1°.0	1.47	−4°.5	1.27	−10°.7	1.08	−4°.9	1.00	0°
¼	1.38	0°	1.37	−1°.0	1.34	−4°.5	1.16	−10°.7	1.02	−3°.3	1.00	0°
½	1.25	0°	1.25	−1°.0	1.22	−4°.2	1.06	−4°.8	1.01	−1°.8	1.00	0°
¾	1.13	0°	1.12	−0°.8	1.10	−2°.6	1.02	−1°.8	1.00	−0°.8	1.00	0°
1	1.00	0°	1.00	0°	1.00	0°	1.00	0°	1.00	0°	1.00	0°

From this table it is seen immediately, that ψ is always negative. The slope of the surface is therefore turned to the right of the direction of the wind, which is also found in practice (see chapter I, paragraph 2).

Further ψ turns out to be always small. We are more particularly concerned with the question as to which value of n yields the closest agreement with observation. FJELDSTADT deduced from his observations, that the best value of n amounts to ${}^3/_4$. From values for μ, given by THORADE (17) it appears also, that this value is probably the best one. The values of ψ connected with this value of n are very small, in very good agreement with the results of PALMÉN ($\psi = -3°$ if $H = 50$ m, see chapter I, paragraph 2). We may say therefore, that the direction of the slope and of the wind are nearly the same. Further it turns out, that the value of k does not change very much with a change in depth. For a more complete discussion of this, it is necessary, to know more about the value of the depth of frictional influence D. PALMÉN obtains experimentally the formula:

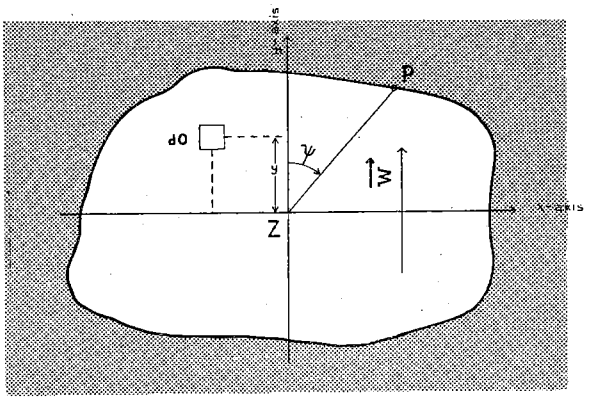

Fig. 4 Windeffect in an enclosed sea

$$D = 35 + 5{,}4\ V.$$

Here D is the value of the depth of frictional influence in meters and V the velocity of the wind in m/sec. We are chiefly interested in the windeffect caused by windvelocities between 15 and 25 m/sec. D has then an average value of 140—150 m. Now the depth of the part of the North Sea to which the windeffect is mainly restricted varies from 40 m to 80 m, that is from 0,3 D to 0,5 D, so that it follows from table 5, that in these

circumstances the value of k does not vary appreciably in this part of the Sea, viz. from 1,12 to 1,10 (for $n = {}^3/_4$!).

Neglecting, therefore, entirely this slight variation of k, we put:

$$k = 1, \ \psi = 0.$$

Hence:

$$\gamma = -\frac{W}{g\varrho H}. \tag{9}$$

For any place on the coast of a perfectly enclosed sea of constant depth the value of the windeffect can be deduced with the aid of formula (9). Assuming that the fluctuations in the sealevel, caused by the wind, remain small in comparison with the depth of the sea, it can be shown, that the height of the sealevel does not change at the centre of gravity of the surface. It was already pointed out, that when the windeffect is due to a homogeneous field of wind, the surface of the sea remains a plane. This plane cuts the undisturbed position of the surface along a straight line. This line is taken as the x-axis (see figure 4). The slope of the surface has everywhere the value $|\gamma|$. The windeffect ζ at a distance y from the x-axis becomes:

$$\zeta = |\gamma| \, . \, y.$$

The volume dI of the column of water with area do and height ζ is:

$$dI = |\gamma| \, . \, y \, . \, do.$$

The total volume of the water is of course constant. Integrating dI over the whole sea, we obtain, therefore:

$$I = \iint |\gamma| \, . \, y \, . \, do = 0.$$

As $|\gamma|$ is a constant:

$$\iint y \, . \, do = 0.$$

But this is exactly the condition, required for the centre of gravity of the whole surface to be situated on the x-axis, the line on which in all points $\zeta = 0$. As for any direction of $\vec{W}$ the centre of gravity is therefore situated on the x-axis, we have in this point always:

$$\zeta = 0.$$

If we wish to know the value of the windeffect in P, we calculate the difference of the height of the sealevel in P and in the centre of gravity Z. Along the line ZP we have:

$$d\zeta = \frac{\partial \zeta}{\partial x} dx + \frac{\partial \zeta}{\partial y} dy = -\vec{\gamma} \, . \, \vec{ds} = -|\gamma| \, . \, ds \, . \cos \psi.$$

Here $\vec{ds}$ is the vector with components dx and dy. The difference $\triangle \zeta$ in height between Z and P is found in the following way:

$$\triangle \zeta = \int_Z^P d\zeta = -|\gamma| \, . \cos \psi \, . \int_Z^P ds = -|\gamma| \, . \cos \psi \, . \, L.$$

Substituting $|\gamma|$ from formula (9), we obtain finally:

$$\triangle \zeta = \frac{|W| \, . \, L \, . \cos \psi}{g\varrho H}.$$

In this formula the value of $|W|$ must be substituted. PALMÉN found: $W = 3{,}2 \times 10^{-6} V^2$ (V = windvelocity in m/sec, W in dyne/cm^2). Expressing L in km and H in m and introducing $g\varrho = 10^3$, we obtain the following formula for the windeffect:

$$\Delta \zeta = \frac{0{,}032\ V^2 L \cos \psi}{H}. \tag{10}$$

This agrees fairly satisfactorily with formula (3) in chapter I. The latter refers, however, to the windeffect in channels, in which conditions may to some extent differ from those at sea. This may explain the difference in the proportionality factors (0,036 as compared with 0,032). We shall, therefore, use in our computation formula (10). For an enclosed sea the windeffect might be completely computed with the aid of this formula as a function of the velocity of the wind V and the directions of the wind ψ. This formula is confirmed quite well by observations of the windeffect in inland seas ("Wadden"-Sea, "Zuider"-Sea). But we are chiefly interested in the question of the applicability of formula (10) to the actual conditions in the North Sea. To investigate this we need a more simplified form of equation (7). First we rewrite (7) in the following form:

$$lS = A \,.\, \frac{W}{\varrho} + B \,.\, gH\gamma. \tag{7a}$$

Substituting in this equation: $S = 0$, we obtain the relation between γ and W:

$$\gamma = -\frac{A}{B} \cdot \frac{W}{g\varrho H}.$$

As it turns out however, that

$$\gamma = -\frac{W}{g\varrho H}, \text{ (equation (9))}$$

holds in close approximation, we have:

$$A/B = 1,\ A = B.$$

Equation (7a) can therefore be brought into the form:

$$lS = A\left[\frac{W}{\varrho} + g\,H\,\gamma\right].$$

If we study, the values of a, b, c and d from equation (7) more closely it turns out that in the case of the North Sea it is allowed to write approximately:

$$lS = \frac{\frac{W}{\varrho} + gH\gamma}{i + \frac{G}{2h}},\quad G = \frac{F + \frac{1}{2}F^2}{1 + F + \frac{1}{2}F^2},\quad h = \frac{\pi H}{D},\quad F = \frac{3\,(1-n)}{nh}.$$

Substituting the numerical values of H, D and n, occurring in a storm surge in the North Sea, we obtain approximately:

$$G = \tfrac{1}{2}.$$

Hence:

$$lS = \frac{\frac{W}{\varrho} + gH\gamma}{i + \frac{1}{4h}}. \tag{11}$$

3. Windeffect in a bay

In this paragraph the windeffect is investigated which occurs in a sea, open to the ocean. The North Sea is represented schematically in figure 5. The length of the sea is assumed to be $2L$, the breadth to be L. This represents fairly well the ratio of the actual dimensions of the North Sea. x- and y-axis have been introduced in the way, shown in the figure. This Sea cannot be considered as an "enclosed sea". For that reason the considerations of the preceding paragraph have to be modified to calculate the value of the windeffect along its coasts, especially for the South coast. For here the centre of gravity ($x = 0$, $y = -L$) cannot be taken as centre of reference, because the level of the sea will fluctuate here also. And besides, the general assumption $S = 0$ does not hold either in this Sea.

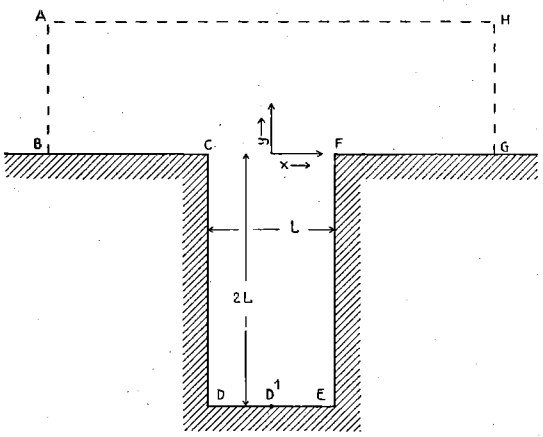

Fig 5.. North Sea (schematically)

For the computation of the windeffect in this Sea we have to add the equations of continuity to the formula for S and the boundary conditions. The equations of continuity formulates the relation between the divergence of the total current and the fluctuations of the Sea-level:

$$\frac{\partial S_x}{dx} + \frac{\partial S_y}{\partial y} = -\frac{\partial \zeta}{\partial t}.$$

As we consider only stationary states:

$$\frac{\partial \zeta}{\partial t} = 0.$$

Hence:
$$\frac{\partial S_x}{\partial x} + \frac{\partial S_y}{\partial y} = 0. \tag{12}$$

We add the equations:

$$lS = \frac{\frac{W}{\varrho} + gH\gamma}{i + \frac{1}{4h}}$$

(equation (11) of the preceding Chapter),

$$S_n = 0, \text{ along the coasts.}$$

But to these equations still another condition has to be added, viz. the condition for the state of the sea on the line CF.

Equation (12) can be satisfied by introducing the *stream function* Φ :

$$lS_x = -\frac{\partial \Phi}{\partial y}, \quad lS_y = \frac{\partial \Phi}{\partial x}.$$

The streamlines of the total current are given by the lines: $\Phi = \text{const.}$

Perpendicular to the streamlines we have everywhere $S_n = 0$. But this is exactly the boundary condition at the coast. Without restricting the generality we may put therefore, $\Phi = 0$, at the coast.

Now a differential equation for Φ has to be found. Solving equation (11) for γ, separating into real and imaginary parts, and introducing the formulas for S, γ and h, we obtain finally:

$$g\frac{\partial\zeta}{\partial x}=\frac{W_x}{\varrho H}+\frac{1}{H}\cdot\frac{\partial\Phi}{\partial x}+\frac{D}{4\pi H^2}\cdot\frac{\partial\Phi}{\partial y},\qquad g\frac{\partial\zeta}{\partial y}=\frac{W_y}{\varrho H}+\frac{1}{H}\cdot\frac{\partial\Phi}{\partial y}-\frac{D}{4\pi H^2}\cdot\frac{\partial\Phi}{\partial x}. \tag{13}$$

In these equations H is assumed to be a function of x and y. In this way these equations are applicable also to the case of a sea of variable depth.

Differentiating the first equation partially with respect to y and differentiating the second one with respect to x and subtracting, we obtain after rearranging:

$$\frac{\partial^2\Phi}{\partial x^2}+\frac{\partial^2\Phi}{\partial y^2}-\frac{\partial\Phi}{\partial x}\cdot\left[\frac{2}{H}\frac{\partial H}{\partial x}+\frac{4\pi}{D}\frac{\partial H}{\partial y}\right]-\frac{\partial\Phi}{\partial y}\cdot\left[\frac{2}{H}\frac{\partial H}{\partial y}-\frac{4\pi}{D}\frac{\partial H}{\partial x}\right]=\frac{4\pi}{\varrho D}\cdot\left[W_x\frac{\partial H}{\partial y}-W_y\frac{\partial H}{\partial x}+\right.$$
$$\left.+H\left(\frac{\partial W_y}{\partial x}-\frac{\partial W_x}{\partial y}\right)\right]. \tag{14}$$

This differential equation must be solved with the condition, that $\Phi=0$ along the coasts and a condition for the line CF, which has still to be established. This will be done in discussing two different cases: a homogeneous field of wind above a sea of constant depth and above a sea of variable depth.

a. Bay of constant depth

In this case we have:

$$\frac{\partial H}{\partial x}=\frac{\partial H}{\partial y}=0.\qquad\frac{\partial W_x}{\partial x}=\frac{\partial W_x}{\partial y}=\frac{\partial W_y}{\partial x}=\frac{\partial W_y}{\partial y}=0.$$

The equations become simply:

$$\frac{\partial^2\Phi}{\partial x^2}+\frac{\partial^2\Phi}{\partial y^2}=0. \tag{14a}$$

$$\Phi=0,\text{ along the coast.}$$

For the line CF no special condition is introduced. But we assume the physically plausible condition, that the disturbance, which the bay causes in the flow in the ocean, extends only to a distance comparable with the dimensions of the bay itself.

The general solution of the differential equation, which satisfies the boundary condition along the line $CDEF$ consists of the superposition of all *special* solutions of the equation:

$$\Phi=\sum_{m=o}^{\infty}A_m\left[e^{(2m+1)\frac{\pi y}{L}}-e^{-(2m+1)\left(4\pi+\frac{\pi y}{L}\right)}\right]\cos\left\{(2m+1)\frac{\pi x}{L}\right\}+$$
$$+\sum_{n=1}^{\infty}B_n\left[e^{2n\frac{\pi y}{L}}-e^{-2n\left(4\pi+\frac{\pi y}{L}\right)}\right]\sin\left\{2n\frac{\pi x}{L}\right\}. \tag{15}$$

But it is difficult to determine the values of the constants A_m and B_n. We use, therefore, a numerical method for the computation of an approximate solution of (14*a*).

When the ocean has the same depth as the bay, the problem can be solved in a simple way. The homogeneous field of wind causes a flow of water in the ocean parallel to the coast (which is assumed to be infinitely long !). This current has everywhere the

same velocity, as the field of wind has everywhere the same strength so that the slope, caused by the wind (see paragraph 4) will be also the same everywhere. The total current in the ocean can be represented therefore by equidistant streamlines, parallel to the coast. We assume (see figure 5), that the influence of the bay does extend only to the line *BAHG* (a larger area would not change the results materially and only increase the work of numerical computation). We assume, therefore, that *AH* is the first undisturbed streamline in the sea, and that the deviation of the disturbed streamlines begins between *A* and *B* and ends between *G* and *H*. The value of Φ along *AB* is, therefore, still "undisturbed", that means, changes linearly. In *B*: $\Phi = 0$, which is also true for the line *BCDEFG*. Along *GH* Φ is again a linear function, along *AH* Φ is a constant. In the numerical example which has been computed, Φ had the value 130 along *AH*.

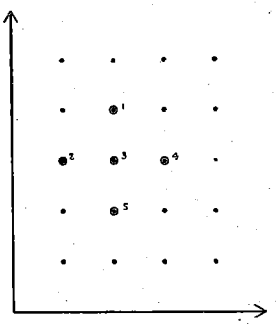

Fig. 6. Lattice for the computation of Φ

In this way the boundary condition is completely established, so that the differential equation can be solved unambiguously. We use a numerical method of computation, the well-known "*method of averaging*" (see e.g. WOLF (64), COURANT (65)). We compute the value of Φ in a set of lattice-points, evenly spaced and covering the whole area, using the theorem, that the value of Φ in a certain point is always the mean of the values of Φ in the neighbouring lattice-points. This is shown in figure 6:

$$\Phi_3 = \tfrac{1}{4}(\Phi_1 + \Phi_2 + \Phi_4 + \Phi_5). \tag{16}$$

This theorem can easily be deduced from the differential equation. When the distance between the lattice-points amounts to h, we have:

$$\Phi_1 = \Phi_3 + \frac{h}{1!}\left[\frac{\partial\Phi}{\partial y}\right]_3 + \frac{h^2}{2!}\left[\frac{\partial^2\Phi}{\partial y^2}\right]_3 + \frac{h^3}{3!}\left[\frac{\partial^3\Phi}{\partial y^3}\right]_3 + \frac{h^4}{4!}\left[\frac{\partial^4\Phi}{\partial y^4}\right]_3 + \cdots\cdots$$

$$\Phi_5 = \Phi_3 - \frac{h}{1!}\left[\frac{\partial\Phi}{\partial y}\right]_3 + \frac{h^2}{2!}\left[\frac{\partial^2\Phi}{\partial y^2}\right]_3 - \frac{h^3}{3!}\left[\frac{\partial^3\Phi}{\partial y^3}\right]_3 + \frac{h^4}{4!}\left[\frac{\partial^4\Phi}{\partial y^4}\right]_3 - \cdots\cdots$$

$$\Phi_2 = \Phi_3 - \frac{h}{1!}\left[\frac{\partial\Phi}{\partial x}\right]_3 + \frac{h^2}{2!}\left[\frac{\partial^2\Phi}{\partial x^2}\right]_3 - \frac{h^3}{3!}\left[\frac{\partial^3\Phi}{\partial x^3}\right]_3 + \frac{h^4}{4!}\left[\frac{\partial^4\Phi}{\partial x^4}\right]_3 - \cdots\cdots$$

$$\Phi_4 = \Phi_3 + \frac{h}{1!}\left[\frac{\partial\Phi}{\partial x}\right]_3 + \frac{h^2}{2!}\left[\frac{\partial^2\Phi}{\partial x^2}\right]_3 + \frac{h^3}{3!}\left[\frac{\partial^3\Phi}{\partial x^3}\right]_3 + \frac{h^4}{4!}\left[\frac{\partial^4\Phi}{\partial x^4}\right]_3 + \cdots\cdots$$

$$\Phi_1 + \Phi_2 + \Phi_3 + \Phi_4 = 4\Phi_3 + h^2\left\{\frac{\partial^2\Phi}{\partial x^2} + \frac{\partial^2\Phi}{\partial y^2}\right\}_3 + \frac{2h^4}{4!}\left\{\frac{\partial^4\Phi}{\partial x^4} + \frac{\partial^4\Phi}{\partial y^4}\right\}_3 + \cdots\cdots$$

But according to the differential equation the second term on the right hand side is zero, so that:

$$\tfrac{1}{4}(\Phi_1 + \Phi_2 + \Phi_3 + \Phi_4) = \Phi_3 + \frac{h^4}{2.4!}\cdot\left\{\frac{\partial^4\Phi}{\partial x^4} + \frac{\partial^4\Phi}{\partial y^4}\right\}_3 + \cdots\cdots$$

If we make h small enough, the terms with h can safely be neglected and equation (16) appears. Now the computation runs as follows: in the lattice-points arbitrary values of Φ are assumed, as a first approximation. In all lattice-points the value of Φ is then successively replaced by the mean value of Φ in the neighbouring points. This operation is repeated until the values of Φ no longer change. We have obtained then, that in each lattice-point Φ has the mean value of Φ in the neighbouring points. In

each lattice-point the differential equation, therefore, is fulfilled. In the figures 7 and 8 the result of the computation is given. The computed values of Φ have been entered in the lattice-points, the streamlines have been drawn and numbered with intervals of 10. The penetrating of the streamlines into the bay, which was to be expected, is clearly visible.

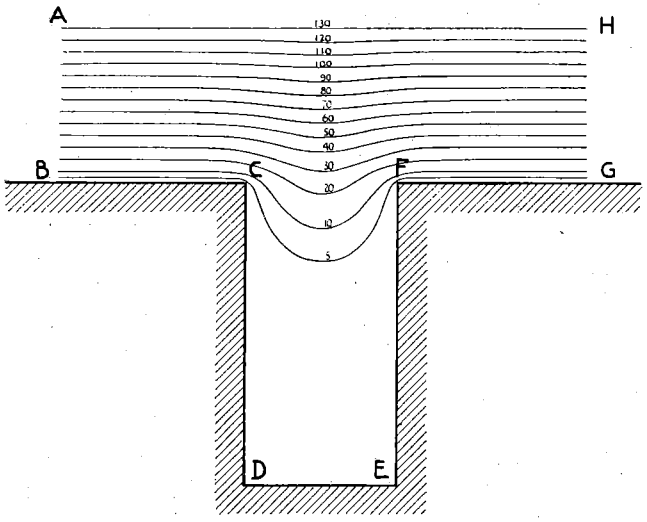

Fig. 7. Streamlines in the North Sea

When we study the values of Φ in figure 8 it appears, that the values in the bay itself can be represented nearly by the simple formula:

$$\Phi_r = 24{,}3\, e^{\frac{\pi y}{L}} \cdot \cos\frac{\pi x}{L}.$$

The values, computed with this formula are also shown in figure 8. Clearly a very satisfactory agreement exists over almost the whole bay. But if we compare Φ_r with formula (15) it turns out immediately, that Φ_r constitutes the first term of the expansion given in (15). We obtain thus the very important result, that we are allowed to neglect all other terms, as the first one gives already a very good approximation of Φ in the bay. Now we confront the result we found with the current which would occur in the bay, if it were closed entirely along the line CF. If Φ must be zero at the coasts and must at the same time satisfy equation (14a) it follows, that we have everywhere:

$$\Phi = 0.$$

This result, viz. that in an enclosed sea of constant depth the current is zero everywhere when the field of wind is homogeneous, has been used already in paragraph 2, in deducing the value of the slope of the surface. In our case one might say, that the Φ, actually found, is a superposition of the Φ for an enclosed sea and the Φ which represents the penetrating of the current from the ocean into the bay. But we can derive very generally the important theorem, that Φ in the North Sea can always be represented as a superposition of two solutions:

$$\Phi = \Phi_i + \Phi_r.$$

In this formula Φ_i is the solution for the sea if it were *enclosed*, and Φ_r is that part of Φ which represents the penetrating of the current from the ocean into the bay. Φ_r is the solution of the *homogeneous* differential equation for the bay, which we obtain from the general equation by putting $W_x = W_y = 0$.

.0 .16 .22 .22 .16 .0	.0 .14½ .23 .23 .14½ .0
.0 .8 .12 .12 .8 .0	.0 .7½ .12 .12 .7½ .0
.0 .4 .6½ .6½ .4 .0	.0 .4 .6½ .6½ .4 .0
.0 .2 .3½ .3½ .2 .0	.0 .2 .3½ .3½ .2 .0
.0 .1 .2 .2 .1 .0	.0 .1 .2 .2 .1 .0
.0 .½ .1 .1 .½ .0	.0 .½ .1 .1 .½ .0
.0 .0 .½ .½ .0 .0	.0 .0 .½ .½ .0 .0
.0 .0 .0 .0 .0 .0	.0 .0 .½ .½ .0 .0
.0 .0 .0 .0 .0 .0	.0 .0 .0 .0 .0 .0
.0 .0 .0 .0 .0 .0	.0 .0 .0 .0 .0 .0
.0 .0 .0 .0 .0 .0	.0 .0 .0 .0 .0 .0
Φ (Computed numerically)	$\Phi_r = 24.3\, e^{\frac{\pi}{5}y} \cos\frac{\pi}{5}x$

Fig. 8. Values of Φ, calculated with two different methods

The proof is simple. In the most general case we have to solve equation (14) with the boundary conditions $\Phi = 0$ along the coasts and the condition that the disturbance caused by the North Sea in the currents in the ocean extends only to a limited distance into the ocean. This leads to fixed values of Φ in the bay: Φ. But we can also solve (14) for the case of an enclosed sea. We obtain then: Φ_i.

Now we consider the difference between Φ and Φ_i, which we call Φ_r:

$$\Phi_r = \Phi - \Phi_i.$$

Then it follows immediately from the theory of linear differential equations that Φ_r is a solution of the *homogeneous* differential equation, which satisfies the condition $\Phi = 0$ along the coasts $CDEF$.

In this way the validity of the theorem is shown. But it is still more important, that Φ_r can always be represented to a very close approximation by the first term of the expansion, which constitutes the general solution of the homogeneous differential equation. This can be shown in an analogous manner as already employed above in the case of a sea with constant depth, etc. We can say, therefore, that this term constitutes the "effect of the opening".

In the case considered above, we had simply:

$$\Phi = \Phi_i + \Phi_r = 0 + \Phi_r = Ae^{\frac{\pi y}{L}} \cos \frac{\pi x}{L}.$$

The value of the constant has been left undetermined, because in our case it has still to be fixed. In our numerical computation we were namely concerned only with the *form* of Φ, not with the *absolute* value of Φ. The windeffect can be derived now from the equations (13):

$$g \frac{\partial \zeta}{\partial x} = \frac{W_x}{\varrho H} + \frac{1}{H} \cdot \frac{\partial \Phi}{\partial x} + \frac{D}{4\pi H^2} \cdot \frac{\partial \Phi}{\partial y}, \quad g \frac{\partial \zeta}{\partial y} = \frac{W_y}{\varrho H} + \frac{1}{H} \cdot \frac{\partial \Phi}{\partial y} - \frac{D}{4\pi H^2} \cdot \frac{\partial \Phi}{\partial x}. \tag{13}$$

The windeffect along a certain path is calculated as follows:

$$\Delta \zeta = \int \left\{ \frac{\partial \zeta}{\partial x} dx + \frac{\partial \zeta}{\partial y} dy \right\} = \int \frac{W_x dx + W_y dy}{g \varrho H} + \int \frac{1}{gH} \left\{ \frac{\partial \Phi}{\partial x} dx + \frac{\partial \Phi}{\partial y} dy \right\} + \frac{1}{4\pi} \int \frac{D}{gH^2} \left\{ \frac{\partial \Phi}{\partial y} dx - \frac{\partial \Phi}{\partial x} dy \right\}.$$

The components of the vector of unit length, indicating the direction of the integration-path, are:

$$\frac{dx}{ds}, \frac{dy}{ds} \quad (ds \text{ is an element of the integration-path}).$$

Hence:

$$W_x dx + W_y dy = W_x \frac{dx}{ds} ds + W_y \frac{dy}{ds} ds = W_s ds.$$

W_s is the component of $\vec{W}$ in the direction of the integration path.

In a analogous way it can be shown that:

$$\frac{\partial \Phi}{\partial y} dx - \frac{\partial \Phi}{\partial x} dy = \frac{\partial \Phi}{\partial n} ds.$$

$\frac{\partial \Phi}{\partial n}$ = gradient of Φ *perpendicular* to the path of integration. Substituting the derived simplifications into the equation for $\Delta\zeta$ we obtain:

$$\Delta \zeta = \int \frac{W_s ds}{g \varrho H} + \int \frac{d\Phi}{gH} + \frac{1}{4\pi} \int \frac{D}{gH^2} \cdot \frac{\partial \Phi}{\partial n} \cdot ds. \tag{17}$$

In order to obtain a condition for the line CF we assume generally, that the height of the sealevel in C and F will not be changed by the wind. In the case of the North Sea we are surely allowed to do that. In C and F holds therefore: $\zeta = 0$. To obtain the height of the sealevel we integrate (17) along the coast.

But along the coast we have everywhere $\Phi = 0$, and therefore $d\Phi = 0$ also. Substituting, we obtain:

$$\zeta = \int \frac{W_s ds}{g\varrho H} + \frac{1}{4\pi} \int \frac{D}{gH^2} \cdot \frac{\partial \Phi}{\partial n} \cdot ds \ .$$

In the general case we have, as shown previously:

$$\Phi = \Phi_i + \Phi_r,$$

where Φ_i is the solution of the *inhomogeneous* equation, solved for the *enclosed* sea, and

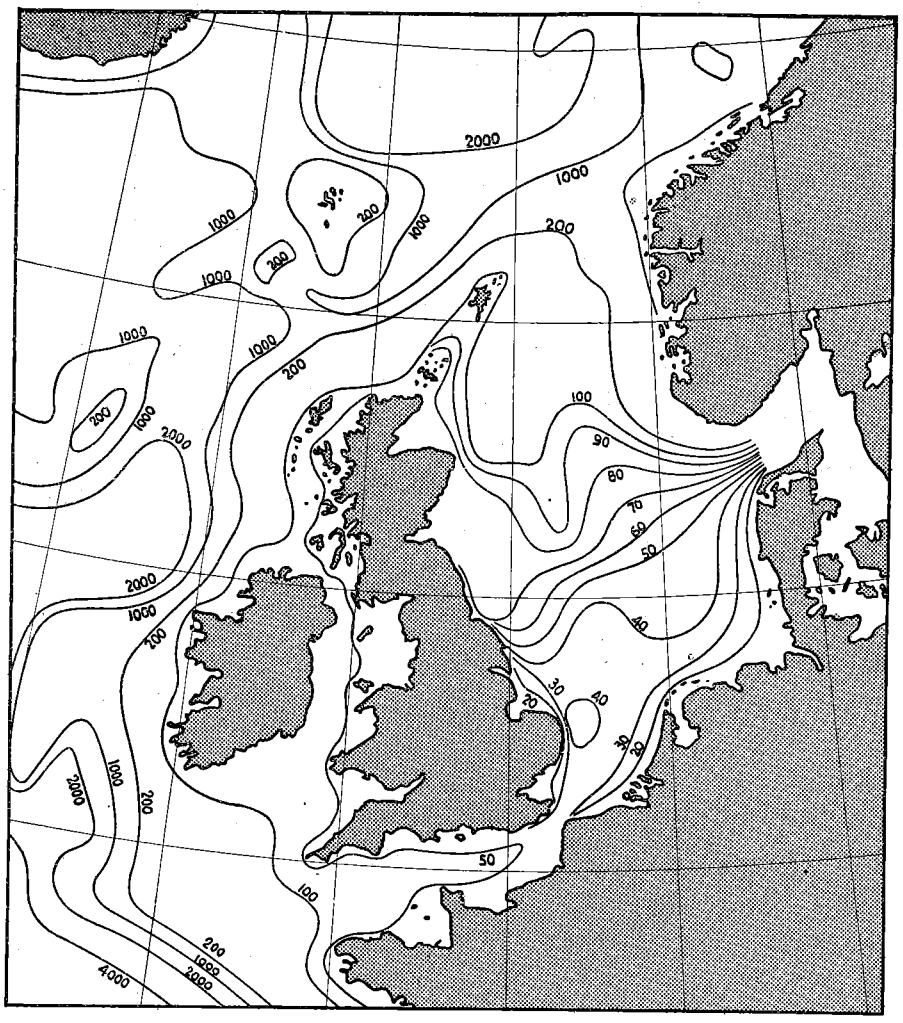

Fig. 9. Depth of the North Sea (in m)

Φ_r is the first term of the expansion constituting the general solution of the *homogeneous* equation, with an as yet arbitrary constant factor. This factor can now be determined by the conditions $\zeta = 0$ in C and F. Integrating (17) along CF:

$$\zeta_F - \zeta_C = 0 = \int_C^F \frac{W_s ds}{g\varrho H} + \int_C^F \frac{1}{gH} \frac{\partial \Phi_i}{\partial x} dx + \int_C^F \frac{1}{gH} \frac{\partial \Phi_r}{\partial x} dx + \frac{1}{4\pi} \int_C^F \frac{D}{gH^2} \frac{\partial \Phi_i}{\partial y} dx + \frac{1}{4\pi} \int_C^F \frac{D}{gH^2} \frac{\partial \Phi_r}{\partial y} dx \ .$$

As Φ_i is fixed completely and only one arbitrary factor occurs in Φ_r, all integrals can be evaluated. In the equation occurs only the still unknown arbitrary factor, which can be solved then from the equation. Then all is known about Φ and the windeffect can be computed.

To evaluate the windeffect for Hook of Holland, we must integrate approximately to the point $x = 0$ on the South coast. Using the method described previously for the computation of the windeffect ζ we obtain finally:

$$\zeta = -\frac{2L W_y}{g\varrho H}.$$

We obtain obviously the result that only the component of the wind along the longitudinal axis of the North Sea influences the sealevel at Hook of Holland. This is very similar to the result of LEVERKINCK (see chapter I, paragraph 2). When it is no longer assumed, that the sea has constant depth, the result is modified. This case is treated sub *b*.

b. Bay with variable depth

In figure (9) the average lines of depth of the North Sea are given. It turns out, that we may assume, that these lines are perpendicular to the longitudinal axis of the Sea. We have, therefore, approximately:

$$\frac{\partial H}{\partial x} = 0, \quad \frac{\partial H}{\partial y} \neq 0.$$

The differential equation obtains a simple form if we assume a linear relation between H and y:

$$H = \tfrac{1}{2} D \left(3 + \frac{y}{L}\right).$$

Hence:

$$\frac{\partial H}{\partial y} = \frac{D}{2L}.$$

Substituting in differential equation (14):

$$\frac{\partial^2 \Phi}{\partial x^2} + \frac{\partial^2 \Phi}{\partial y^2} - \frac{2\pi}{L}\frac{\partial \Phi}{\partial x} = \frac{2\pi}{L} \cdot \frac{W_x}{\varrho}.$$

By numerical computation, analogous to that previously carried out sub *a*, we find that Φ_i can be represented approximately by the formula:

$$\Phi_i = \frac{L W_x}{\varrho} e^{\frac{\pi x}{2L}} \cos\frac{\pi x}{L} \sin\frac{\pi y}{2L}.$$

Φ_r becomes:

$$\Phi_r = A\, e^{\frac{\pi x}{L} + \frac{\pi y \sqrt{2}}{L}} \cos\frac{\pi x}{L}.$$

Hence:

$$\Phi = \Phi_i + \Phi_r = \frac{L W_x}{\varrho} e^{\frac{\pi x}{2L}} \cos\frac{\pi x}{L} \sin\frac{\pi y}{2L} + A\, e^{\frac{\pi x}{L} + \frac{\pi y \sqrt{2}}{L}} \cos\frac{\pi x}{L}.$$

The windeffect at Hook of Holland can be found with the method discussed sub *a*. We obtain:

$$\zeta = \int_C^D \frac{W_y\, dy}{g\varrho H} + 0{,}7 \int_D^{D'} \frac{W_x\, dx}{g\varrho H}.$$

D' is the position of Hook of Holland ($DD' = D'E$) on the line DE. The formula for ζ is derived assuming a linearly changing depth in the North Sea. We assume,

however, that this formula also holds for the actual configuration in the North Sea. Writing H_o for the nearly constant depth of the Southern part of the sea, we obtain:

$$\zeta = -\frac{4}{3} \cdot \frac{L W_y}{g \varrho H_o} + \frac{1}{3} \cdot \frac{L W_x}{g \varrho H_o}.$$

In this formula L is half of the "length" of the North Sea. We put: $L = 450$ km. Introducing the angle ψ between the direction of the wind and the direction of the longitudinal axis of the North Sea, the formula for ζ can be rewritten:

$$\zeta = \frac{1{,}4\, L W}{g \varrho H_o} \cdot \cos(\psi - 15°).$$

W = absolute magnitude of the influence of the wind.

ψ = angle between direction of the wind and direction of the longitudinal axis of the North Sea (positive, if the direction of the wind is West of the direction of the axis of the Sea).

According to the formula the wind has its maximum effect, when the direction of the wind is about 15° West of the axis of the sea. As regards the angular distribution, the cosine-law holds, in agreement with the results of SCHULZ and WITTING.

Analogous to the derivation of formula (10) in paragraph 2, we can introduce the formula of PALMÉN for W. We get:

$$\zeta = 1{,}4\ L \cdot \frac{0{,}032\ V^2 \cos(\psi - 15°)}{H_o}.$$

Introducing: $L = 450$ (km), $H_o = 40$ (m), $V = 20$ (m/sec), $\psi = 15°$, we obtain: $\zeta = 201$ (cm).

From table 3 and figure 1 in Chapter I, however, appears, that the maximum windeffect connected with a windvelocity of 20 m/sec (9 Beaufort) amounts to 150 cm approximately. That is less than the theoretical value. It turns out, therefore, that the windeffect caused by *wind in the North Sea only* is quite sufficient to yield the observed values. Even if the observed value of the windeffect is greater dan 150 cm, no "distant causes" (on the ocean, etc.) need be considered: the windeffect can be explained in terms of the field of wind on the North Sea only.

Now maximum values of the windeffect occur with NW-wind. It will be shown, in the following paragraph, that indeed in this case the wind on the ocean cannot cause an extra windeffect in the North Sea.

In the same way as indicated above, we can calculate the part of the windeffect which is caused in the Southern part of the North Sea (South of the line Dunbar—Skagen, cf. paragraph 5). We obtain approximately: 160 cm ($V = 20$ m/sec !). We see, therefore, that the greatest part of the windeffect is caused in this section of the North Sea. This result will be used later.

4. Influence of the Channel

Until now we have always assumed, that the North Sea is closed at its South end. But we have to investigate still the modification in our results, caused by the Channel. We shall study therefore first the windeffect in an infinitely long channel. We use equation (11) for the current S:

$$lS = \frac{\frac{W}{\varrho} + gH\gamma}{i + \frac{D}{4\pi H}}. \qquad (11)$$

Taking the x-axis parallel to the longitudinal axis of the channel, we can write down the condition for the current in the channel: $S_y = 0$.

Physically it is clear, that the slope of the surface will be directed perpendicularly to the coast. Hence:

$$\gamma_x = 0.$$

Separating equation (11) into real and imaginary parts, we obtain:

$$lS_y = \frac{1}{1 + \frac{D^2}{16\pi^2 H^2}} \cdot \left[\frac{1}{\varrho} \left\{ \frac{D}{4\pi H} \cdot W_y - W_x \right\} - gH \left\{ \gamma_x - \frac{D}{4\pi H} \cdot \gamma_y \right\} \right].$$

Substituting $S_y = 0$ and $\gamma_x = 0$:

$$\gamma_y = \frac{4\pi}{g\varrho D} \cdot \left[W_x - \frac{D}{4\pi H} \cdot W_y \right].$$

In a very deep sea $D << H$ holds. Hence:

$$\gamma_y = \frac{4\pi}{g\varrho D} \cdot W_x.$$

The slope becomes independent of the depth of the sea. The variable value of H is substituted by the constant quantity $1/4\pi\ D$.

Moreover it turns out, that only the component of the wind *parallel to the coast* causes the windeffect. This is an important result. For the windeffect on the western coast of Europe by wind on the ocean can acquire an appreciable value only when the wind is parallel to this coast, viz. a South-Westerly wind. A North-Westerly wind has no influence at all. And this is generally the direction of the wind when a storm surge occurs. We arrive, therefore, at the conclusion, that in general *no* additional windeffect is caused by the wind on the ocean, when a storm surge occurs. This result is quite different from GALLÉ's result (6), who assumed that part of the windeffect of the storm surges was caused by the action of the wind on the ocean. Our conclusions are also in perfect agreement with our previous result (paragraph 2), that differences in the value of the windeffect in the North Sea can be attributed wholly to differences in the field of wind on the North Sea itself. We arrive, therefore, at the very important conclusion, that in the working up of the material it is not necessary to take into account the wind on the ocean. Only the wind on the North Sea, and eventually also in the Channel need be considered.

Now we return to the windeffect in the Channel. The depth of this part of the sea is much smaller. We put:

$$D = 2H$$

Substituting this, we get:

$$\gamma_y = \frac{2\pi}{g\varrho H} \cdot \left[W_x - \frac{1}{2\pi} W_y \right].$$

If we introduce here also the angle between the direction of the wind and the axis of the Channel (positive, when the direction of the wind lies in the 1st or 2nd quadrant), and also the absolute value W of the influence of the wind, we obtain:

$$\gamma_y = \frac{2\pi}{g\varrho H} W \cos(\psi - 9°).$$

In this case, too, the sealevel is chiefly influenced by the component parallel to the coast. It follows, that a maximum windeffect is caused in the Channel by a WSW-wind.

The evaluation of the windeffect is rather difficult, as we do not know exactly the "effective width" of the Channel. If we assume, however, that the opening near Calais can be taken as "effective width", we should obtain a value of 30 km. In this evaluation it must be taken into account, that the windeffect must be considered relatively to the *middle* of the Channel, so that the distance over which the windeffect is caused, amounts to only 15 km. Introducing L and H_o of the formula of paragraph 3, we get:

$$\zeta = 0{,}2 \,.\, \frac{LW}{g\varrho H_o} \,.\, \cos(\psi - 9°) \,.$$

When we compare this with the formula of the windeffect in the North Sea:

$$\zeta = 1{,}4 \,.\, \frac{LW}{g\varrho H_o} \,.\, \cos(\psi - 15°),$$

it turns out, that the effect of the Channel is much smaller than the effect of the North Sea. The Channel can, therefore, be considered as a basin with nearly constant height of the sealevel. This basin influences the windeffect in the North Sea: as the water flows away to this basin a *levelling* of the sea surface is caused, which results in a decrease of the windeffect. As we are allowed to assume, that this decrease is proportional to the windeffect itself, we obtain instead of the previous formula the following one:

$$\zeta = k \,.\, 1{,}4 \,.\, \frac{LW}{g\varrho H_o} \,.\, \cos(\psi - 15°),\ 0 < k < 1.$$

In this equation k is a constant, denoting the "decreasing influence" of the Channel. It can be shown, that the value of k is not much less than 1, for example 0,8 or there about. But these estimates are very arbitrary.

As the effect of the Channel is much smaller than the effect of the North Sea, it will simply be superposed upon the effect of the North Sea. If we try to combine the two effects in one formula, it is essential that the direction of the wind in both places be taken with reference to the same fundamental direction. *We take the direction due West as the fundamental one.* The formula for the windeffects have then to be modified a little. It was measured in the North Sea with reference to the longitudinal axis of the North Sea, which makes an angle of about 70° with the direction due West. And ψ was measured in the Channel with reference to the direction of the axis of the Channel, which we assume to be $-40°$ ($= W\,40°\,S$!). Taking this into account and representing the direction and influence of the wind in the Channel by ψ_1 and W_1 respectively, and of the wind in the North Sea by ψ_2 and W_2, we obtain finally:

$$\zeta = 0{,}2 \,.\, \frac{LW_1}{g\varrho H_o} \,.\, \cos(\psi_1 + 30°) + k \,.\, 1{,}4 \,.\, \frac{LW_2}{g\varrho H_o} \,.\, \cos(\psi_2 - 55°).$$

5. Effect of an inhomogeneous field of wind

Until now we have treated in our investigations only homogeneous fields of wind. But it is quite possible, that the field of wind is *not* homogeneous. In this case the direction and the force of the wind vary so strongly on the North Sea, that they can not be replaced by their mean value. If the isobars are only slightly curved, we are still allowed to treat the field of wind as homogeneous, provided we consider only part of the North Sea, for example the Southern part of it. We derived previously (paragraph 3), that in this section of the sea is caused the greater part of the windeffect.

This section is indicated in figure 10 by the number II. The other sections, which we take into account, are also indicated in figure 10, numbered I and III. In accordance

with the results of our previous investigations, we try to represent the data obtained in actual storm surges by the equation:

$$\zeta = A_1 V_1^2 \cos(\psi_1 - \varepsilon_1) + A_2 V_2^2 \cos(\psi_2 - \varepsilon_2) + A_3 V_3^2 \cos(\psi_3 - \varepsilon_3).$$

$A_1\, A_2\, A_3$ = constants, valid in the three "windsections".
$\psi_1,\ \psi_2,\ \psi_3$ = mean direction of the wind in the three sections I, II and III respectively.
$\varepsilon_1,\ \varepsilon_2,\ \varepsilon_3$ = directions of maximum influence in the three sections.
$V_1,\ V_2,\ V_3$ = velocity of the wind in the three sections.

With this formula most cases can be described. But it is possible, that a depression has its centre above the North Sea. Then the field of wind is inhomogeneous even in the indicated smaller sections of the sea. This case must therefore be treated separately. We assume again, just as in paragraph 3:

$$H = \tfrac{1}{2} D \left(3 + \frac{y}{L}\right).$$

But we are no longer allowed to assume, that W_x and W_y are constants. In this case the differential equation becomes:

$$\frac{\partial^2 \Phi}{\partial x^2} + \frac{\partial^2 \Phi}{\partial y^2} - \frac{2\pi}{L}\frac{\partial \Phi}{\partial x} - \frac{D}{HL}\frac{\partial \Phi}{\partial y} =$$

$$= \frac{4\pi}{\varrho} \cdot \left[\frac{W_x}{2L} + \frac{1}{2}\left(3 + \frac{y}{L}\right)\left(\frac{\partial W_y}{\partial x} - \frac{\partial W_x}{\partial y}\right)\right].$$

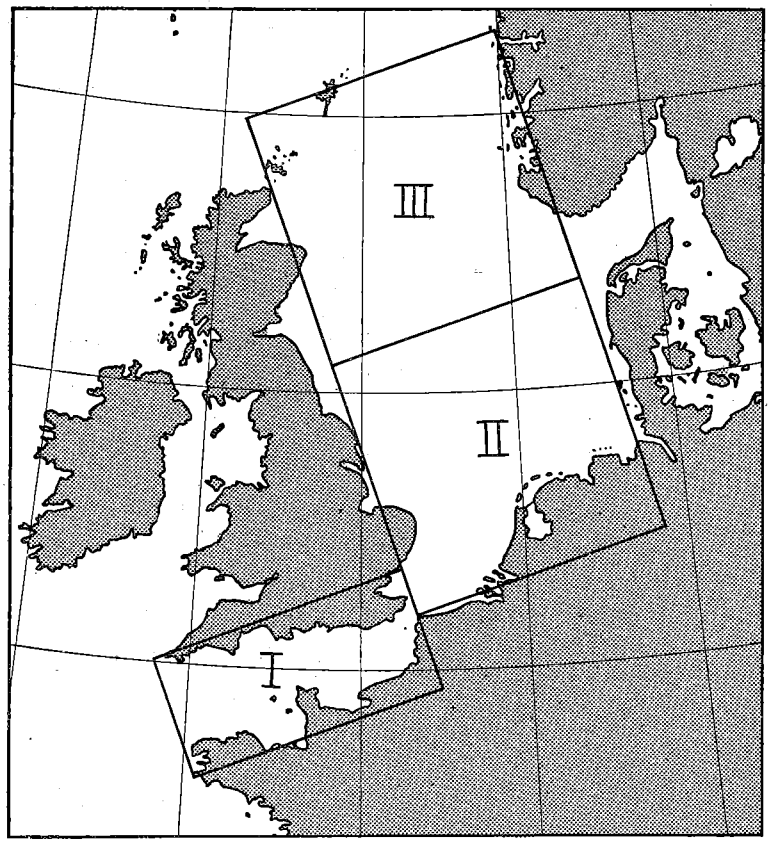

Fig. 10. The "windsections" of the North Sea

The right hand side of the equation takes a simpler form, if we assume, that the depression has a circular form, that the wind blows parallel to the isobars and that we are allowed to write for $|W|$:

$$|W| = r \frac{W_0}{L},$$

r = distance from the centre of the depression,
W_0 = value of $|W|$ at the distance L from the centre.

Substituting the formula for $|W|$ we obtain:

$$\frac{\partial W_y}{\partial x} - \frac{\partial W_x}{\partial y} = \frac{2W_o}{L}.$$

When we consider the first term on the right hand side of the differential equation, it turns out, that in practice the *average* value of this term will be small compared with the second term. For that reason the first term is neglected. Neglecting also the term with $\partial\Phi/\partial y$ on the left hand side, we obtain finally:

$$\frac{\partial^2 \Phi}{\partial x^2} + \frac{\partial^2 \Phi}{\partial y^2} - \frac{2\pi}{L} \cdot \frac{\partial \Phi}{\partial x} = \frac{4\pi W_o}{\varrho L} \cdot \left(3 + \frac{y}{L}\right).$$

In accordance with the methods, developed in paragraph 2, we evaluate Φ as a superposition of Φ_i and Φ_r, Φ_i being the solution of the inhomogeneous equation in the case

of an enclosed sea, and Φ_r being the solution of the homogeneous equation, which has the same form as in paragraph 3. The computation is quite analogous to the computations in paragraph 2 and paragraph 3, so that only the final result is given here:

$$\zeta = \int \frac{W_s\, ds}{g\varrho H} - 0{,}2 \oint \frac{W_s\, ds}{g\varrho H}.$$

The second term is the "circular integral" round the whole North Sea. The value of this integral is certainly > 0, as in the case of a depression on the North Sea we have always: $W_s > 0$. The first integration must be performed along the line CDE (see figure 5).

The windeffect is to a first approximation again represented by the simple formula $\int \frac{W_s\, ds}{g\varrho H}$. It is true, that the second term decreases the value of the windeffect, but the influence of this term is much smaller than the influence of the first term. ζ is, therefore, mainly represented by the first term.

If we consider a circular depression with a constant gradient, we are able to calculate the velocity of the wind at any distance from the centre (see Chapter III,

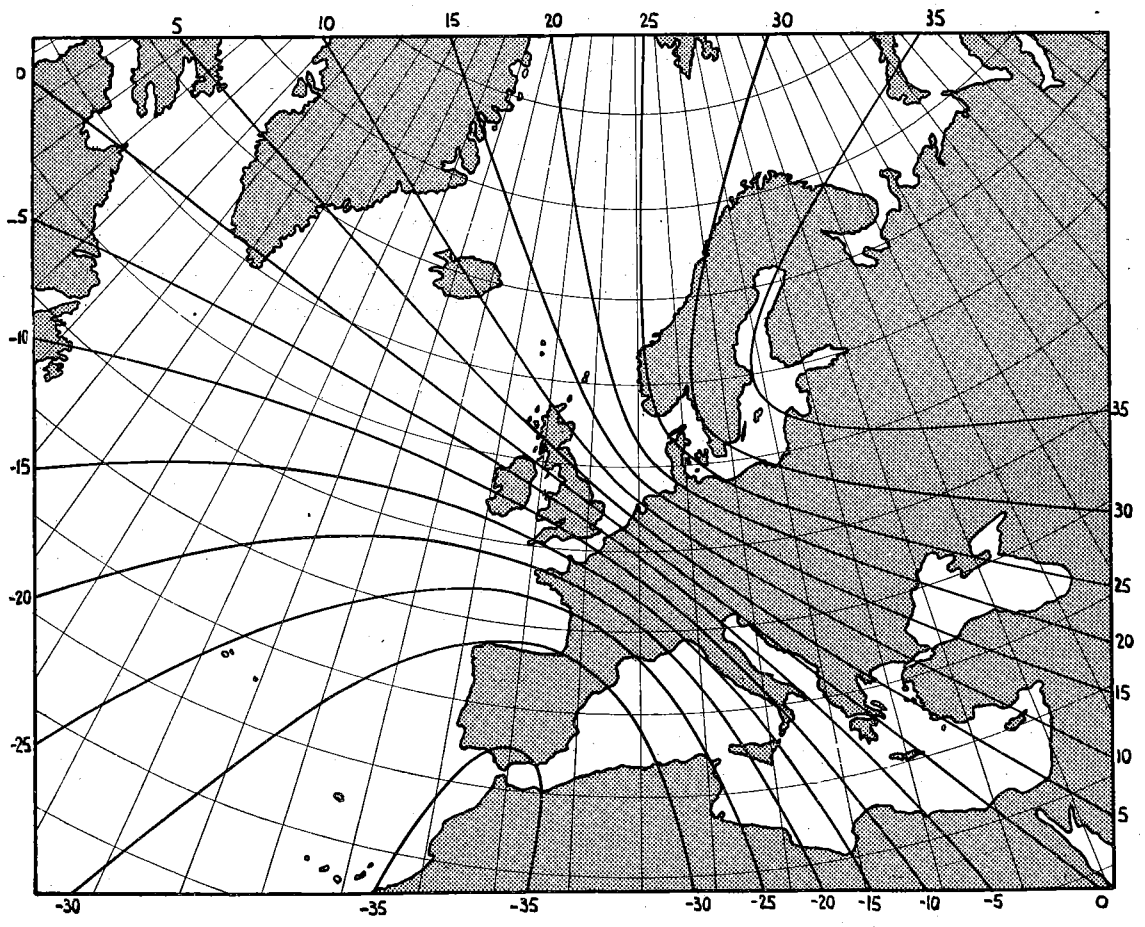

Fig. 11. Windeffect caused by depressions in different positions

paragraph 2). When we know V we also know V^2, and it is then possible to calculate the value of $\int \frac{W_s\, ds}{g\varrho H}$ for any position of the centre. The result of this computation is given in figure 11. The windeffect has been calculated in cm, assuming a constant gradient in the depression of 10 mb/500 km. This has been done for all positions of the centre indicated on the chart. We have entered in the chart the values of the windeffect and

drawn isopleths with intervals of 5 cm. The result is shown in the figure. This must be compared with practice. But the following should be borne in mind: in computing figure 11, we have used already the results of chapter IV for the homogeneous fields of wind. We studied namely these cases first and of course it is clear, that the isobars will become nearly straight on the North Sea, when the centre of the depression is situated far from the North Sea. In these cases the windeffect on the coast can be calculated immediately with the formula, resulting from the investigation of the homogeneous fields of wind. In this way the "asymptotical directions" of the isopleths have been found.

6. Nonstationery state

In the preceding paragraphs we have studied the stationary states of the sea. But in practice the sea is practically never in a stationary state, when a storm surge occurs. On that account the phenomena connected with inertia have to be investigated, for it is our purpose to reduce all states to stationary ones, as the simple formulas, derived in the preceding paragraphs, only hold for the state of equilibrium.

In order to investigate the non-stationary states the differential equations involving the time have to be used. In these considerations, just as in the case of paragraphs 2, 3, 4 and 5, we want the formula for the *total* current, because only for the total current the equation of continuity takes the simple form:

$$\frac{\partial S_x}{\partial x} + \frac{\partial S_y}{\partial y} = -\frac{\partial \zeta}{\partial t}.$$

The fundamental equations of motion, however, hold for the velocities of the *individual* waterparticles. To obtain equations of the form we need, an artifice has to be used. We write the fundamental equations in complex form (cf. paragraph 1):

$$\varrho \frac{\partial w}{dt} = \frac{\partial}{\partial z}\left(\mu \frac{\partial w}{\partial z}\right) - il\varrho w + g\varrho\gamma.$$

Integrating with respect to z from 0 to H:

$$\varrho \int_0^H \frac{\partial w}{\partial t}\, dz = \int_0^H \frac{\partial}{\partial z}\left(\mu \frac{\partial w}{\partial z}\right) dz - il\varrho \int_0^H w dz + g\varrho\gamma \int_0^H dz.$$

Substituting

$$S = \int_0^H w dz.$$

$$\varrho \frac{\partial S}{\partial t} = \left(\mu \frac{\partial w}{\partial z}\right)_H - \left(\mu \frac{\partial w}{\partial z}\right)_0 - il\varrho S + g\varrho\, \gamma H.$$

But the boundary condition at the surface was:

$$-\mu\left(\frac{\partial w}{\partial z}\right)_0 = W.$$

Hence:

$$\varrho \frac{\partial S}{\partial t} = \left(\mu \frac{\partial w}{\partial z}\right)_H + W - il\varrho S + g\varrho\gamma H.$$

The term $\left(\mu \frac{\partial w}{\partial z}\right)_H$ represents the frictional force along the bottom. For this force we had also a condition, in which however, proportionality with the velocity at the

bottom was assumed. And in our new equations only the *total* current S occurs. We must therefore replace this term by another expression. To this end we again use the stationary state. For this state we have:

$$\frac{\partial S}{\partial t} = 0.$$

Substituting, we obtain a relation for S:

$$0 = \left(\mu \frac{\partial w}{\partial z}\right)_H + W - il\varrho S + g\varrho\gamma H.$$

But in paragraph 2 we obtained:

$$lS = \frac{\frac{W}{\varrho} + gH\gamma}{i + \frac{1}{4h}},$$

or, rewritten:

$$0 = -il\varrho S - \frac{\varrho lS}{4h} + W + g\varrho\gamma H.$$

This equation is nearly identical with the first equation for S. But both equations refer to the same thing, viz. the relation between the total current and the external forces, acting on the water in the stationary state. They must, therefore, be *exactly* identical. Hence:

$$\left(\mu \frac{\partial w}{\partial z}\right)_H = -\frac{\varrho lS}{4h}.$$

And the equation for $\partial S/\partial t$ becomes after some rearranging:

$$\frac{\partial S}{\partial t} = -l\left(iS + \frac{S}{4h}\right) + \frac{W}{\varrho} + g\gamma H.$$

With the aid of this equation of motion we shall investigate the oscillations caused by: *a*) suddenly, and *b*) gradually varying fields of wind.

a. Suddenly varying field of wind

As a first approximation we neglect the force of Coriolis. In the case of the North Sea this is certainly allowed. We replace the North Sea by a channel, which is closed at one end (in $x = 0$). In this channel only motions parallel to the axis of the channel occur. The equation of motion reads:

$$\frac{\partial S}{\partial t} = -\frac{lS}{4h} + \frac{W}{\varrho} + gH\gamma.$$

As γ will not remain constant, we introduce again:

$$\gamma = -\frac{\partial \zeta}{\partial x}.$$

Substituting:

$$\frac{\partial S}{\partial t} = -\frac{lS}{4h} + \frac{W}{\varrho} - gH\frac{\partial \zeta}{\partial x}.$$

The equation of continuity becomes (neglecting the transversal motions):

$$\frac{\partial S}{\partial x} = -\frac{\partial \zeta}{\partial t}.$$

The boundary conditions become:

$$x = 0 : S = 0.$$

$$x = 2L : \zeta = 0.$$

In order to determine the motion completely, the initial condition has to be added. In the beginning the whole sea is in its normal state. Hence, we have everywhere:

$$t = 0 : S = 0, \ \zeta = 0.$$

In order to be able to integrate the equations of motion we first eliminate the term W/ϱ. This term does not depend on the time: at the time $t = 0$ the "wind" suddenly takes the value W but remains constant thereafter. Substituting:

$$\zeta = \zeta' + (x - 2L) \cdot \frac{L}{g\varrho H},$$

we obtain:

$$\frac{\partial S}{\partial t} = -\frac{lS}{4h} - gH\frac{\partial \zeta'}{\partial x}, \qquad \frac{\partial S}{\partial x} = -\frac{\partial \zeta'}{\partial t}.$$

The initial condition for ζ' is:

$$\zeta' = -(x - 2L) \cdot \frac{W}{g\varrho H}.$$

The other conditions remain the same.

By numerical computation it was shown, that a satisfactory approximation to reality was obtained by substituting:

$$\zeta' = e^{-\frac{lt}{8h}} \cdot \zeta''. \qquad S = e^{-\frac{lt}{8h}} \cdot S'.$$

ζ'' and S' satisfy the equations:

$$\frac{\partial S'}{\partial t} = -gH\frac{\partial \zeta''}{\partial x}, \tag{18}$$

$$\frac{\partial S'}{\partial x} = -\frac{\partial \zeta''}{\partial t}. \tag{19}$$

Boundary conditions and initial conditions remain again the same:

$$x = 0 : S' = 0.$$

$$x = 2L : \zeta'' = 0.$$

$$t = 0 : S' = 0, \ \zeta'' = -(x - 2L) \cdot \frac{W}{g\varrho H}.$$

Equations (18) and (19) are the well-known equations of motion, describing the propagation of a disturbance in all sorts of media. In our case the solving of the equations necessitate the definition of the function $F(x)$, which is represented graphically in figure 12. AB represents the surface of the water in the undisturbed state. $A'B$ is the initial position of ζ''. The line $A'B$ has to be extended in the way, indicated in figure 12. This "curve" constitutes the function $F(x)$ we want. This function satisfies the conditions:

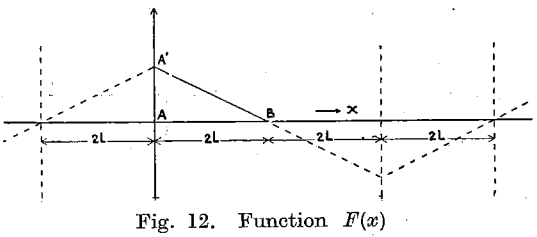

Fig. 12. Function $F(x)$

$$F(x) = F(-x),$$

$$F(x) = -F(4L - x).$$

ζ'' and S' are represented by the following formula, which can easily be verified:

$$S' = -c/2\,[F(x-ct) - F(x+ct)],$$

$$\zeta'' = -\tfrac{1}{2}\,[F(x-ct) + F(x+ct)],$$

$$c = \sqrt{gH}.$$

Substituting the equations for ζ' and ζ we obtain finally:

$$\zeta = (x-2L)\cdot\frac{W}{g\varrho H} - \tfrac{1}{2}\,e^{-\frac{lt}{8h}}\cdot[F(x-ct) + F(x+ct)].$$

We are chiefly interested in the value of ζ for $x = 0$. Substituting in the equation for ζ: $x = 0$, and taking into account:

$$F(x) = F(-x),$$

we obtain:

$$\zeta = -\frac{2LW}{g\varrho H} - e^{-\frac{lt}{8h}}\cdot F(ct), \tag{20}$$

$$F(0) = \frac{2LW}{g\varrho H}.$$

Oscillations are thereby found to occur indeed. For $F(x)$ is a periodical function, and so, therefore, is $F(ct)$. Formula (20) may be interpreted in the following way: neglecting the exponential factor ζ behaves, as if the "waves" represented by the function $F(x)$ (cf. figure 12 !) were propagated towards the coast with the velocity c. This result is important.

The period of the oscillation follows from the equation (cf. figure 12):

$$cT = 8\,L,$$

hence:

$$T = \frac{8L}{c}.$$

Assuming, that the windeffect is caused only in the Southern part of the North Sea (section II, cf. figure 10), we should obtain:

$$T = 28 \text{ (hours)}.$$

This is a period of approximately one day. The maximum value of the windeffect, however, is reached after $^1/_4\,T$, or 7 hours. This would be in agreement with the result of Ortt. Schulz (cf. Chapter I, paragraph 2), however, found a much smaller "time-lag" (3 hours). This is explained sub *b*. Considering the windeffect in the whole sea, the value of T can no longer be calculated with the simple formula given above, as the depth in the whole sea changes considerably. Assuming , that the average depth of section III (cf. figure 10) amounts to 160 m, we calculate the time in which a disturbance is propagated from the Southern end to the Northern end of the Sea. We find: 10 hours. According to this result the period of a full oscillation would amount to 40 hours. From the actually observed period we can therefore derive, which part of the sea is partaking in the oscillation. This result will be used in Chapter V.

But the extinction-factor is also important. It has the form:

$$e^{-\frac{lt}{8h}}.$$

Considering first the southern part of the North Sea only, we obtain approximately:

$$\frac{l}{8h} = \frac{lD}{8\pi H} = 10^{-5}.$$

This means, that the amplitude of the oscillation is reduced to the fraction $1/e$ of its original value after 10^5 seconds, i. e. nearly one day. This rate of extinction only holds for a storm. Otherwise the rate of extinction is much smaller, as the value of D decreases with decreasing velocity of the wind (cf. PALMÉN, 44).

The rate of extinction is also modified a little, if we also take the Northern part of the Sea into account. We calculate this in the following way. It was shown previously, that the changes in the level of the Sea could be interpreted as the propagating of disturbances of the surface of the Sea. We calculate therefore the decrease of the amplitude of a disturbance after having been propagated around the whole Sea. We assume that section II and section III of the Sea (cf. figure 10) both have the length L, and moreover, that in section II the depth of the Sea is H_0 and in section III: $4\,H_0$. If the velocity of propagation in section II is c, it is $2c$ in section III ($c_{III} = \sqrt{gH} = \sqrt{4gH_0} = 2\sqrt{gH_0} = 2c$). In T seconds the disturbance has traversed section II. We have:

$$L = cT.$$

Then section III is traversed in $\frac{1}{2}T$ seconds.

After traversing section II the amplitude of the disturbance is reduced by a factor: $e^{-\frac{lTD}{8\pi H_0}}$. Then it traverses section III, in which its amplitude is reduced again, this time by the factor $e^{-\frac{lTD}{64\pi H_0}}$.

If the original value of the amplitude is A_0, and its final value A, we have consequently:

$$A = A_0 \cdot e^{-\frac{lTD}{8\pi H_0}} \cdot e^{-\frac{lTD}{64\pi H_0}} = A_0 e^{-\frac{lTD}{\pi H_0}\left(\frac{1}{8}+\frac{1}{64}\right)}.$$

We try to bring this into the form:

$$A = A_0 e^{-\alpha \cdot \frac{ltD}{8\pi H_0}}$$

For the time t in the last formula the total time required to traverse the two sections must be substituted, hence:

$$t = T + \tfrac{1}{2}T = 1\tfrac{1}{2}T.$$

Equating the exponents of both powers of e, we obtain:

$$\alpha = {}^3/_4.$$

The rate of extinction of the travelling disturbances is in this case, therefore, not proportional to $e^{-\frac{ltD}{8\pi H}}$, but to $e^{-\frac{3}{4}\frac{ltD}{8\pi H}}$. The difference is only small. To a fair approximation it is allowed, therefore, to take only the extinction caused in the southern part of the North Sea into account, as the order of magnitude of the rate of extinction can only be estimated.

In all the preceding calculations the force of Coriolis has been neglected. It is possible, however, to take this force into account by numerical computation. The results obtained previously remain mainly the same. Only transverse currents occur, which results in a transformation of the "oscillation" of the North Sea into a wave, swinging around

the sea from right to left, just as in the case of tidal waves. This phenomenon may be explained qualitatively in the following way. When a North-Westerly wind suddenly starts, the water will accumulate in the southern part of the sea. This is accompanied by a current towards this southern part. But the force of Coriolis, acting on this current, causes a deflection to the right, which results in an accumulation of water against the Eastern coast of England. The maximum of this effect is reached *before* the maximum effect on the South coast of the North Sea occurs. When the water swings back, a heaping up of the water against the Eastern coasts of the North Sea is caused in the same way. Thus a kind of wave is generated, which swings around the North Sea from right to left, in the same sense as a tidal wave. This was found also by DOODSON (20).

An other consequence of the influence of the force of Coriolis is, that the oscillations are slowed down a little. TAYLOR (66) has numerically solved an analogous problem. He found, that in the case of a basin like the North Sea the proper period of the basin was increased, but only by 10—20 %. Bearing this in mind, it was therefore surely allowed to neglect the rotation of the earth in our more or less approximate considerations.

b. Gradually varying fields of wind

When the wind does not vary suddenly but gradually, the development of the wind-effect may be calculated using the results of section *a*. We start from the formula:

$$\zeta = -\frac{2LW}{g\varrho H_o} - e^{-\frac{lt}{8h}} \cdot F(ct) .$$

We have shown (cf. *a*), that $F(t)$ is a periodical function. But the actual form of $F(t)$ is not suitable for computations. For that reason we substitute $F(t)$ by a cosine-function. If the period of the oscillation is T, we assume:

$$F(ct) = -\frac{2LW}{g\varrho H_o} \cdot \cos\frac{2\pi t}{T} .$$

We put also:

$$\frac{l}{8h} = \frac{\beta}{T} .$$

Hence:

$$\zeta = -\frac{2LW}{g\varrho H_o} \cdot \left[1 - e^{-\beta \cdot \frac{t}{T}} \cdot \cos\frac{2\pi t}{T}\right] .$$

Finally we substitute:

$$-\frac{2LW}{g\varrho H_o} = \zeta_o .$$

ζ_o is the stationary value of ζ ultimately reached. Substituting, the equation becomes:

$$\zeta = \zeta_o \cdot \left[1 - e^{-\beta \cdot \frac{t}{T}} \cdot \cos\frac{2\pi t}{T}\right] .$$

This formula is generalized in the case of non-stationary fields of winds (PROUDMAN, HORROCKS, NOMITSU). The method we use is based upon the linear form of all differential equations and other conditions used in the computation. We only assume, that the period of the oscillations of the Sea is independent of the variations of the field of wind.

The fact that the field of wind changes with time may be formulated in this way, that ζ_o is no longer a constant, but a function of time. For, generally, with every state of the field of wind an other value of ζ_o is connected. Now as all equations are linear,

it is immediately clear, that all *fluctuations* in the windfield cause corresponding *fluctuations* of ζ_o, which are simply superposed upon the motion and the state of the surface already present. If at the time τ we superpose a variation $d\zeta_o$ on ζ_o, a $d\zeta$ will be superposed upon the ζ already present, for which the equation holds:

$$d\zeta = d\zeta_o \cdot \left[1 - e^{-\frac{\beta (t-\tau)}{T}} \cdot \cos \frac{2\pi (t-\tau)}{T} \right].$$

But for $d\zeta_o$ we can write:

$$d\zeta_o = \left(\frac{d\zeta_o}{dt}\right)_{t=\tau} d\tau.$$

Hence:

$$d\zeta = \left(\frac{d\zeta_o}{dt}\right)_{t=\tau} \left[1 - e^{-\frac{\beta (t-\tau)}{T}} \cdot \cos \frac{2\pi (t-\tau)}{T} \right] d\tau .$$

All fluctuations in ζ, caused by fluctuations of the field of wind after $t = 0$, are simply superposed. We obtain:

$$\zeta = \int_0^t d\zeta = \int_0^t \left(\frac{d\zeta_o}{dt}\right)_{t=\tau} \cdot \left[1 - e^{-\frac{\beta (t-\tau)}{T}} \cdot \cos \frac{2\pi (t-\tau)}{T} \right] d\tau .$$

Using this formula the effect of changes in the field of wind are easily calculated. Special cases will now be considered. As a first case we take:

$$\zeta_o = A \sin \omega t.$$

This is the case of the development of a storm: the wind increases, which corresponds with an increase in the height of the level of the sea, which is in "equilibrium" with the wind. After reaching a maximum the wind decreases again. Most storms show this development. Only rarely the wind remains at its maximum for one or two days on end. And even in this case ζ_o may show a marked maximum as well, because probably the direction of the wind will change during the storm, which causes also variations in ζ_o. We obtain the following equation for ζ:

$$\zeta = \int_0^t A\omega \cos \omega\tau \cdot \left[1 - e^{-\frac{\beta (t-\tau)}{T}} \cdot \cos \frac{2\pi (t-\tau)}{T} \right] d\tau =$$

$$= A \sin \omega t - \omega T A \cdot \left[\beta a_o \cos \omega t + \omega T a_1 \sin \omega t - e^{-\frac{\beta . t}{T}} \left\{ \beta a_o \cos \frac{2\pi t}{T} + 2\pi a_2 \sin \frac{2\pi t}{T} \right\} \right].$$

$$a_o = \frac{\beta^2 + 4\pi^2 + \omega^2 T^2}{(\beta^2 + 4\pi^2 + \omega^2 T^2)^2 - (4\pi\omega T)^2}.$$

$$a_1 = \frac{\beta^2 - 4\pi^2 + \omega^2 T^2}{(\beta^2 + 4\pi^2 + \omega^2 T^2)^2 - (4\pi\omega T)^2}.$$

$$a_2 = \frac{-\beta^2 - 4\pi^2 + \omega^2 T^2}{(\beta^2 + 4\pi^2 + \omega^2 T^2)^2 - (4\pi\omega T)^2}.$$

Three cases are considered:

1. $\omega << 2\pi/T.$

In this case the wind varies slowly compared with the characteristic period of the Sea. We obtain approximately:

$$\zeta = A \sin \omega t.$$

As might be expected, the sea has evidently the opportunity to adjust itself at every moment in accordance with the wind, being permanently in the stationary state.

2. $\omega = 2\pi/T.$

The wind varies with the same period as the characteristic period of the sea (resonance). We obtain approximately:

$$\zeta = A\left[\tfrac{3}{4}\sin\omega t - \frac{\pi}{\beta}\cos\omega t + e^{-\beta\cdot\frac{t}{T}}\cdot\left\{\frac{\pi}{\beta}\cos\omega t - \tfrac{1}{4}\sin\omega t\right\}\right].$$

Evidently the phase of the sea differs from the phase of the wind. For further comments we must know the value of β. We have:

$$\beta = \frac{l}{8h}\cdot T.$$

Both $8h/l$ and T are of the order of magnitude of one day (cf. *a*). Hence:

$$\beta \approx 1.$$

The factor of $\cos\omega t$ in the equation for ζ becomes π. It appears, therefore, that the phase of ζ is changed nearly 90°. The amplitude is much greater than the amplitude of the "equilibrium value". This effect occurs sometimes in practice.

3. $\omega >> 2\pi/T.$

The wind is varying rapidly, which is the case in a very gusty wind. We obtain approximately:

$$\zeta = 0.$$

The sea is not influenced by the fluctuations of the wind. This is important. For we find here, that in working out the material we must use only the mean value of the wind during periods comparable with the characteristic period of the sea.

In practice we have in most cases approximately:

$$\omega = \frac{\pi}{T}.$$

The case:

$$\omega = \frac{\pi}{T}, \quad \beta \approx 1,$$

is, therefore, evaluated completely. The result is shown in figure 13, in the same way as in figure 3. The line A shows the function $A \sin \omega t$. It is assumed that the wind after decreasing again to zero remains zero. The line B represents the fluctuations of the sea caused by the storm. The oscillations, occurring after the wind has ceased, are clearly visible.

In figure 14 analogous curves are shown. Only the curve A has a somewhat different form, and the calculations have been performed with an other value of $\beta(\beta = 2)$. In its general features this figure is very similar to figure 13. But attention should be drawn to the following feature of these curves: when the sea has attained its maximum rising-velocity the curves A and B are nearly parallel. The same is true, but in a less pronounced manner, for the falling part of the curves. In these parts we obtain curve B by shifting curve A to the right over a certain distance: the "time-lag" $\triangle t$. The

value of $\triangle t$ for the rising part of the curves differs from the value for the sinking parts. We shall try to verify all these results in the working out of the material. But to do that we want the curve A in the practical cases. This line is found, however, by comparison with figure 13. For in this figure also a curve C has been drawn which is

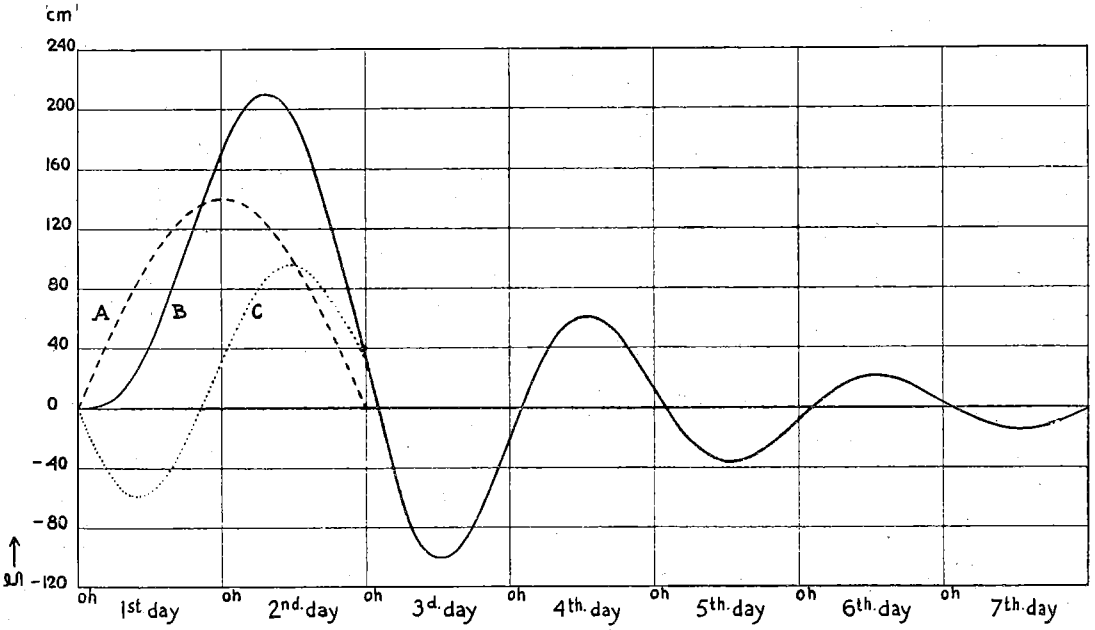

Fig. 13. Fluctuations caused by a gradually varying field of wind (storm surge)

obtained by subtracting curve A from curve B. The curve is practically symmetrical with respect to the point $t = T$. But from our material we can only deduce the line B. Now C is found approximately by reflecting the part of curve B after the storm has

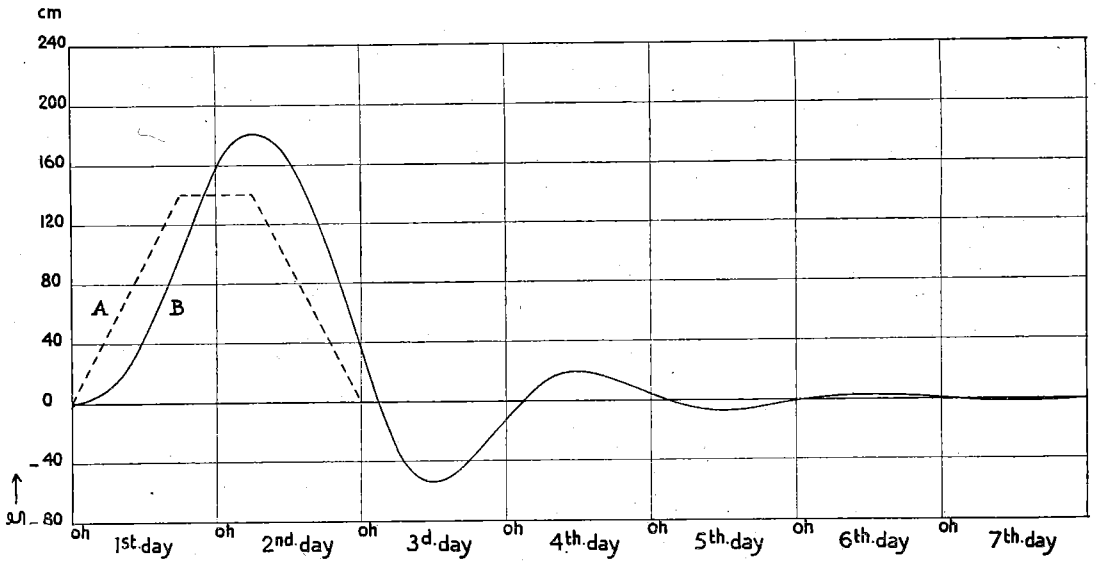

Fig. 14. Fluctuations caused by a gradually varying field of wind (storm surge)

ceased in the point $t = T$. Subtracting this curve from B we obtain approximately curve A, which constitutes the stationary state. And this state can be correlated with the field of wind according to the considerations of the paragraphs 2—5.

The conclusions, here arrived at, throw also some light on the assumption of GALLÉ (cf. Chapter I, paragraph 1), that the water, accumulated in the North Sea on the days preceding the day of the actual storm surge, aids also in raising the level of the Sea

on this day itself. From our calculations it follows, however, that the Sea adjusts itself according to the variations in the field of the wind only with a "time-lag" amounting at most to 6 hours. Here we neglected the oscillations. Only these oscillations, caused by wind on the preceding days, can to some extent influence the height of the Sea during the storm surge. But these oscillations are on this day already rather strongly diminished so that their influence is small. Our final conclusion as regards the "distant effect of the ocean", is therefore, that we may safely neglect this effect in our investigations.

In this paragraph only a changing *homogeneous* field of wind above the whole of the North Sea has been considered. For that reason we have still to treat the phenomena of inertia, caused by non-stationary *inhomogeneous* fields of wind. We are concerned here with very complicated oscillations of the Sea. We assume, however, that in these cases the same value of the characteristic period T occurs as in the case of homogeneous fields of wind. But sub b no special assumptions were made concerning the nature of the field of wind causing the "equilibrium value" ζ_o, so that if T is the same, all equations remain the same and we are allowed to apply all results of the case of homogeneous fields also to the case of inhomogeneous fields of winds.

CHAPTER III. THE MATERIAL

It is most important for the Warning-Service for Storm Surges to be able to predict the development of each individual storm surge. In the same way as the government-committee "Rotterdamsche Waterweg", we have therefore selected a set of storm surges, which have been studied in accordance with the results of the previous chapters.

The selection of the storm surges was guided by the principle, that if possible all high surges should be investigated, but that on the other hand the test-material should not become too extensive, as its complete study would then take too much time. In this way 14 storm surges were selected out of the period 1920—1940.

Next the place (or places) on the coast must be selected for which to compute the meteorological effect. It was more or less self-evident, to choose Hook of Holland, as thereby our results would be more easily comparable with the results of the government-committee "Rotterdamsche Waterweg" and of ORTT, who both investigated the meteorological effect at Hook of Holland. Moreover the place to be selected, should not lie at the entrance of an estuary, as this would to a certain extent complicate matters. For that reason Hook of Holland was chosen.

We selected the storm surges for our study from the period 1920—1940 for three reasons. First because the *recent* storm surges should also be included; secondly because only in this period reliable records of the direction and force of the wind along our coast were available. And thirdly it was desirable, that four times a day a weather-map was available for studying the field of wind and atmospheric pressure over the whole North Sea.

From the records of the wind on our coasts and the weather-maps the field of wind on the North Sea was deduced. From the records of the sealevel at Hook of Holland the meteorological effect was derived. How this was done is described in the following paragraphs.

1. Elimination of the tides

From the department of "Waterstaat" [1]) records were obtained of the sealevel at Hook of Holland for the following periods, covering the selected storm surges:

4—7 December 1920
17—22 January 1921
4—11 November 1921
24 November—1 December 1925
9—16 October 1926
22 November—2 December 1928
11—22 January 1930
21—28 November 1930
16—20 January 1931
18—22 October 1935
14 October —4 November 1936
29 November—9 December 1936
28 Januari —5 February 1938.

These periods do not cover the actual storm surges only, but also the oscillations of the whole North Sea after the storm. From these records the astronomical tides had to be eliminated. The best method for this purpose is that already previously used (see Chapter I, paragraph 1) of calculating the tides with the aid of harmonic analysis. The tides were evaluated according to the method developed by VAN DER STOK (*7a*, *7b*). The tide is represented as a sum of partial tides:

$$\xi(t) = \sum_n A_n \cos(\omega_n t + V_n - \varkappa_n). \tag{1}$$

$\xi(t)$ = fluctuation of the sealevel, caused by the astronomical tides.
A_n = amplitude of the n'th partial tide.
ω_n = angular velocity of the n'th partial tide.
V_n = astronomical argument of the n'th partial tide.
$\varkappa_n$ = phase constant of the n'th partial tide.

[1]) Department for the maintenance of dykes, roads, bridges and the navigability of canals.

The formula holds for any arbitrary day. For a certain tide ω_n is the (constant) angular velocity, which is known with great accuracy. The astronomical argument V_n changes from day to day, but is a constant for one and the same day. The value of V_n is tabulated by VAN DER STOK for the different tides. The phase constant $\varkappa_n$ is a constant for each place on the coast, but its value changes from place to place. This constant has been derived from the tidal phenomena for many places on the Dutch coast. The amplitude A_n is for a definite spot on the coast also nearly a constant. Its value changes only slightly with a period of 19 years (Sarosperiod). The tabulated values of A_n are the mean values for this period. Table 6 contains the values of the tidal constants, used in the computation. These partial tides have been selected in accordance with the condition: $A_n \geqq 4$ (cm).

In this way 16 tides were selected for Hook of Holland (P_1 and λ_2 are slightly smaller than 4, but they should be taken into account too). Besides the tables for V_n VAN DER STOK tabulates also the variation of a tide during its own period. The corresponding tables for Q_1, ν_2, L_2, λ_2, MN_4 and M_6 were omitted, however. They had to be computed from the values of ω_n. The values of the constants, tabulated in table 6, were all kindly communicated to us by the department of "Waterstaat".

TABLE 6 *Values of the tidal constants for Hook of Holland*

Partial tide	A_n (cm)	$\varkappa_n$ (°)	ω_n (°/hour)
K_1	7.86	351°.4	15.0410686
O_1	11.15	181°.3	13.9430356
P_1	3.86	341°.3	14.9589314
Q_1	4.76	135°.9	13.3986609
M_2	75.26	70°.6	28.9841042
S_2	18.65	130°.8	30.0
N_2	11.62	45°.4	28.4397296
K_2	5.41	132°.8	30.0821372
ν_2	6.10	34°.1	28.5125830
$2MS$	8.25	189°.7	27.9682084
L_2	8.25	76°.5	29.5284788
λ_2	3.74	100°.1	29.4556254
M_4	17.45	130°.1	57.9682084
MS_4	10.45	185°.8	58.9841042
MN_4	6.97	114°.7	57.4238338
M_6	4.42	62°.3	86.9523126

With the aid of all these data the height of the tide was calculated with intervals of half an hour for each day of the selected period, covering 117 days in all. Subsequently the height of the tide was subtracted from the corresponding height of the sealevel, which was derived from the records at Hook of Holland. In this way about 5600 values of the meteorological effect were computed. These were plotted against the time. From these curves it was at once clear, that in many cases the tide had not been removed altogether. An oscillation with a period of 6 hours was especially conspicious with great persistancy. These oscillations were removed from the disturbed curves by an averaging of overlapping intervals: the mean value of all 13 values of the meteorological effect ranging from $(t-3)$ to $(t+3)$ was considered to be the true value of the effect at the time t. For straight portions of the curves this method yielded excellent results. But for the more strongly curved portions wrong values were obtained, as the curves were "flattened" more or less by the process of averaging, which for that matter is only plausible, as it is this very "flattening" of the curve, which is the object of the whole procedure. For that reason a special device was used for these

portions of the curves. A smooth curve was drawn, which represented the general course of the disturbed curve. The differences between this estimated curve and the actual curve were evaluated. And the method of overlapping averaging was then applied to these differences. This is allowed, because the curvature of the curve has been artificially removed. With the aid of the averaged values of the differences the estimated curve is afterwards corrected. In this way the oscillations with a period of six hours were removed.

But in some cases the corrected curves still showed slight but clearly perceptible oscillations with the period of the M_2-tide. These oscillations could not be removed with the method of overlapping averaging, as the period of M_2 becomes comparable with the periods connected with the storm surges themselves. On that account an other method was used. The "points of inflexion" of the superposed oscillations constitute also "points of inflexion" of the compound curve. In these points the amplitude of the oscillations becomes zero. By drawing through these points of the compound curve a smooth curve, we obtain a fair idea of the undisturbed curve. The difference between the compound curve and the estimated curve can now be plotted. This difference constitutes the tidal oscillations, which were superposed upon the curve of the pure meteorological effect. We change the estimated curve so long, till the curve of the differences shows a nearly purely harmonic oscillation. By means of this graphical method all remaining tidal fluctuations were eliminated with complete success. The curves for the pure meteorological effects obtained in this way, are represented in figures 33*a*—46*a*. The curves are plotted against Greenwich mean time.

2. The wind on the North Sea and in the Channel

It was shown already in paragraph 2 of Chapter II, that we must know the mean value of the wind in the three sections of the North Sea shown in figure 10. Until now the wind on the Sea was computed from the isobars on the Sea, derived from weathermaps. Also the gradient was computed sometimes from the difference in atmospheric pressure between two conveniently situated places. The direction of the wind is derived from the isobars by assuming a constant angle between the wind and the direction of the isobars or the gradient of the atmospheric pressure. Also the velocity of the wind may be computed from isobars or gradient.

In our investigation the wind on the Sea will likewise be computed from the isobars. The observations on board the ships at sea are few and unreliable, especially concerning the velocity of the wind, so that they cannot be used as a base for the computation of the wind on the Sea. We used the daily weather-maps issued by the Deutsche Seewarte for the determination of the field of barometric pressure on the Sea. But in each separate case the relation between the field of pressure and the wind was established by comparing the field of pressure above Holland with the wind on the coast, derived from the records of the wind at Flushing, Hook of Holland, IJmuiden, Helder, Vlieland and Rottumeroog. Moreover, the estimates of the wind, made on board the light-ships "Noord-Hinder", "Haaks" and "Terschellingerbank" were used as material for comparison. From all these data the wind on the coast was derived. Also the gradient of the field of atmospheric pressure above the coast was computed from the isobars of the weather-maps and the difference in atmospheric pressure between Dutch Meteorological stations. The relation between the velocity of the "wind on the coast" and the gradientwind, computed from the gradient of the barometric field, was used afterwards to calculate the velocity of the wind on the Sea from the isobars on the Sea.

a. The wind on the coast

For each station the wind at a height of 6 meters above the earth has been derived from the records (cf. e.g. BRAAK, 67, 68). Only in this way the values of the windvelocity at the different stations become mutually comparable. But even after

reduction in the indicated way large differences of the windvelocity remain. The recorded windvelocities at Rottumeroog, Vlieland and Flushing are mostly lower than the corresponding velocities at Hook of Holland, IJmuiden and especially Helder. Generally these last stations are in good agreement with each other. But when however differences occur also between these stations, the most "probable" value of the windvelocity has to be found. In this case we make use of the estimates of the light-ships. It should be borne in mind, however, that the velocity-equivalents of the estimates at sea are not altogether identical with the internationally adopted equivalents of the scale of Beaufort. At sea the estimates are generally low (KUHLBRODT, 69, BLECK, 70). The velocity-equivalents of the Beaufort estimates at sea are for that reason higher than the internationally fixed scale of Beaufort equivalents. According to BRAAK (personal communication) the equivalents given by BLECK are better than the international equivalents. Both have been tabulated in table 7. Combining in this way the data of the coast stations and the lightships we obtain at last a value of the velocity of the wind at the coast.

TABLE 7 *International and* BLECK *equivalents of the Beaufort scale*

Degrees Beaufort	1	2	3	4	5	6	7	8	9	10	11	12
International equivalent . . .	1.1	2.5	4.3	6.3	8.6	11.1	13.8	16.7	19.9	23.3	27.1	> 29.0
BLECK equivalent	1.8	4.4	7.0	9.6	12.2	14.8	17.4	20.0	22.6	25.2	27.8	> 29.1

Not only the *velocity*, however, but also the *direction* of the wind on the coast is fixed. This is computed as the mean of the directions of the wind at all stations along the coast. Only Rottumeroog is omitted, because this station shows often a direction of the wind which is largely different from the direction on the other places.

b. The gradient-wind

After having computed the velocity of the wind at the coast, the velocity of the gradientwind must be obtained also. We put:

V = velocity of the gradientwind,
ϱ = density of the air,
R = radius of curvature of the paths of wind,
G = gradient of the atmospheric pressure,
l = $2\omega \sin \varphi$ (for definitions cf. Chapter II).

Introducing these symbols we obtain the following relation, when the wind paths are curved cyclonically:

$$lV + \frac{V^2}{R} = \frac{G}{\varrho}. \tag{2}$$

ϱ depends on the temperature and density of the air. Putting:

ϱ_o = density of the air at 0° C and a pressure of 76 cm (p_o),
t = temperature of the air in °C,
p = atmospheric pressure,
α = coefficient of expansion of the air ($\alpha = 0{,}00366$),

we obtain:

$$\frac{1}{\varrho} = \frac{1+\alpha t}{\varrho_o} \cdot \frac{p_o}{p}.$$

Introducing:

$$\triangle p = p_o - p,$$

we obtain approximately, as can easily be verified:

$$\frac{1}{\varrho} = \frac{1}{\varrho_o} \cdot \left(1 + \frac{\triangle p}{p} + \alpha t\right) = \frac{1}{\varrho_o} \cdot (1 + \delta), \qquad \delta = \frac{\triangle p}{p} + \alpha t. \tag{3}$$

The value of δ is fixed with sufficient accuracy if we take permanently:

$$p = 1000 \text{ mb.}$$

We must then express $\triangle p$ in *mb* too. Substituting also the value of α, we obtain:

$$100\ \delta = 0{,}1 \triangle p + 0{,}366\ t. \tag{4}$$

Substituting (3) into (2):

$$lV + \frac{V^2}{R} = \frac{G}{\varrho_o} \cdot (1 + \delta) = \frac{G_o}{\varrho_o}, \quad G_o = G(1 + \delta). \tag{5}$$

In this equation δ is represented by (4).

For the derivation of V from the values of G, R, t and p, we constructed two graphs. With the first graph the value of δ was obtained in a simple way from the values of p and t. Then G_o was evaluated with the aid of equations (5). And finally the value of V, corresponding with the values of G_o and R, was read from a graph, showing the relation between G and V for different values of R.

In our investigation the value of G was calculated from the differences of air-pressure between Flushing, Helder and de Bilt. Moreover the value of G was derived from the distance of the isobars on the weathermaps as a check. Through the values of G a smooth curve was drawn, yielding an additional correction. The value of p was read simply from the weathermap, the value of t was derived from the observations made on board the lightships. The radius of curvature of the windpaths were simply assumed to be equal to the radius of curvature of the isobars. This is however not true in general. Only in the stationary case blows the wind (nearly) parallel to the isobars. But we are interested precisily in non-stationary cases. The wind fluctuates strongly: *storm* surge ! The evaluation of the right windpaths, however, is very complicated and inaccurate. For that reason we preferred to use simply the curvature of the isobars. Besides the error, made in this way, is nearly compensated. We calculate namely the ratio between the velocity of the actual wind on the coast and the velocity of the gradientwind, obtained according to the indicated method; we derive the wind on the Sea however from the value of the gradientwind, calculated according to the same method, and the ratio, previously found. It is evident, that in this way an error, caused by a wrong value of the R, is nearly compensated. For if we calculate a value of the gradientwind which is too high, the other value of the gradientwind will most probably be also too high, and nearly in the same ratio.

A particularity, connected with the computation of the ratio between gradientwind and wind on the coast, is the correlation of this ratio with the difference in temperature between air and sea. It turns out, namely, that this ratio is much greater in the case of higher temperature of the Sea ("cold air mass") than in the case of higher temperature of the air ("warm air mass"). Averagely we find:

case 1. $T_{air} < T_{sea}$ (cold air mass): ratio = 0,76,

case 2. $T_{air} > T_{sea}$ (warm air mass): ratio = 0,60.

This difference can easily be explained by taking into account that the greater turbulence in the cold air causes a stronger mixing of the air at the sealevel with the air at greater heights of which the velocity is nearly that of the gradientwind.

The mean value of the ratio amounts to 0,75. This is very close to the ratio for cold air, owing to the fact that only a few cases of warm air are present. PALMÉN (46) also determined the value of this ratio. He obtained the value 0,76, in perfect agreement with our result.

c. Wind on the Sea

In order to determine the velocity of the wind in the three sections of the North Sea, shown in figure 10, the mean value of G, R and p was derived from the weathermaps for each section. The value of t was assumed to be identical with the temperature, measured on board the lightships. With the method, described in section *b*, the velocity of the gradientwind was calculated. From this value the velocity of the wind at the surface of the Sea was calculated with the aid of the ratio between the velocity of the wind at the surface and the velocity of the gradientwind, computed for the Dutch coast from the observations. The values for the wind on the Sea obtained in this way, were plotted against the time and a smooth curve was drawn through them. Finally from these curves the values of the wind were read, which are tabulated in the tables 25—38. These tables give also the average direction ψ of the isobars in the three sections, taking (cf. Chapter II, paragraph 4) $\psi = 0°$ when the direction is West, $\psi > 0°$ when the direction is North of West and $\psi < 0°$ when the direction is South of West. We choose the direction of the isobars, for it turned out, that on the coast the relation between the direction of the wind and the direction of the isobars was very poorly defined. As it is rather probable, however, that on the Sea the direction of the wind is much the same as the direction of the isobars, we decided to use the directions of the isobars in stead of the direction of the wind. We calculated only the average of the angle between the direction of the isobars and the direction of the wind on the Dutch coast, and we obtained: 8°. This value is somewhat smaller than the values assumed by other investigators:

LEVERKINCK: 16°,
WITTING: 15°—20°,
DOODSON: 20°,
BAUR and PHILIPPS: 13°.

On that account we shall use a value of 10°, when we discuss the results of our investigations (cf. Chapter V).

The accurate method, described above, for calculating the wind on the Sea, has been applied only to the wind on the days of the actual storm surges. For the days after (or before) the storm surges, on which only small fluctuations of the Sea occur, the wind (especially the velocity) needs not be known with the same utmost accuracy. It turned out, that it was sufficient, to deduce the values for the wind from the Beaufort estimates of the wind on the weatherstations, surrounding the North Sea. The values, obtained in this way, are indicated in the tables by printing in italics.

The considerations given so far are applicable only to the cases in which it is possible to evaluate an average value of the wind in the indicated sections. But it is also possible, that the centre of a depression is situated above the North Sea. The field of wind is then so inhomogeneous, that the computing of a mean value of the wind would cause the investigation of the material to become erroneous. For that reason we determine the structure of the field of pressure by indicating the position of the centre of the depression, the direction of the long axis of the depression, the average value of the gradient of the pressure on the short axis, and the ratio of short and long axis. If a depression has a circular form no difference is present between long and short axis. In this case only the mean value of the gradient of the air pressure is noted. In the investigation of the material the depressions are studied separately.

All data have been derived from the synoptic weathermaps for 1 h, 7 h, 13 h and 18 h G.M.T., so that our data for the wind refer to *these* times. To simplify our calculations we have therefore plotted the values of the meteorological effect against G.M.T. too.

CHAPTER IV. INVESTIGATION OF THE MATERIAL

The various storm surges can be compared only after elimination of the effects of inertia. The field of wind can then be correlated with the remaining stationary state, and it is exactly for this stationary state that the formulas hold, which were derived in the first 5 paragraphs of Chapter II.

When we have obtained the curves for the stationary state, the effect of the barometric pressure is first eliminated from these curves. Thus the pure windeffect remains, which is studied in connection with the field of wind. This investigation is again divided into two sets of cases: those with a homogeneous field of wind in the three sections of figure 10, and those in which the centre of a depression is situated on the North Sea or in its immediate vicinity. As a check, the formulas, obtained in this investigation, are used for computing the development of the various storm surges from the fields of wind, whereupon the results are compared with the actually observed values of the meteorological effect. In this way we obtain a fair idea of the extent to which the computed values tally with the observed ones.

1. Elimination of the oscillations due to inertia

We eliminate the oscillations of inertia with the aid of the results of paragraph 6 of Chapter II. For that purpose we have first to determine from our material a value of T (the period of the characteristic oscillations of the North Sea) and of β, the quantity which regulates the extinction of the oscillations. We derive the value of these quantities from the oscillations occurring after the storm. We can represent them by the formula:

$$\zeta = Ae^{-\beta t} \cos \frac{2\pi t}{T}. \tag{1}$$

As T and β have to be determined from the oscillations, the oscillatory part of the curves must be separated from the pure windeffect, which may be present. We perform this by means of the method, explained in Chapter III for the elimination of the remaining traces of the M_2-tide. Just as in that case we connect in the present one the points of inflexion by a smooth curve and subtract this estimated curve from the compound curve. The differences constitute the superposed oscillations of inertia of the whole Sea. We change the position of the estimated curve so long till this curve and the curve of the oscillations both run smoothly. It is possible, that after removal of the oscillation with the shortest period fluctuations with longer periods still remain. These oscillations are then removed in the same way. The result in shown in the figures 33*b*—46*b*. The periods 8—10 Nov. 1921; 13—16 Oct. 1926; 28 Nov.—2 Dec. 1928; 18—22 Jan. 1930 and 25—28 Nov. 1930, are instances of cases in which only one oscillation was superposed upon the windeffect. More superposed oscillations are found for example in the period 30 Oct.—4 Nov. 1930. Of course, the final curve shows also fluctuations with time. As, however, the longest period of oscillation of the North Sea amounts theoretically to 40 hours, we are able to decide whether the observed fluctuations are due to real oscillations or to a gradually changing windeffect.

In this way those parts of the figures 33*b*—46*b*, which are *not* related with a storm, are constructed. We take fully into account the tables of the wind, so as to analyse only those periods, in which only a gradual variation of the windeffect is to be expected.

From the curves for the oscillations, obtained in this way we derive the values of β and T according to formula (1). The value of T often changes during a period. The average value must then be determined from the positions of maxima and minima or zero-points. Moreover the average value of β can be deduced from the decrease of the amplitude with

time. In this way the values have been found, which are tabulated in table 8. In this table the periods are given for which the values of β and T have been derived.

TABLE 8 *Values of β and T as functions of V*

Period	T	$\beta \times 10^6$	V	Period	T	$\beta \times 10^6$	V	Period	T	$\beta \times 10^6$	V
Dec. 6—7, 1920 . .	63	6	6.7	Jan. 11—14, 1930 . .	32	9	12.3	Oct. 24—26, 1936 . .	39	—	—
Jan. 20—22, 1921 . .	37	8	12.3	Jan. 18—21, 1930 . .	53	1	7.7	Oct. 30—Nov. 1, 1936	28	6	6.6
Nov. 7—11, 1921 . .	46	5	6.5	Nov. 21—22, 1930 . .	36	—	—	Oct. 30—Nov. 3, 1936	62	5	6.3
Nov. 27—29, 1925 . .	36	7	7.7	Nov. 25—28, 1930 . .	48	4	8.3	Nov. 2—4, 1936 . . .	33	5	6.9
Nov. 30—Dec. 1, 1925	47	7	7.4	Jan. 19—20, 1931 . .	32	2	4.0	Dec. 7—9, 1936 . . .	46	5	7.1
Oct. 13—16, 1926 . .	31	1	5.0	Oct. 21—22, 1935 . .	38	6	7.4	Febr. 1—5, 1938 . . .	31	5	11.7
Nov. 30—Dec. 2, 1928	38	1	10.0	Oct. 21—23, 1936 . .	48	4	7.0				

The values of T are expressed in hours. For β the value of $\beta \times 10^6$ is entered and finally the values of the windvelocity averaged over the whole North Sea in the periods considered (in m/sec) are also given. The latter quantity has been determined too, because, according to theory, the value of β depends on the value of D, and D depends in its turn on the value of V. We compare, therefore, also the theoretical predictions with practice with reference to this point.

On studying first the values of T, it turns out, that a large scattering exists. But the values of T are distributed more or less systematically around the average value:

$$T_o = 41 \text{ (hours)}.$$

This is in excellent agreement with theory, which predicts a value of 40 hours (cf. Chapter II, paragraph 6).

For β we have to study its relation with V. Here also large individual fluctuations occur. Averaging, however, the 18 cases in which both β and V have been determined so as to obtain three mean values of β and V, yields the values tabulated in table 9. It turns out, that a linear relation exists between the two quantities:

$$\beta \times 10^6 = 2{,}0 + 0{,}37\ V. \tag{1a}$$

TABLE 9 *Relation between β and V*

V (m/sec)	$\beta \times 10^6$	$2.0 + 0.37\ V$
5.9	4.2	4.2
7.3	4.7	4.7
10.0	5.7	5.7

The values of β, calculated with the aid of formula (1a) have also been entered in table 9. The fact that perfect agreement exists is a strong argument in favour of the linear law.

This can be compared with the theoretical formula for β, which was derived in paragraph 6 of Chapter II. For the *whole* North Sea we obtained:

$$\beta = \tfrac{3}{4} \cdot \frac{lD}{8\pi H_o}.$$

The value of T_o refers to an oscillation in which the whole North Sea partakes. For that reason we have to use also for β the formula which holds for an oscillation of the whole Sea. In the formula H_o is the average depth of the Southern part of the North Sea.

We assume:

$$H_o = 40 \text{ (m)}.$$

For D we use again the formula of PALMÉN:

$$D = 35 + 5{,}4\ V.$$

In our geographic latitude we have:

$$l = 10^{-4}.$$

Substituting D and l in the equation for β we obtain:

$$\beta \times 10^6 = 2{,}6 + 0{,}40\ V.$$

These values are slightly higher than the values we obtained experimentally. But taking into account the approximative character of the theoretical considerations and the rather uncertain derivation of equation (1a) from the observations the agreement between theory and "experiment" is very satisfactory.

We now calculate β for the case of a storm. Using our empirical formula and assuming that an average value of the windvelocity of 20 m/sec occurs during the storm surge, we obtain:

$$\beta = 10^{-5}.$$

But we computed figure 13 with the value:

$$\beta T = 1,$$

and figure 14 with the value:

$$\beta T = 2.$$

In our case we obtain, substituting the value $T_o = 41$ (hours):

$$\beta T = 1{,}4.$$

It is therefore to be expected, that for the actual development of a storm surge conditions will be intermediate between those of the two figures. This result has been used in constructing the curve for the stationary states. Here again the graphical method has been applied: the oscillation, existing after the storm, has been extrapolated backwards during the period of the storm surge itself. The amplitude was found approximately by taking the first negative maximum after the storm. The phase of the oscillation was found by a careful comparison of the actually recorded curve for the meteorological effect with the curves, given in figure 13. In this way some arbitrariness is introduced. But as, so far, the graphical method has yielded reliable results, we ventured to suppose, that also in this case reality would be approximated fairly well.

The oscillation, found by extrapolating backwards, was subtracted from the curve of the actual storm surge. Once more the estimated curve was altered so long till the course of both this curve and the curve obtained by subtraction became smooth. In this way for all storm surges a perfect separation was obtained of the stationary state from the oscillations caused by inertia. The results are shown in figures 33b—46b. From these curves we read the value ζ_o of the stationary meteorological effect present at the synoptic hours (1 hour G.M.T. etc.). The values of ζ_o have also been tabulated in the tables 25—38. They have served as a base for the next investigations.

2. Elimination of the barometric effect

The pure windeffect is obtained, after subtracting the barometric effect from the values of the total meteorological effect ("stationary" value !).

The values found for the meteorological effect, after having carried out the processes explained in paragraph 1, refer to the stationary state of the sea, connected with the field of

wind and barometric pressure. We have therefore investigated the barometric effect during periods with very feable winds and slowly changing fields of pressure, so that the state of the sea could be considered as stationary. This investigation was carried out for Helder. For days, on which a windforce of at most 1 or 2 degrees Beaufort was noted at the Dutch coast stations, the predicted values in the tide-table were compared with the actually found values of high water and low water. When such a feable wind blows, the windeffect can be neglected. The difference between actual and predicted values of the tides are then entirely due to the influence of the field of pressure, so that we can correlate these differences with the local barometric pressure in Helder, neglecting the influence of the *gradient* of the field of pressure.

The differences calculated from the value of high tide yielded the same relation with the barometric pressure as the differences calculated from the values of low tide. This relation turned out to be linear:

$$(\triangle \zeta)_p = 0{,}45\,(1004{,}5 - p), \tag{2}$$

$(\triangle \zeta)_p$ = barometric effect of the Sea,
p = local pressure (in mb).

If the *local* pressure were compensated hydrostatically the coefficient of p should be nearly 1. As we have neglected the direction and absolute value of the *gradient* of the field of pressure, however, this coefficient will be smaller. For it can be shown, that this omission will result always in a *decrease* of this coefficient. This is confirmed by our empirical result. An other investigation of this relation yielded a somewhat greater value of the coefficient. Therefore rounding off a little we assume as the relation for the barometric effect:

$$(\triangle \zeta)_p = \tfrac{1}{2} \cdot (1003 - p). \tag{2a}$$

With the aid of this formula the values of the "pressure effect" have been computed. The values of $(\triangle\zeta)_p$ have been tabulated in the tables 33—46. The values of the pure windeffect, which have been tabulated in the 12th column of the tables 33—46, have been obtained by subtracting $(\triangle \zeta)_p$ from ζ_o (the "stationary" value of the meteorological effect, cf. paragraph 2).

3. The relation of the windeffect with the windvelocity

In the investigation of the windeffect the relation with the *velocity* of the wind was considered first of all. According to paragrahp 5 of Chapter II a quadratic relation should be found. This can be checked by selecting cases with a perfectly homogeneous field of wind and then comparing the values of the windeffect caused by different windvelocities all having the same direction. It turns out, however, that a fixed direction of the wind provides only very few values, which can be compared, so that more directions of the wind must be considered. These directions must, however, be chosen in such a way, that the same windvelocity yields nearly the same windeffect for these different directions. Only then are we allowed to use more directions of the wind. For that reason we choose these directions in the vicinity of $\psi = 50°$. For it was shown in Chapter II, that a homogeneous field of wind yields the maximum value of the windeffect, when $\psi \approx 50°$. And in the vicinity of the maximum the windeffect changes only slowly with the direction: the value of $\cos(\psi - 50°)$ changes only by 1 % — 2 % if ψ changes from 40° to 60°. We consider therefore directions in the vicinity of $\psi = 50°$.

In this way we have extended the number of cases in which the windeffects can be compared with each other. Nevertheless few cases are found in which the field of wind is perfectly homogeneous. On that account we have to reduce our conditions still further. Now in Chapter II was found, that the windeffect was mainly caused by the wind in the Southern part of the North Sea (section II, cf. figure 10). We now select

therefore all cases, in which the wind in sections I and III does not differ much from the wind in section II. As, however, the wind in section II causes the greater part of the windeffect, we correlate the values of the windeffect only with the velocity of the wind in this section, neglecting the (very small) influence of differences between the wind in section II and the wind in sections I and III (causing differences of a few % in the windeffect). In this way we have selected the cases of table 10, in which the direction

TABLE 10 *Relation between windeffect and velocity of the wind*

Date	Hour	ψ	V	ζ	Date	Hour	ψ	V	ζ	Date	Hour	ψ	V	ζ
Jan. 19, 1921	1	50°	20.8	155	Nov. 26, 1928	18	59°	15.0	86	Oct. 20, 1935	18	50°	12.4	44
Jan. 19, 1921	7	58°	19.0	134	Nov. 27, 1928	1	55°	13.0	74	Oct. 20, 1936	18	46°	11.0	54
Jan. 19, 1921	13	64°	16.7	99	Nov. 27, 1928	7	54°	12.1	71	Dec. 1, 1936	1	43°	18.3	141
Jan. 19, 1921	18	55°	14.6	70	Nov. 27, 1928	13	58°	12.3	71	Dec. 1, 1936	7	44°	18.2	176
Nov. 25, 1928	18	53°	17.4	115	Jan. 17, 1931	7	40°	18.9	133	Dec. 2, 1936	18	47°	13.6	71
Nov. 26, 1928	1	59°	20.1	172	Jan. 17, 1931	13	51°	18.4	139	Jan. 30, 1938	1	42°	17.7	119
Nov. 26, 1928	7	61°	19.3	142	Jan. 18, 1931	18	47°	12.5	45					
Nov. 26, 1928	13	60°	17.0	105	Oct. 20, 1935	13	50°	14.3	71					

of the wind in section II and also the velocity of the wind (in m/sec) have been tabulated. The values of the windeffect have been entered also. We now examine the question as to whether the relation between the velocity of the wind and the windeffect is quadratic or not. To this end we have plotted the values of ζ against the values of V^2. It turned out, that considerable scattering was present. We determined therefore the average value of ζ and V^2 for 4 sets of cases. The results are given in table 11. In order to obtain nearly the same mean value of ψ in all sets, so that the average values should be comparable, it was necessary to introduce slightly different statistical weights of the groups. These statistical weights are also given in the table.

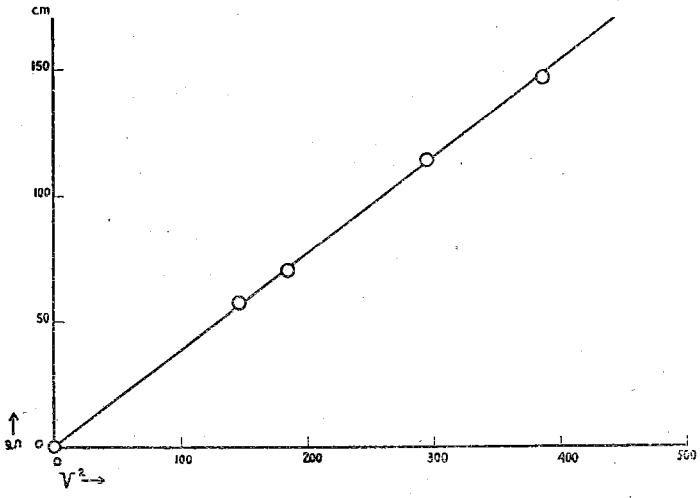

Fig. 15. Average relation between ζ and V^2

TABLE 11 *Average relation between ζ and V^2*

Mean value of φ . . .	51°	51°	53°	54°
„ „ „ V^2 . .	146	184	293	385
„ „ „ ζ . . .	57	70	114	147
Statistical weight . . .	1	1	2	1

The values in this table have been plotted in figure 15. If the law for the windeffect is really quadratic in the velocity, the points of figure 15 should lie on a straight line. This line should pass through the origin, as of course the windeffect is zero when the velocity of the wind is zero. Looking at figure 15, we see immediately, that the points lie indeed on a straight line, passing through the origin.

We arrive at the conclusion, therefore, *that the quadratic law holds*. We use this result in the determination of the influence of the *direction* of the wind.

4. The relation of the windeffect with the direction of the wind

The investigation of the relation of the windeffect with the direction of the wind is carried out first for the cases in which the velocity of the wind is accurately known.

Afterwards the other cases are studied (cf. Chapter III, paragraph 2c). According to the previous paragraph, we are allowed to put for the windeffect:

$$\zeta = a(\psi) \,.\, V^2. \tag{3}$$

V = velocity of the wind (in m/sec),
$a(\psi)$ = windeffect caused by wind with a direction ψ and velocity 1 (m/sec).

With the aid of formula (3) we can calculate from any value of ζ the corresponding value of a. In this way we obtain a great number of values of a. By averaging all these values we can determine the curve showing the relation between a and ψ.

But in averaging simply all values of a errors would be introduced. To show this we consider the formula for ζ derived in Chapter II, which we may write as:

$$\zeta = aV^2 \cos(\psi - \psi_o).$$

We substitute for $\cos(\psi - \psi_o)$ the scalar product of the vectors $\vec{i}$ and $\vec{i}_o$ of unit length indicating the direction ψ of the wind and the direction ψ_o of the direction of maximum windeffect respectively:

$$\cos(\psi - \psi_o) = \vec{i} \,.\, \vec{i}_o \,.$$

Hence:

$$\zeta = aV^2 \vec{i} \,.\, \vec{i}_o.$$

Now if we average N values of ζ, corresponding to slightly different values of ψ, we obtain:

$$\frac{1}{N} \sum_{n=1}^{N} \zeta_n = \frac{a}{N} \left\{ \sum_{n=1}^{N} V_n^{\,2} \vec{i}_n \right\} \,.\, \vec{i}_o \,.$$

It is clear, therefore, that the values of V^2 have to be averaged *vectorially*.

According to this result in each case the North- and West-components of the vector with absolute value V^2 and direction ψ have been computed. These values are arranged according to the value of ψ and then averaged. From the components of these "average" vectors we compute again the length and direction of the vectors. The values of ζ are also averaged. We have obtained in this way the value of the windeffect, caused by the wind with a direction coinciding with the direction of the "mean" vector and a velocity equal to the root of this "mean" vector.

This process of averaging has been carried out for all three sections of the Sea. For each section 22 values of ζ, V and ψ have been obtained. All these values were the result of averaging approximately 20 cases. A first preliminary investigation showed at once, that the angular distribution did not follow the cosine law. This is caused chiefly by the windeffect in section II. As the influence of the wind in sections I and III is only small, we are allowed to assume for them a pure cosine distribution, whereas the angular distribution of the influence of the wind in section II must be taken as arbitrary. We put therefore

$$\zeta = a_1 V_1^{\,2} \cos(\psi_1 - \varepsilon_1) + a_2(\psi_2) \,.\, V_2^{\,2} + a_3 V_3^{\,2} \cos(\psi_3 - \varepsilon_3), \tag{4}$$

where:

V_1, V_2, V_3 = windvelocities in sections I, II and III respectively;
a_1, a_3 = constants;
ψ_1, ψ_2, ψ_3 = directions of the wind in sections I, II and III respectively;
ε_1, ε_2, ε_3 = directions for maximum windeffect in sections I, II and III respectively;
$a_2(\psi_2)$ = angular distribution of the windeffect in section II.

It turned out, that by this formula actual conditions could indeed be very well represented. As a first approximation the first row of values of a and ε tabulated in

table 12 were found. The values of a_2 and ε_2 give only the values of $a_2\,(\psi_2)$ and ψ_2 for the direction of the wind causing the maximum windeffect.

TABLE 12 *Values of a and ε in different approximations*

	Section I		Section II		Section III	
	a_1	ε_1	a_2	ε_2	a_3	ε_3
First approximation	0.09	— 25°	0.33	65°	0.05	90°
Second „	0.087	— 26°	0.333	66°	0.048	92°
Third „	0.087	— 26°	0.333	66°	0.048	92°

From these values is seen at once, that the influence of the Channel and the Northern part of the Sea is indeed small. These influences may be treated therefore as small disturbances.

The values of a_1, ε_1; a_3, ε_3; and the form of $a_2\,(\psi_2)$ (given more or less by a_2, ε_2 in the table) are now improved in the following way. For *each* case we calculate the value of ζ_2, defined by the equation:

$$\zeta_2 = \zeta - a_1 V_1^2 \cos(\psi_1 - \varepsilon_1) - a_3 V_3^2 \cos(\psi_3 - \varepsilon_3). \tag{5}$$

In this computation the values for a_1, ε_1; a_3, ε_3; obtained in first approximation (cf. table 12) are used.

Then we should have:

$$\zeta_2 = a_2(\psi_2) \,.\, V_2^2.$$

From this set of values for ζ_2 we compute, averaging vectorially as explained above, an improved curve for $a_2\,(\psi_2)$ (second approximation). With the aid of this curve we can calculate values of "ζ_1":

$$\zeta_1 = \zeta - a_2(\psi_2) \,.\, V_2^2 - a_3 V_3^2 \cos(\psi_3 - \varepsilon_3).$$

ζ_1 should be represented by:

$$\zeta_1 = a_1 V_1^2 \cos(\psi_1 - \varepsilon_1).$$

From the set of values for ζ_1 we can derive improved values of a_1 and ε_1 (second approximation).

With the values of the second approximation for $a_2\,(\psi_2)$ and a_1, ε_1; we can calculate values for "ζ_3", and calculate improved values of a_3 and ε_3 (second approximation).

With the values of the second approximation the whole process can be repeated and a third approximation computed. The successive approximations have been tabulated in table 12. It turns out, that the third approximation yields the same values as the second one. These values are therefore the correct ones to be used in equation (4). The angular distribution, found in this way for $a_2\,(\psi_2)$ is tabulated in table 13 and is also shown in

TABLE 13 *Values of the angular distribution of $a_2\,(\psi_2)$*

ψ_2. . .	— 36°	— 23°	— 12°	0°	12°	24°	38°	48°	56°	71°	88°
$a_2\,(\psi_2)$.	0.071	0.070	0.123	0.171	0.210	0.270	0.297	0.308	0.330	0.328	0.317

figure 16. It appears at once from figure 16, that the points representing the different values of $a_2\,(\psi_2)$ lie closely to the smooth curve drawn through them. This curve can be drawn accurately, however, only for the values of ψ in the interval: $-50° \leqq \psi \leqq 100°$.

A striking feature of the curve is its assymmetrical character. The maximum is situated near 66°, whereas the point half way the two zero-points is situated near 46°. This asymmetry will be discussed later (Chapter V).

We have used until now only the values of ζ for which accurate values of the wind-velocity had been derived. Now also the other values of ζ are considered. To check, whether or not, different results are yielded, we calculate in each case the value of ζ_2 with the aid of equation (5), using the correct values of a_1, ε_1; a_3, ε_3 (third approximation).

Considering the values of ζ_2 obtained in this way, we find, that more values should be averaged here than in the preceding investigation, because of the stronger scattering of the individual values. In order to obtain the form of the curve we have, moreover, to effect the averaging of overlapping intervals for the Easterly directions of the wind.

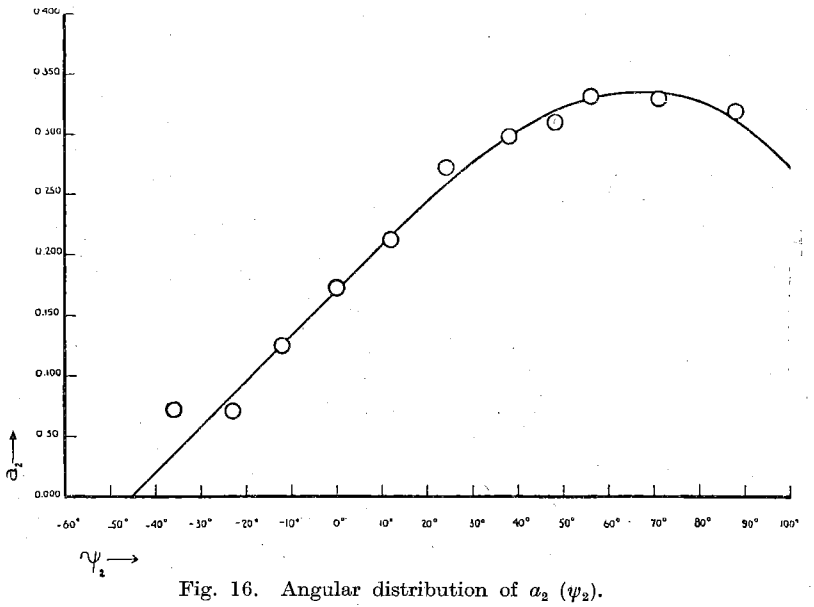

Fig. 16. Angular distribution of a_2 (ψ_2).

TABLE 14 *Values of a_2 (ψ_2) from the cases with estimated windvelocities*

ψ_2	— 63°	— 29°	— 7°	15°	58°	132°	— 148°	— 178°
a_2 (ψ_2). . .	— 0.043	0.058	0.149	0.223	0.345	— 0.046	— 0.280	— 0.260

TABLE 15

Angular distribution of the windeffect in the three Sections of the North Sea and in the whole North Sea (a (ψ))

ψ	a_1 (ψ_1)	a_2 (ψ_2)	a_3 (ψ_3)	a (ψ)	ψ	a_1 (ψ_1)	a_2 (ψ_2)	a_3 (ψ_3)	a (ψ)
— 40°	0.084	0.020	— 0.032	0.072	140°	— 0.084	— 0.019	0.032	— 0.071
— 30°	0.087	0.055	— 0.025	0.117	150°	— 0.087	— 0.098	0.025	— 0.160
— 20°	0.087	0.093	0.018	0.162	160°	— 0.087	— 0.169	0.018	— 0.238
— 10°	0.084	0.131	— 0.010	0.205	170°	— 0.084	— 0.220	0.010	— 0.294
0°	0.078	0.171	— 0.002	0.247	180°	— 0.078	— 0.254	0.002	— 0.330
10°	0.070	0.209	0.007	0.286	— 170°	— 0.070	— 0.271	— 0.007	— 0.348
20°	0.060	0.246	0.015	0.321	— 160°	— 0.060	— 0.280	— 0.015	— 0.355
30°	0.049	0.278	0.023	0.350	— 150°	— 0.049	— 0.277	— 0.023	— 0.349
40°	0.035	0.303	0.030	0.368	— 140°	— 0.035	— 0.268	— 0.030	— 0.333
50°	0.021	0.322	0.036	0.379	— 130°	— 0.021	— 0.253	— 0.036	— 0.310
60°	0.006	0.331	0.041	0.378	— 120°	— 0.006	— 0.234	— 0.041	— 0.281
70°	— 0.009	0.333	0.045	0.369	— 110°	0.009	— 0.207	— 0.045	— 0.243
80°	— 0.024	0.327	0.047	0.350	— 100°	0.024	— 0.177	— 0.047	— 0.200
90°	— 0.038	0.306	0.048	0.319	— 90°	0.038	— 0.150	— 0.048	— 0.160
100°	— 0.051	0.271	0.048	0.268	— 80°	0.051	— 0.118	— 0.048	— 0.115
110°	— 0.063	0.212	0.046	0.195	— 70°	0.063	— 0.086	— 0.046	— 0.069
120°	— 0.072	0.136	0.042	0.106	— 60°	0.072	— 0.052	— 0.042	— 0.022
130°	— 0.079	0.058	0.038	0.017	— 50°	0.079	— 0.017	— 0.038	0.024

In figure 17 the curve of figure 16 has been drawn once more and besides the points, representing the values of a_2 (ψ_2) in table 14, have been plotted. We see, that the points in the interval $-50° \leq \psi \leq 100°$ lie very closely to the curve. This justifies the

assumption of the reliability of the other points too, so that these points have served to complete the curve of figure 17.

The curve of figure 17 has been tabulated in table 15, together with the values of $a_1 \cos(\psi_1 - \varepsilon_1)$ and $a_3 \cos(\psi_3 - \varepsilon_3)$. Moreover the sum $a(\psi)$ of the three separate windeffects

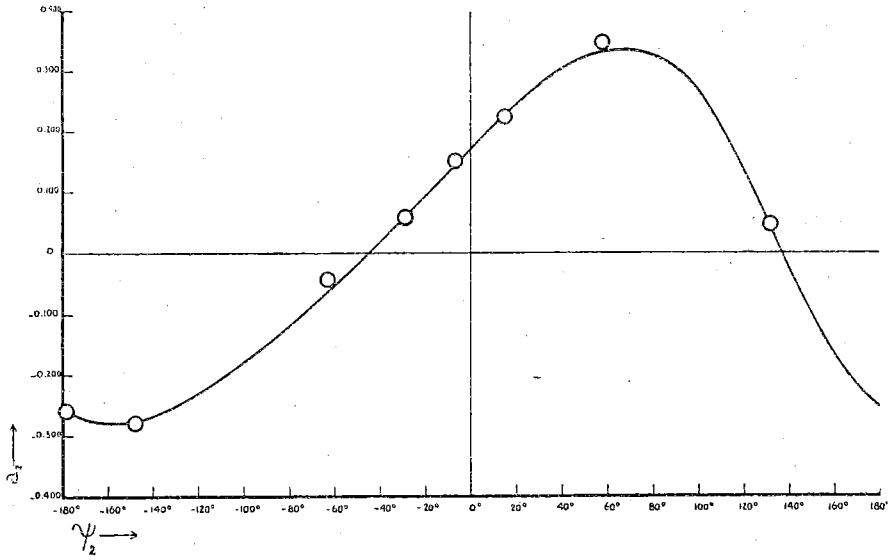

Fig. 17. Values of $a_2(\psi_2)$ derived from the cases with estimated windvelocities

has been computed. This represents the windeffect caused by a wind having the same direction and velocity on the whole Sea and the Channel.

These values have been plotted in figure 18.

Here, too, the asymmetrical character is clearly perceptible. We see also, that the negative windeffect is less pronounced than the positive one. This result was also found

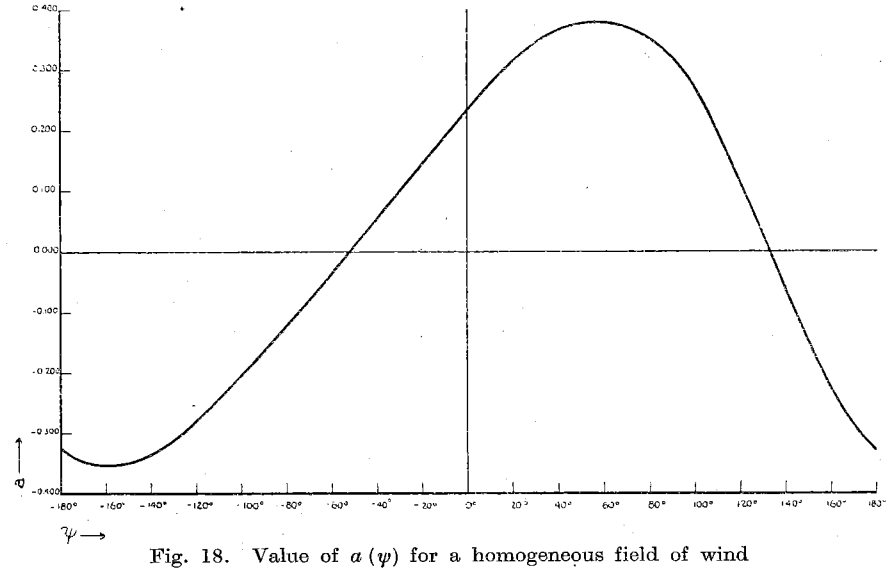

Fig. 18. Value of $a(\psi)$ for a homogeneous field of wind

by other investigators. If we represent the new curve by the formula $a = a(\psi)$, the windeffect, caused by a homogeneous field of wind with direction ψ and velocity V would be:

$$\zeta = a(\psi) \cdot V^2. \tag{6}$$

With the computation of table 15 and the plotting of the figures 17 and 18 our task: "the investigation of homogeneous fields of wind" is completed. For with the aid of this table (resp. figures) and the formula (4) or (6) the windeffect can be calculated for any case.

5. Depressions

In paragraph 5 of Chapter II we derived the value of the windeffect, caused by depressions with different positions of the centre. Isopleths for the windeffect as a function of the position of the centre were calculated. But we mentioned already in Chapter II, that in the computation in question the results of the preceding paragraph had been taken into account. When the centre of the depression is namely situated at a great distance from the North Sea, the field of wind in the different sections may be taken to be homogeneous, and the windeffect can be calculated from the direction of the isobars and the velocity of the wind. The velocity of the wind can be calculated from the gradient (which is taken to be constant everywhere and equal to 10) and the curvature of the isobars, using the ratio between gradient wind and surface wind obtained in Chapter III. In this way the far off parts of the isopleths have been computed. The parts on the North Sea, however, were computed with the formula, derived in paragraph 5 of Chapter II. In practice, therefore, the position of the far off parts of the isopleths need not be examined. Only the parts on the North Sea should be checked. And in investigating this problem, we are allowed to use the fact, that the isopleths must have positions, already fixed for those parts which lie at a certain distance from the North Sea.

In order to study the windeffect of the depressions on the North Sea, we examine first the relation between the windeffect and the value of the gradient G of the barometric

TABLE 16 *Numerical data concerning depressions situated on the North Sea*

Data	Hour	Latitude	Longitude	G	θ	Ratio of the axes	ζ	ζ'_{10}	$\frac{\zeta}{\zeta'_{10}}$	$\frac{\zeta}{\zeta'}$	ζ_{10}	g	ζ''_{10}
4 December 1920	1	54½°	— 5½°	25½	—	—	122	16	7.6	1.23	19.2	13	15.5
4 December 1920	7	54°	— 9°	27	—	—	149	20	7.5	1.07	20.4	15	20.7
4 December 1920	*13*	*53°*	— *5½°*	*27*	—	—	*130*	*10*	*13.0*	—	*17.8*	*15*	*12.0*
4 December 1920	*18*	*51°*	— *4½°*	*21*	—	—	*72*	*2*	*36.0*	—	*16.3*	*9*	*3.5*
6 November 1921	7	55°	— 2½°	21	98°	1 : 2	46	13	3.5	0.85	8.7	4	11.0
6 November 1921	13	53°	— 6½°	28	73°	2 : 3	148	13	11.4	1.54	16.1	16	14.0
6 November 1921	18	53½°	—10°	26	60°	1 : 2	141	20	7.1	1.10	18.9	14	21.8
25 November 1925	1	57°	— 5°	15	—	—	38	21	1.8	0.86	16.9	2	18.7
30 November 1925	13	54°	— 1°	10	—	—	— 15	6	—	—	— 15.0	2	7.5
30 November 1925	18	52½°	— 2°	8	—	—	— 15	2	—	—	— 23.4	2	3.9
1 December 1925	1	50½°	— 4½°	6	—	—	— 10	— 2	—	—	— 27.8	1	1.6
9 October 1926	13	57½°	— 1°	18½	—	—	30	16	1.9	0.56	8.8	4	13.2
9 October 1926	18	57½°	— 2½°	23	— 30°	1 : 2	65	18	3.6	0.72	13.8	3	15.4
13 October 1926	1	58°	2°	18	—	—	37	12	3.1	1.00	11.4	6	15.2
13 October 1926	7	56½°	— 1½°	17	20°	1 : 2½	29	15	1.9	0.70	11.9	6	12.2
13 October 1926	13	56°	— 7°	14½	3°	1 : 2½	28	22	1.3	0.64	16.9	4	12.2
14 October 1926	7	58½°	— 3°	13½	—	—	35	20	1.8	1.00	19.2	4	17.2
23 November 1928	13	57½°	2½°	28	—	—	60	11	5.5	0.73	7.7	16	13.4
23 November 1928	18	57°	— 1°	27	—	—	73	15	4.9	0.70	10.0	15	12.3
24 November 1928	1	58½°	— 5°	25	—	—	115	22	5.2	0.86	18.4	6	20.3
24 November 1928	7	58°	— 7½°	24½	—	—	142	25	5.7	1.14	23.7	6	23.8
24 November 1928	13	58°	— 7½°	24	—	—	145	25	5.8	1.20	25.2	6	23.8
25 November 1928	13	57½°	— 2½°	20	78°	1 : 2	72	18	4.0	1.06	15.1	2	15.4
22 November 1930	18	58½°	1½°	21	—	—	68	14	4.9	1.14	15.4	9	11.1
23 November 1930	1	57½°	— 6½°	23	70°	1 : 3	124	23	5.4	1.07	20.2	5	21.8
19 October 1935	13	59½°	— 3½°	24	—	—	81	21	3.9	0.71	14.1	12	18.9
19 October 1935	18	57½°	— 5°	27	—	—	130	22	5.9	0.86	17.8	4	19.3
20 October 1935	1	58°	— 8°	25	—	—	160	26	6.2	1.04	25.6	13	24.6
20 October 1935	7	56½°	— 8°	21½	—	—	120	24	5.0	1.13	26.0	9	23.3
19 October 1936	13	55°	— 4°	16	—	—	48	15	3.6	1.30	18.8	3	13.9
19 October 1936	18	55°	— 7°	18	—	—	77	20	3.9	1.25	23.8	3	14.6
5 December 1936	13	57½°	— 4°	15	30°	2 : 3	44	20	2.2	1.03	21.9	2	17.8
5 December 1936	18	57°	— 6°	15	20°	1 : 2	46	22	2.1	0.98	24.3	5	20.4
6 December 1936	1	57°	— 9°	15	— 5°	2 : 3	52	26	2.0	0.92	29.2	5	25.8
6 December 1936	7	56½°	— 7½°	15	—	—	60	23	2.6	1.22	26.7	2	22.3
6 December 1936	13	56°	— 6½°	16	98°	2 : 3	68	21	3.2	1.33	22.1	5	20.2
6 December 1936	18	56°	— 6°	17	93°	1 : 2	73	21	3.5	1.26	20.9	6	14.2
7 December 1936	1	56½°	— 8°	16	94°	1 : 2	80	24	3.3	1.38	25.8	5	23.5
7 December 1936	7	56°	— 8°	15	87°	1 : 2	52	23	2.3	1.04	19.1	5	22.7

pressure, occurring in the depression. We cannot use here, as in the case of the homogeneous fields of wind, the velocity of the wind, for this velocity changes throughout the depression (from zero in the centre to a maximum value in a certain distance from the centre). For that reason the *gradient* is here used.

To find the relation with the gradient, we compare the value of the windeffect, obtained in each individual case, with the theoretical value of the windeffect caused by a depression with the same position of the centre, but having circular form and gradient = 10 (mb/500 km). This value is derived from figure 11. We denote it by ζ'_{10}. In table 16 we have tabulated all available depressions, situated on the North Sea or in the immediate vicinity of the North Sea. The value of ζ'_{10} introduced above, is tabulated in column 9. In column 10 the ratio between the actual value of the windeffect ζ and ζ'_{10} is given. Studying the values of these ratios, we perceive that for the cases of 4 Dec. 1920, 13 h and 18 h, this ratio differs largely from the other values. For that reason these cases have been printed in italics and have been neglected in the further investigation.

The other values show, however, also some scattering, so that mean values have been calculated and tabulated in Table 17.

TABLE 17. *Mean relation between windeffect and gradient of atmospheric pressure*

Mean value of the gradient $(\overline{G})$.	14.7	16.4	20.4	24.4	27.2
„ „ „ „ ratio ζ/ζ'_{10} . .	1.99	3.09	3.97	5.66	7.05
$\overline{G}^2$	216	269	416	595	740

We try to find the relation between ζ/ζ'_{10} and G. To this end we put:

$$\frac{\zeta}{\zeta'_{10}} = aG^p$$

or:

$$\log \frac{\zeta}{\zeta'_{10}} = \log a + p \log G.$$

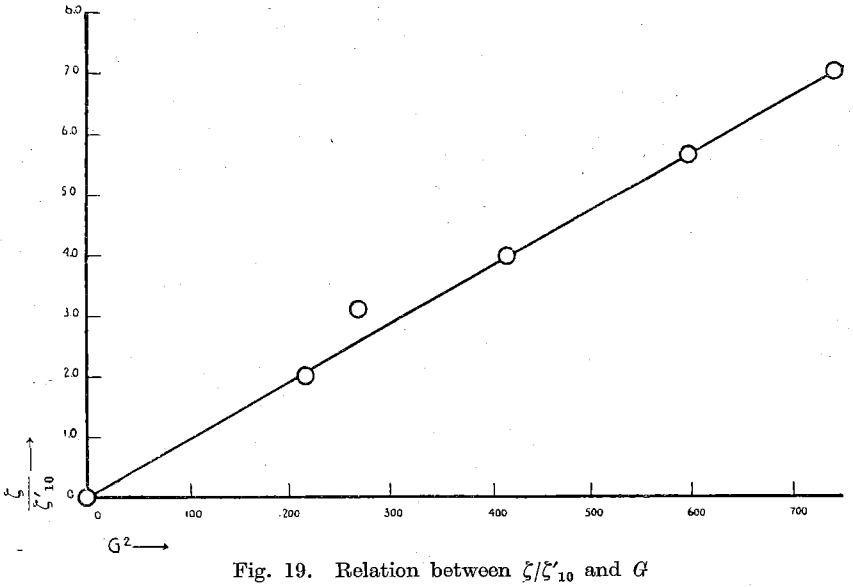

Fig. 19. Relation between ζ/ζ'_{10} and G

By plotting $\log G$ against $\log \zeta/\zeta'_{10}$ and drawing the smooth average curve best adjusted to the points we obtain:

$$p \approx 1{,}9.$$

We see, that the relation is almost quadratic. To check this we plot in figure 19 ζ/ζ'_{10} against G^2. We have tabulated the value of G^2 also in table 17. It turns out, that nearly all points of figure 19 lie closely to a straight line, passing through the origin. Only one point lies outside this line. We derive from the figure:

$$\frac{\zeta}{\zeta'_{10}} = 0{,}0095\ G^2. \tag{7}$$

In these computations we neglected the deviation of many depressions from the circular form. We next investigate therefore the influence of these deviations. We write formula (7) in the following form:

$$\zeta = 0{,}0095\ \zeta'_{10}\ G^2. \tag{7a}$$

With the aid of this formula the value of ζ for "circular form" is computed for each depression from the values of ζ'_{10} and G. When the depression has not a circular form, the calculated value of ζ, ζ', will generally deviate from the value of ζ actually found (ζ !). For all cases under consideration we compute the ratio of ζ/ζ'. Denoting this ratio by a, we have:

$$\zeta = a\zeta'.$$

We calculate first the mean value of a for the depressions with circular form. We obtain:

$$a = 1{,}00.$$

so that formula (7) holds for circular depressions. We consider now the ratio between the axes in the depressions of elliptic form. In more than half of the total number of cases this ratio amounts to $^1/_2$, the other depressions not differing much from this "standard form". As the number of elliptic depressions is too small to investigate the influence of a change in the ratio between the axes, we investigate only the influence of "elliptic form", assuming all depressions to have nearly the *same* ellipticity. In this investigation we try to find the relation between the value of a and the direction θ of the longer axis. Of course this relation is also a function of the position of the centre of the depression, but we neglect this influence.

When we plot the values of a against the values of θ we obtain clearly a definite relation. Great individual scattering occurs, however. In order to obtain a formula, we consider again mean values (cf. table 18). We assumed the following formula for a:

$$a = 1 - a_0 \cos(2\,\theta - \varepsilon).$$

TABLE 18 *Mean values of a and* θ

θ	2°	62°	94°
a	0.79	1.16	1.17

We must, indeed, have a periodic function of 2θ; as when the direction of the depression has turned through 180°, its position is the same as before and we must have the same value of a. We obtain:

$$a = 1 - 0{,}21 \cos 2\,\theta. \tag{8}$$

In figure 20 this curve is shown with reference to the points of table 18.

Finally, therefore, we obtain for an elliptic depression the following formula:

$$\zeta = 0{,}0095\,(1 - 0{,}21 \cos 2\,\theta)\,\zeta'_{10}\,G^2.$$

In this formula ζ'_{10} is still the value of ζ_{10} in figure 11. With the aid of formula (8) we are able to reduce all depressions to "circular" ones, by calculating a new value of the windeffect (ζ') from the observed one (ζ) with the formula:

$$\zeta' = \frac{1}{a} \cdot \zeta.$$

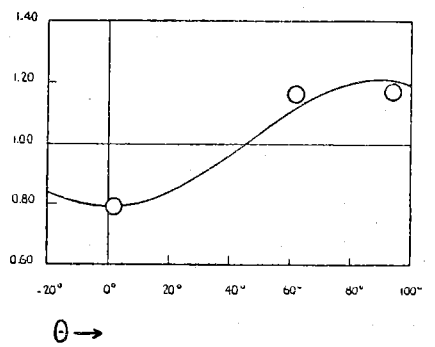

Fig. 20. Relation between a and θ

With the aid of the quadratic law in G we further reduce all values of ζ' to the value of ζ' for $G = 10$. We call these values ζ_{10}. They have been tabulated in column 12 of table 16. These values have been plotted on a map. They should all lie on isopleths. As, however, individual scattering exists, mean values have again been computed, giving

statistical weights to the different values of ζ_{10} according to the values of G^2, tabulated in column 13 of table 16. The mean values, obtained in this way are indicated by crosses in figure 21. But the scattering even in these values is too great, so that mean values were again computed, this time indicated by little circles in figure 21.

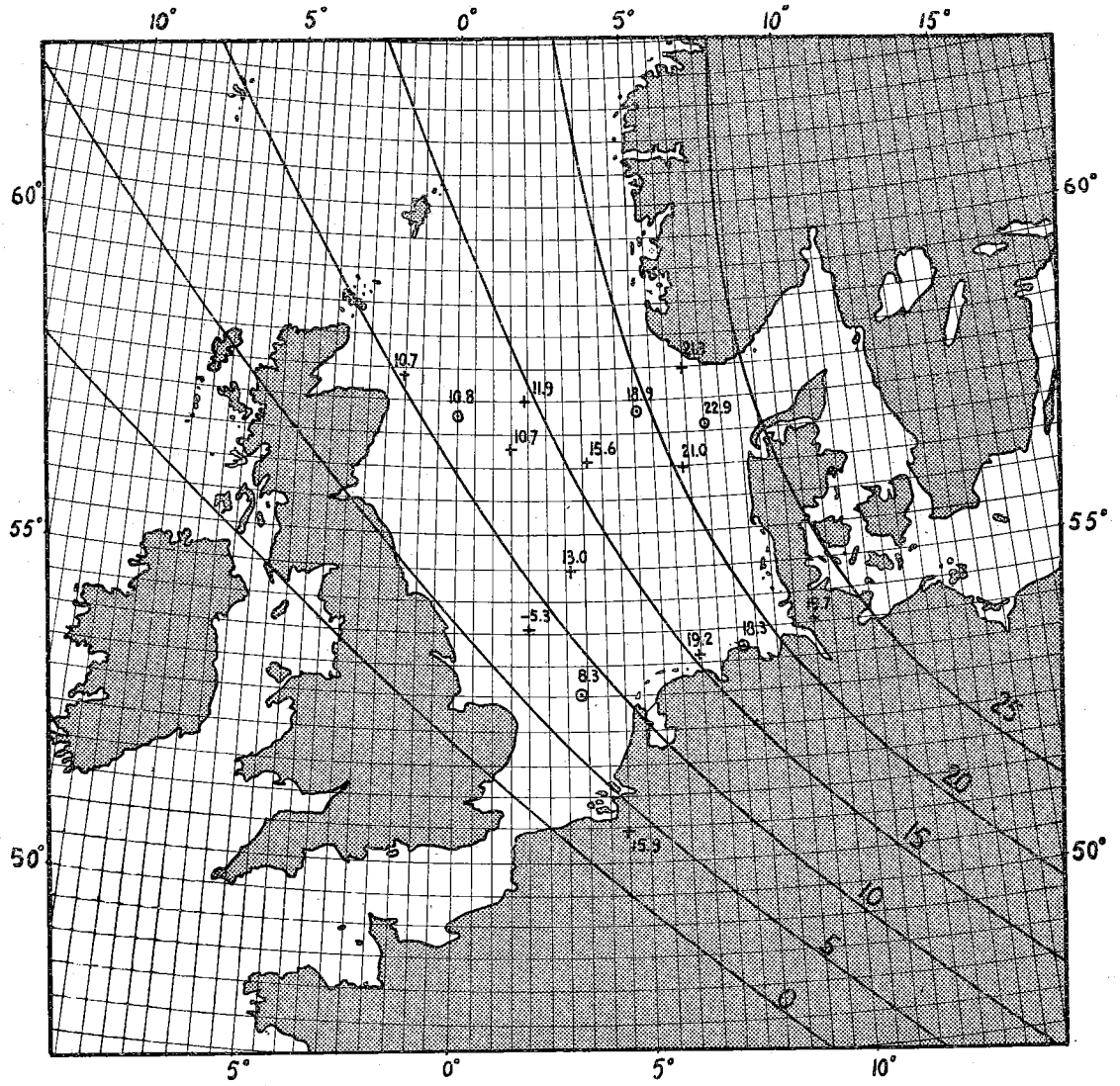

Fig. 21. Isopleths for ζ''_{10}

Through these points isopleths should be drawn for ζ_{10}. In doing this it should be borne in mind, that the position of the isopleths at a greater distance from the North Sea must be the same as in figure 11, as was pointed out previously. Taking into account all conditions we obtain finally the isopleths, drawn on figure 21. Comparing these isopleths with the lines of figure 11, we see that differences occur in the Northern part of the Sea. The empirical values of ζ_{10} are lower than the theoretical ones. In the Southern part, however, the empirical values are higher. For the rest, however, the agreement between theoretical and empirical values is satisfactory.

From these curves is read the value of ζ_{10} for the positions of the various depressions under consideration (ζ''_{10}!). ζ''_{10} has been tabulated in column 14. Comparing them with the values of ζ_{10} (column 11) we see large deviations. This scattering compelled us previously to work with mean values!

6. Time-lags

In the preceding paragraphs the stationary states have been analysed, now only the question of the time-lags must still be investigated.

We do this in the following way. With the aid of table 16 and formulas (4) and (2*a*) for all cases of homogeneous field of wind the value of ζ is computed. We omit in these computations the cases in which depressions occur, as we saw in the previous paragraph, that in these cases large individual scattering exists. The values of ζ obtained are now compared with the actual ones, especially for those cases, in which the windeffect increases or decreases. For these cases we compute the difference between the stationary (calculated) and non-stationary (actually found) value of ζ, that is $\triangle \zeta$.

We next consider the stretches of the rising and falling parts of the curves, that are nearly straight. When a constant time-lag exists, these stretches of the stationary and non-stationary curves must be parallel and for the difference $\triangle \zeta$ we should have everywhere:

$$\triangle \zeta = \frac{d\zeta}{dt} \cdot \triangle t \, .$$

$\triangle t$ = constant time-lag,
$d\zeta/dt$ = variation of ζ with time (e.g. cm/hour).

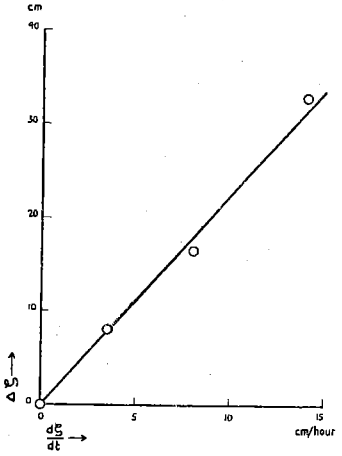

Fig. 22. The relation between $\triangle \zeta$ and $d\zeta/dt$ (rising part)

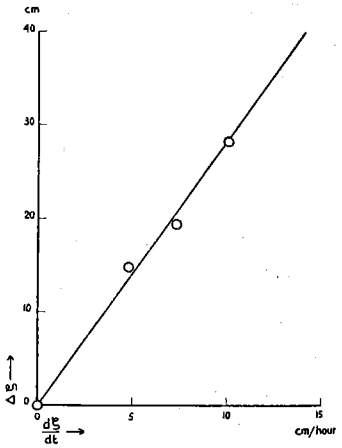

Fig. 23. The relation between $\triangle \zeta$ and $d\zeta/dt$ (falling part)

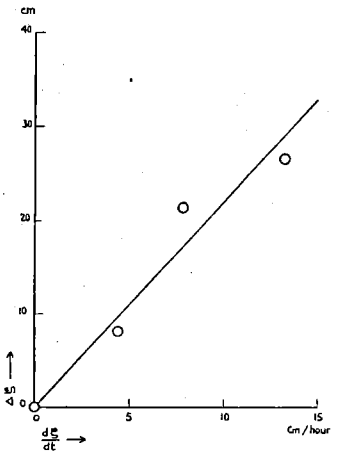

Fig. 24. The relation between $\triangle \zeta$ and $d\zeta/dt$ (oscillations)

When we plot $\triangle \zeta$ against $d\zeta/dt$, we should find a linear relation. This is found indeed; only a difference in time-lag exists between the rising and the falling part of the curve. Mean values of $\triangle \zeta$ and $d\zeta/dt$ are tabulated in table 19. These values are also plotted in figures 22 and 23. Clearly the linear relation holds very well, so that the assumption of a constant time-lag is fully justified. We compute the value of the time-lags from the figures. These values are also tabulated in table 19.

TABLE 19 *Mean values of $\triangle \zeta$ and $d\zeta/dt$*

Phenomenon		$\triangle \zeta$ (cm)			$\triangle t$ (hours)
Retardation occurring in rising part of the windeffect	$d\zeta/dt$	3.5	8.0	14.0	2,2
	$\triangle \zeta$	8.0	16.5	32.8	
Retardation occurring in sinking part of the windeffect	$d\zeta/dt$	4.8	7.3	10.1	2,8
	$\triangle \zeta$	14.8	19.4	28.2	
Difference between stationary and non-stationary value of the maximum	$d\zeta/dt$	4.4	7.8	13.2	2,2
	$\triangle \zeta$	8.1	21.4	26.6	

An other phenomenon connected with inertia is the fact, that the maximum oscillates to higher values than the stationary one. Hence we have also investigated the relation between the *maximum rising velocity* and the difference between the stationary and non-stationary values of this maximum (cf. table 19, and figure 24). It appears, that this relation is very nearly also a linear one, so that, here too, a sort of time-lag can be introduced, which has the meaning, that the difference between stationary and non-stationary values of the maximum is found by multiplying the maximum rising velocity by the (constant) value of the time-lag, which, according to figure 24, amounts to 2,2 hours. This is the same value as that of the time-lag for the rising part of the curve.

We also examined the difference in time between the reaching of the stationary and the non-stationary maximum. It appears, that this difference is rather constant and amounts likewise to:

$$\triangle t = 2{,}2 \text{ hours.}$$

It turns out, therefore, that all time-lags, for the rising part of the curve, amount to 2,2 hours. The time-lag for the falling part of the curve is somewhat greater: 2,8 hours. With the aid of these time-lags we are now able to compute approximately the actual development of a storm surge from the computed stationary curve and this stationary curve can be determined in its turn by means of table 16 and formulas (4) and (2a), so that we can now compute completely the actual development of the storm surges under consideration. A discussion of the results of this computation and of the other results is given in Chapter V.

CHAPTER V. RESULTS

In the preceding Chapters we studied theoretically and empirically the conditions in the North Sea. In the present Chapter the theoretical and empirical results will be compared. We shall try to explain the differences between them and discuss the accuracy, which can be reached in practice in the prediction of storm surges.

1. Agreement between theoretical and empirical results

a. Homogeneous fields of wind

For the homogeneous fields of wind the theoretical and empirical results concerning the stationary state are tabulated in table 20. We have given the values of maximum windeffect for $V = 10$ (m/sec) and the direction of the wind, causing this maximum effect.

TABLE 20 *Theoretical and empirical results compared*

	ζ_{max} (exp.)	ζ_{max} (theor.)	ψ_{max} (exp.)	ψ_{max} (theor.)
Section I	8,7 (cm)	6 (cm)	— 36°	— 15°
„ II	33,3 (cm)	40 (cm)	56°	50°
„ III	4,8 (cm)	8 (cm)	82°	80°

We have taken into account, that throughout our empirical investigations the direction of the *isobars* has been used. To obtain the corresponding direction of the *wind*, we subtracted 10° from the empirically derived values of the optimum directions of the isobars. On the whole a fair agreement between theory and practice is found, which is very satisfactory, as no perfect agreement between these two could be expected, the theoretical investigations being rather approximative.

It turns out, therefore, that the assumption of a bay, which is practically closed at its Southern end, as used in our theoretical considerations, is justified. Starting from this conclusion, we study once again the value and angular distribution of the windeffect in section II. The theoretical value, computed for this section, applies to a perfectly enclosed sea. Already in Chapter II we remarked, that this value will not be reached, due to the lowering influence of the Channel. For this value of the windeffect in section II applies to the case, that *no* wind is blowing in section I and III, so that the accumulated water can flow away to the "basin with normal level" constituted by the Channel. Thus a lower value of a_2 should be found, than the one theoretically calculated for a perfectly enclosed sea. We obtain indeed a lower value. The difference is, however, not appreciable, indicating that the influence of the Channel is not very large, which also was predicted in Chapter II. These theoretical considerations being all of them confirmed quite well, we should expect, that the theoretically computed *angular distribution* would also be confirmed by the empirical data. And this is not the case. In figure 21 we notice a very marked asymmetry instead of the cosine-law, which we expected to hold. This asymmetry cannot be explained by the presence of the Channel. For the effect of section II can be considered to be the total effect, if no wind blew in sections I and III. As in that case no fluctuations of the Channel occur, it acts only as a basin with constant sealevel, which reduces all values of the windeffect nearly in the same ratio. *Asymmetry*, however, is not caused by this fact, so that we have to look for another explanation. To this end we calculate:

$$\zeta' = 0{,}243 \cos(\psi - 46°).$$

We calculate also the ratio between ζ (the actual values of the windeffect, caused in section II, cf. table 15) and ζ'. We plot in figure 25 the values of this ratio ζ/ζ' against

the corresponding direction of the wind. A nearly symmetrical curve results, with a maximum near $\psi = 125°$. Besides, we calculate mean values of the difference in temperature, $\triangle T$ between the air and the sea ($\triangle T = T_{air} - T_{sea}$), which follow from the observations on the lightships, made during the periods of the storm surges considered. These values have been tabulated in table 21 and also plotted against ψ in figure 26.

Comparing figure 25 with figure 26 we see a striking analogy between the two curves in both, namely a strong rising setting in between $\psi = 0°$ and $\psi = 30°$, which in both curves continues till $\psi = 90°$. Here the curve for $\triangle T$ ends, as no sufficient data were available to extend it. But the analogy between the two parts of the curves is striking enough. This offers an explication of the asymmetry of the angular distribution, which is shown in figure 25. Other investigations (SEILKOPF, 71; KIMBALL, 72) already drew attention to the fact, that the height of the waves depends not only on the velocity of the wind, but is besides strongly influenced by the difference in temperature between air and sea.

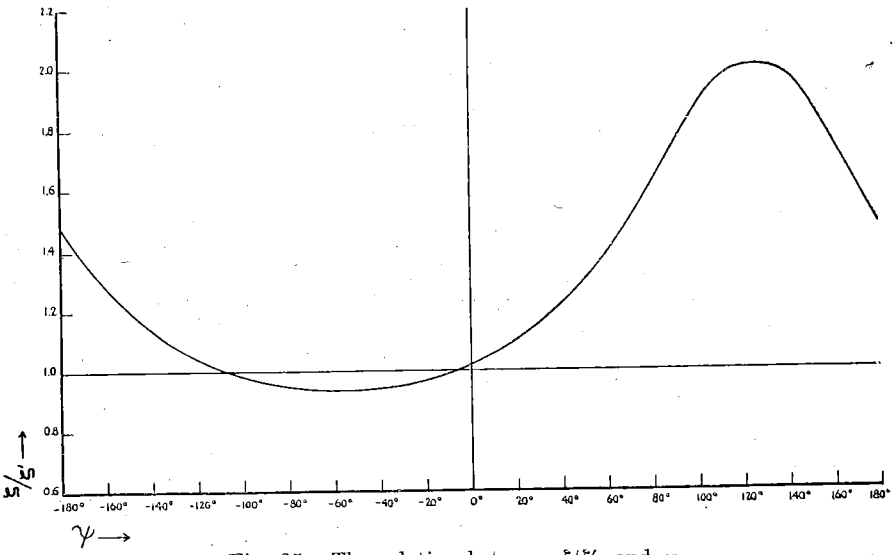

Fig. 25. The relation between ζ/ζ' and ψ

TABLE 21 *Relation between $\triangle T$ and the direction of the wind*

ψ	— 35°	— 22°	— 12°	— 1°	11°	22°	33°	43°	49°	55°	65°	84°
$\triangle T$.	— 0.3	— 0.5	— 0.6	— 0.7	— 0.5	— 0.6	— 1.3	— 1.6	— 2.0	— 2.1	— 2.4	— 3.4

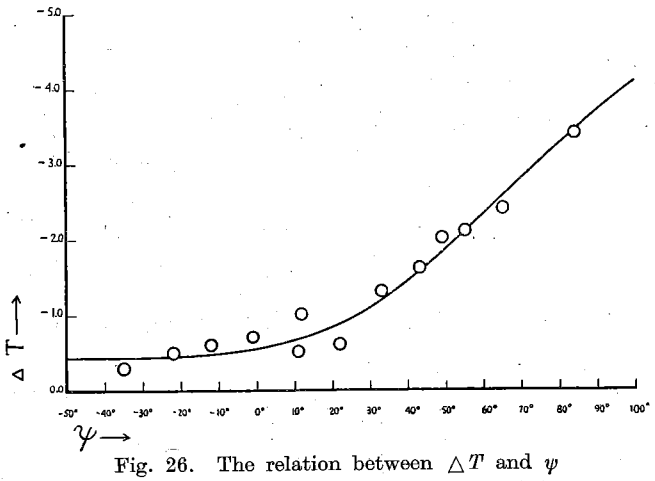

Fig. 26. The relation between $\triangle T$ and ψ

In a cold mass of air (air colder than the sea) the waves are much higher and more irregular than in warm air masses (air warmer than the sea). But if in a cold mass of air the sea is more disturbed by the wind than in a warm mass of air, the frictional forces will also be greater, the contact between air and water being clearly more pronounced. Greater frictional forces, however, cause also greater windeffects. For that reason the analogy between the curves of figure 25 and 26 may be assumed to result from this effect. We arrive, therefore, at the conclusion, that the asymmetry of the angular distribution of section II is, at least partly, explained by the influence of the difference in temperature between the air and the sea.

A second cause for the asymmetry, shown in figure 25, is, however, surely present. The size of the waves on the surface of the sea (which determines to a great extent the amount of the friction between wind and sea) is determined partly by the "*fetch*" of the wind over the water (cf. a. o. THORADE, 17). Applying this result to the North Sea, it turns out, that the highest waves will be present in the Southern part of this Sea, when

the wind blows parallel to the longitudinal axis of the sea, that means for $\psi = 80° - 90°$ (ψ refers to the *isobars*!) Now the maximum of the curve of figure 26 occurs near 125°. This is not perfectly in agreement with the value of ψ, just mentioned. Taking into account, however, the more or less approximative character of the curve for ζ in this interval, we are allowed to conclude, that this effect will also contribute to the asymmetry of the windeffect.

As this second effect is doubtlessly present, no quantitative results can be given concerning the influence of $\triangle T$ on the windeffect. Nevertheless these effects should certainly be borne in mind, in particular when comparing other investigations with the present results.

b. Depressions

The researches on the depressions were somewhat less satisfactory than those on the homogeneous wind fields. It is true, that the computed position of the isopleths (fig. 21) is in rather good agreement with the theoretical position (fig. 11), but a rather large scattering in the individual cases remains. This can be explained in the following way. We have determined the field of wind, connected with the depression, only by giving the *form* of the depression (direction and ratio of axes, gradient), but the wind is also influenced by the *motion* of the depression. For in a moving depression the paths of the airparticles acquire quite an other radius of curvature than can be computed from the isobars only, and this results in other values of the velocity of the wind. For that reason the mean position of the isopleths of figure 21, in which the motion of the depressions have been averaged out more or less is close to theory, but deviations occur in the individual cases. On that account we also reduced the number of cases of "depressions" as much as possible by considering them as "homogeneous" in the three separate sections of the sea and used the *actually recorded* wind, which was only *extrapolated* by the form of the isobars and the magnitude of the gradient in the sea. In this way we obtained in the cases of homogeneous wind a rather good approximation to the actual windvelocity on the sea. We should, therefore, use this method also in practice as much as possible.

c. Nonstationary state

We obtained the same time-lag, viz. 2,2 hours, for all effects, connected with the *rising* part of the storm surge: namely the retardation in the rising part, the excess of the real maximum over the stationary one, the retardation in the *time* of the maximum. It is easily explained why the retardation in the rising part and the oscillating up of the maximum are both ruled by the same time-lag, when namely both effects have the same time-lag, they have also the same *magnitude* (cf. Chapter IV, paragraph 6). And when the level of the sea was previously too low, it is only plausible, that it will oscillate upward afterwards, and become too high, and nearly by the same amount by which it was too low.

The time-lag by the falling part of the storm surge is greater than the time-lag for the rising part: 2,8 hours. This can also be explained easily: if no upward oscillating-effects were present the retardation would be the same as for the rising part, but the first-named effect adds to the "retardation" in adding to the height of the recorded windeffect. This is also in agreement with theory (cf. figures 13 and 14). The values of the time-lags themselves must, however, also be explained. In Chapter II we obtained as a result, that, when the wind rises suddenly and remains constant afterwards, the stationary value of the windeffect is only reached after 7 hours, if we omit the oscillations. Here we have, therefore, a time-lag of 7 hours. But if the wind varies "linearly" (viz. the value of the corresponding stationary state of the windeffect) it can easily be shown, that the stationary and non-stationary curves become nearly parallel after a short time and show a time-lag of $3\frac{1}{2}$ hours. This holds, however, only for a sea with constant depth. If we take into account the variation of the depth in the North Sea, a still smaller value of the time-lag is obtained, viz. $2\frac{1}{2}$ hours, approximately. This is rather close to the empirical values, which are therefore explained satisfactorily.

2. Comparison with previous investigations

In this paragraph we compare our results with the results obtained by previous investigations, concerning the conditions on the Dutch Coast (cf. Chapter I).

Like ORTT, we obtained a quadratic law for the windeffect as a function of the windvelocity. This result is different from the result of the committee "Rotterdamsche Waterweg", which obtained curves with a pronounced "point of inflexion". The explanation can easily be given. The parts of the curves, given by the committee (cf. figure 1), in which the slope decreases, are namely connected with very high velocities of the wind (11—12 Beaufort grades). These velocities were, however, not measured on the whole sea, but only at Hook of Holland. Now these high velocities of the wind rarely extend over a large area. They occur generally only in the "trough" of a depression, which covers only a certain limited area. For that reason the measured very high windvelocities at Hook of Holland correspond probably with a lower *mean windvelocity on the whole North Sea*! On that account the windeffect observed in connection with these windvelocities are also too low. And this naturally results in a "flattening" of the curves of figure 1.

Our results concerning the angular distribution are different from both ORTT's and the committee's results. Our curve has on the whole been shifted towards greater values of ψ. This can be explained by the fact that we correlated the windeffect with the direction of the wind (isobars) on the *Sea*. And generally the isobars on the Sea are veered with reference to the isobars on the coast, so that we obtain the same values of the windeffect for greater values of ψ than investigations who use the direction of the isobars on the *coast*.

The angular distribution, found by ORTT and the "committee" show very little asymmetry. In the case of the "committee" it can be shown that this results also from the different directions of the isobars on the *sea*. This is also true for ORTT, but in the latter case a second reason is present. His results are namely mean values of the windeffect during a *whole* year. And in this case air masses with other temperature-effects will be present also. This tends to reduce the effect which we held partly responsible for the asymmetry of our curves.

Finally we obtained a much lower value of the time-lag (2,2 and 2,8 hours) than ORTT (6 hours). The value of ORTT, however, will probably be connected with the fact, that he had only at his disposal the value of the windeffect with intervals of 6 hours (high and low tide!). This had as a quite natural effect, that the influence of the wind could not be perceived in the "simultaneous" value of the windeffect, but in the "next" one, so that his value of the time-lag could only be given in multiples of 6.

We arrive at the conclusion, that the differences between our results and those of former investigations can be explained quite satisfactorily and must be attributed chiefly to shortcomings in the methods previously used.

3. Prediction of storm surges in practice

By means of the results of Chapter IV we have calculated the values of the meteorological effect in the non-stationary state for all storm surges, which we have investigated. These values are at once comparable with the values actually found. In this way we can make out, whether our formulas give satisfactory results for the actual development of each individual storm-surge. The computation ran as follows. First the stationary curve was calculated. From this curve the time and position of the actual maximum was derived by means of the time-lags and the position of the rising and falling parts of the non-stationary curve were determined. These points were connected by a smooth curve. The values, obtained in this way for the meteorological effect, are shown in the figures 33*a*—46*a* by little circles. Besides, they were tabulated in tables 25—38. The oscillations *after* the storm

surges have not been calculated, as it is rather difficult to predict the actual period of these oscillations. We have, therefore, only calculated the stationary state for these parts of the curves.

If we consider the results, obtained in this way, it turns out, that the development of every individual storm surge is indeed represented very satisfactorily. This justifies the conclusion, that we are able to predict in practice also the development of future storm surges with considerable accuracy, by means of the results of Chapter IV. The different aspects of the computation will now be discussed in some detail.

a. Superposition of meteorological effect and the tides

It was found in Chapter III, that even when we calculated the astronomical effect from a great number of partial tides, the elimination of the tides was not perfect. Evidently the phase and the amplitude of the tidal waves change more or less during a storm surge in an unknown way. The superposition of the astronomical and meteorological effects is not wholly additive, as also other investigators found. But in practice it is just the height of high tide, which we need, as this is of the greatest importance in causing danger. We can calculate this height only by superposing the calculated meteorological effect and the value of high tide predicted in the tide-tables. Here, too, errors can therefore be made in an unknown way. This should be borne in mind in predicting the height of high tide, as well as in criticizing afterwards the results of a warning for storm surges.

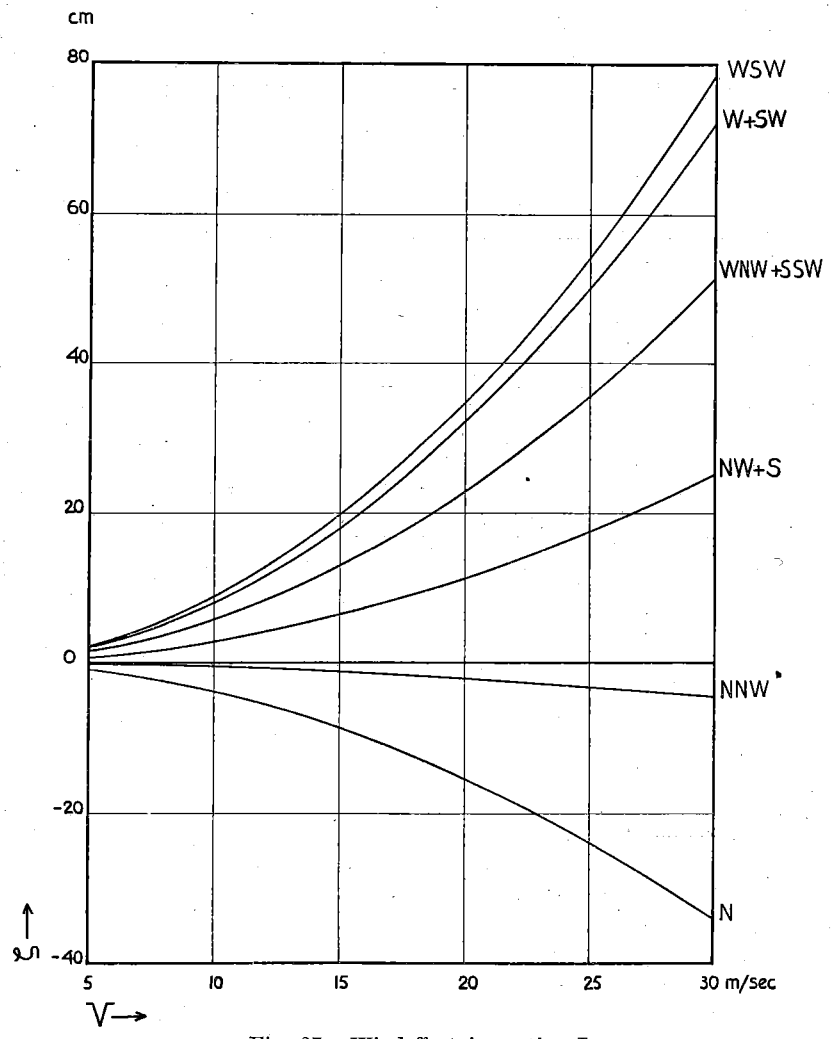

Fig. 27. Windeffect in section I

b. Phenomena of inertia

These are of importance for the determination of the actual development of a storm surge (e. g. the time of high water can occur in the period of rising meteorological effect). But we are chiefly interested in the maximum height of the meteorological effect. To evaluate this height we have to make an estimate of the maximum "rising-velocity" of this effect. In most cases this can easily be done. From figure 23 can be read immediately the amount, which must be added to the computed "stationary" value of the maximum. From the distribution of the points in figure 23 we see, that in most cases the "rising-velocity" amounts to 20—30 cm/hour. Although in many cases this rather rough approximation will be sufficient, a more accurate value will generally be needed.

c. Relation between windeffect and windvelocity

We found, that the windeffect is proportional to the square of the windvelocity. The highest mean value of the windvelocity for which this law was checked, amounted, however, only to 19 m/sec. In this mean value velocities up to 23 m/sec. were averaged, so that we can only conclude, that the quadratic law has been checked up to velocities of 20—23 m/sec. However, windvelocities higher than 25 m/sec will rarely be present above the *whole* Southern part of the North Sea. An extrapolation of the quadratic law up to 25 m/sec is justified, but extrapolation up to 30 m/sec becomes a little doubtful: HELLSTRÖM (48) obtained his value of 1,6 for the exponent of V exactly by taking into account the windeffect caused by very large windvelocities (up to 52 m/sec !) on an American lake. For that reason the parts of the curves between 25 m/sec and 30 m/sec in the curves of figures 27, 28, 29 and 30 should be used with some caution.

From these curves it follows also, that a large error is introduced into the value of the windeffect, if we make an error of 1 Beaufort in the estimated windforce (i. e. an error of 3 m/sec in the estimated windvelocity !), when this windforce is great (10 Beaufort or more). The windvelocity should, therefore, be estimated very carefully. Moreover we are concerned with the windvelocity on the *Sea*. It must be borne in mind that the average value of the ratio between the velocity of the actual wind and the velocity of the gradient wind was found to be 0,75 in our in vestigations, as otherwise in the practice of the Weather Service the windvelocity on the Sea might be estimated too low. Also the influence of warm or cold air mass must be taken into account.

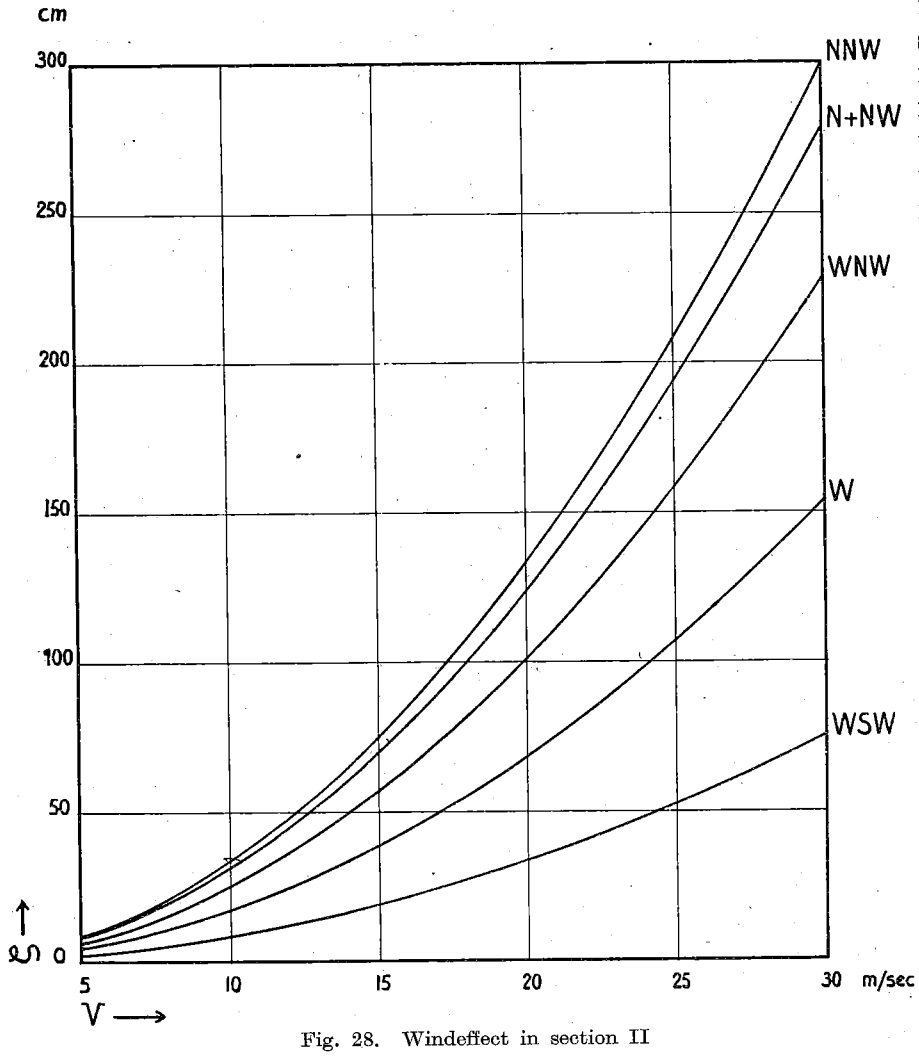

Fig. 28. Windeffect in section II

d. Relation between windeffect and direction of the wind

The graphs in figure 16—18 have been computed for the direction of the *isobars*. The graphs in previous investigations were always computed for the direction of the *wind*. But in the practice of the Weather Service the direction of the isobars can be predicted with greater accuracy than the direction of the wind. On that account we use in our graphs also the direction of the isobars.

Now the figures 16—18 give only curves for the quantity $a(\psi)$, which is used in the equation:

$$\zeta = a(\psi) \cdot V^2.$$

But in practice it is desirable to have a set of curves analogous to figure 1. We calculate, therefore, the value of the windeffect for a fixed direction of the isobars as a function of the velocity of the wind. The figures 27—29 refer to the three sections of the North Sea, figure 30 has been computed for a perfect homogeneous field of wind on the whole sea.

In using these graphs in practice, it should be borne in mind, however, that the windeffect is influenced also by the difference in temperature between the air and the sea (cf. paragraph 1 of this chapter).

All cases, investigated in the present investigation, occurred in autumn or in winter. But, though rare, a storm surge may also occur in summer. It is possible, that in such a case somewhat different conditions prevail, which would influence the value of the windeffect. This will hardly ever be the case, however.

For the prediction of the windeffect of *depressions*, the isopleths of figure 21 and formula 8 of chapter IV should be used. The accuracy of these predictions is not so great, however, as in the case of homogeneous fields of wind.

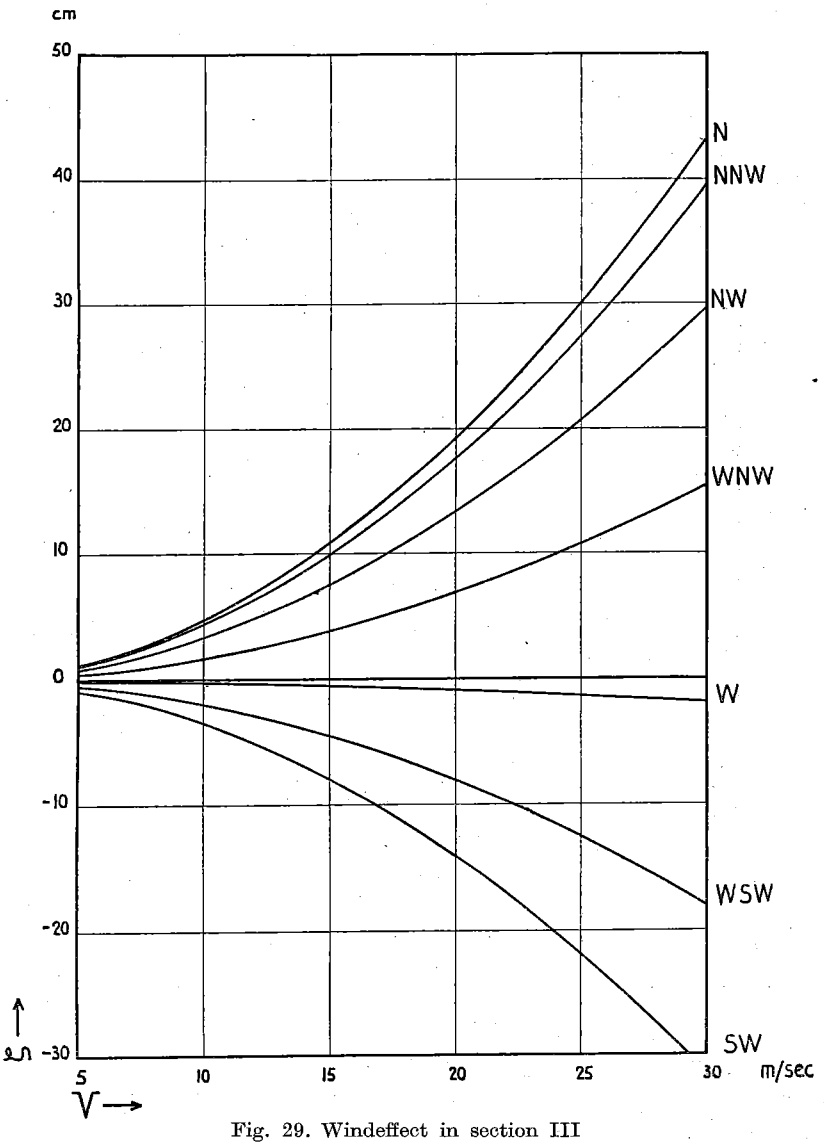

Fig. 29. Windeffect in section III

e. Effect of atmospheric pressure

For the average effect of the atmospheric pressure we obtained the formula:

$$(\triangle \zeta)_p = \tfrac{1}{2}(1003 - p).$$

With the aid of this formula the effect of the atmospheric pressure can in practice be calculated very simply. This formula does not yield absolutely reliable results, as it represents the *average* effect of the atmospheric pressure. The direction of the isobars, which is sure to influence this effect, has been neglected. As, however, the values of this "pressure-effect" always remain small, these omissions will not cause serious errors, as they would necessitate "corrections to a correction".

f. "Distant effects"

In the previous Chapters it was shown that the wind on the Atlantic needs only be taken into account, when a South-Westerly wind is present there over a large area. But this is very seldom the case. Moreover, in these cases there is never caused such a high windeffect on our coasts, that a "storm surge" results. If the wind on the Atlantic has an other direction, no windeffect will be caused at all. We may, therefore, neglect the wind on the Atlantic in the prediction of storm surges. The only "distant effect" we have to take into account is the wind in the Northern part of the North Sea. The influence of this section of the sea, however, is small, and has been fully determined by the graphs of figure 29.

In this section on "distant effects" we discuss also the influence of preceding storms ("distant in time" !). For preceding storms cause oscillations of the whole North Sea, which may yield additional height to the height of the next storm surge.

If such a case occurs, we have to take into account the period, amplitude and extinction of the oscillations caused by the preceding storm. It is rather difficult to estimate the amplitude. For in the storm surges we studied previously these amplitudes were found only after a careful elimination of the tides and after studying closely the remaining curves for the meteorological effect. In practice, however, an analogous analysis of the conditions of the sea cannot be carried out immediately after a storm surge has occurred, so that the amplitude of the oscillations must be estimated in an other way. We use to this end the graphs of figure 24, substituting here the *descending-velocity*. In this way we obtain an estimate of the amplitude of the oscillation after the storm. For evaluating easily the rate of extinction we computed the graphs of figure 31. For different values of the windvelocity we calculated with the aid of equation (1*a*) of Chapter IV the factor which must be multiplied by the initial value of the amplitude, so as to obtain the value of the amplitude at any moment.

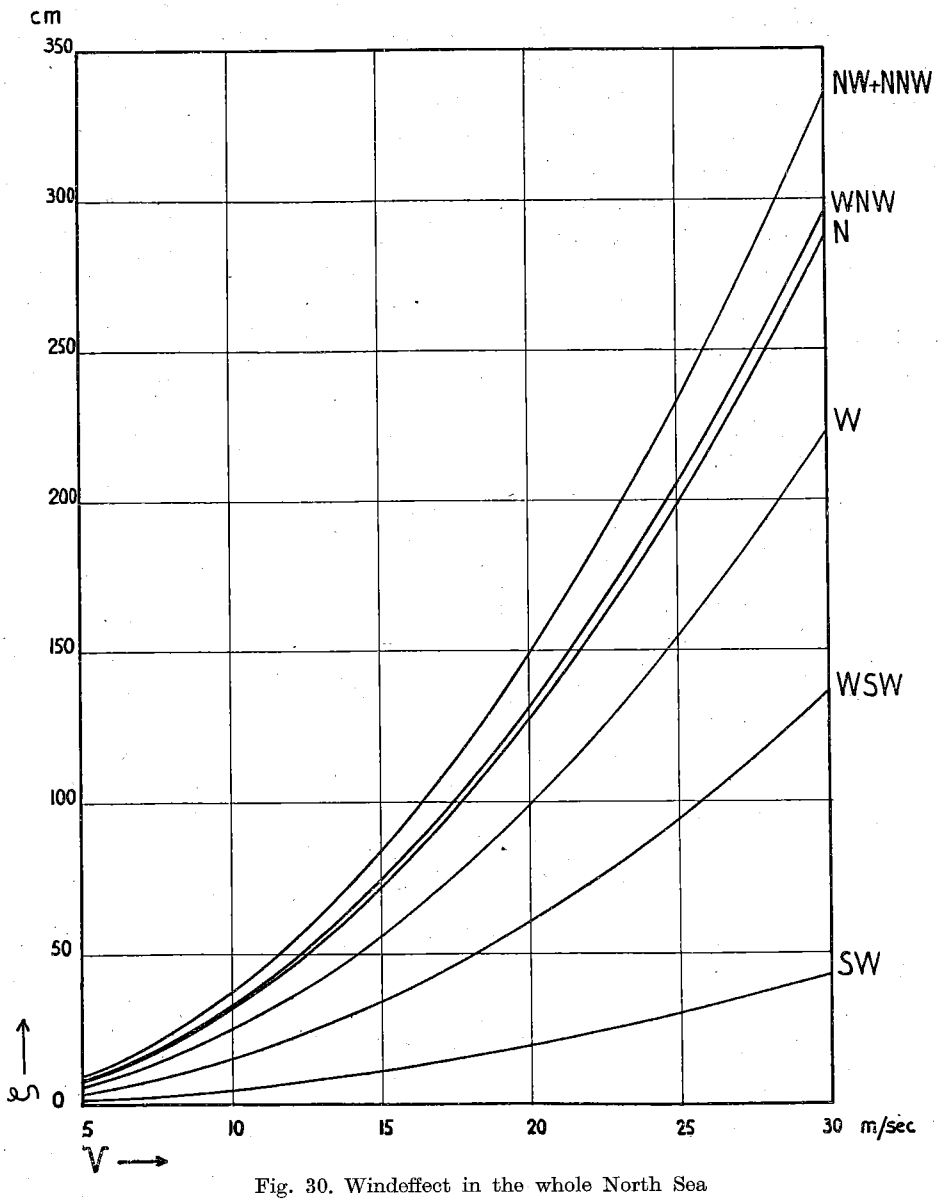

Fig. 30. Windeffect in the whole North Sea

If we assume a period of 40 hours it can be estimated whether or not the next storm surge can be influenced by the oscillations. The windvelocity should be taken into account, as it influences the rate of extinction considerably.

It will be generally found, that the influence of preceding storms is rather small.

g. Differences in the meteorological effect between places along the coast

This subject has not been investigated in the present study. ORTT, however, found, that the difference of the meteorological effect between Hook of Holland and Ymuiden was negligible. In practice, however, warnings for storm surges are given chiefly for places

in the vicinity of Hook of Holland, so that the study of the variation of the meteorological effect along the coast was superfluous. It turns out, in practice, that no serious errors are introduced by assuming the same value of the meteorological effect for all places on the coast between Flushing and Hook of Holland.

But farther North (up to the Helgoland Bight) the value of the meteorological effect is sure to vary. For Cuxhaven, for example, were observed the maximum values of the meteorological effect tabulated in table 22. The corresponding values at Hook of Holland have also been entered, from which a change in the effect along the coast appears, which must be perceptible already on the Dutch part of the coast. This can be explained theoretically by means of the formulas of Chapter II and Chapter IV. Besides, the theoretically computed values for Cuxhaven are also given in table 22. They are in perfect agreement with the empirical data. We shall here, however, not enter further into this question.

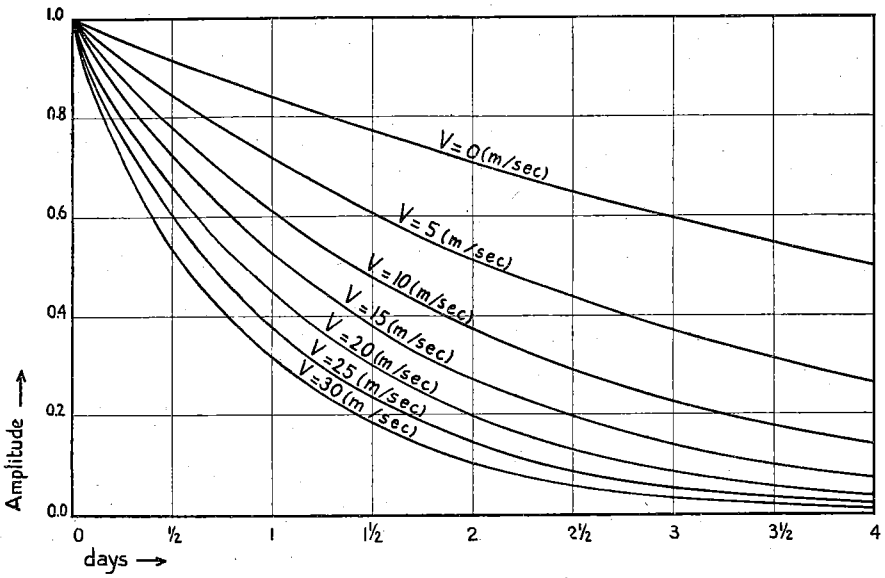

Fig. 31. Rate of extinction

In practice the prediction of a storm surge will run as follows. After having estimated the direction of the isobars and the velocity of the wind, which will occur in the three sections of the Sea, the stationary value of the windeffect is derived from the graphs of figures 27—30. The effect of the atmospheric pressure is subsequently added. In the case of a depression the isopleths of figure 21 must be used.

TABLE 22 *Meteorological effect at Cuxhaven*

Place \ Date	Oct. 18, 1936	Oct. 27, 1936
Hook of Holland . . .	155	140
Cuxhaven	320	330
Cuxhaven (theor.). . .	315	335

After having obtained the "stationary value" of the meteorological effect the maximum rising-velocity of the rising part of the effect is estimated. From the graph, given in figure 24, the additional height of the actual maximum is obtained. The time of this maximum is found by shifting the time of the "stationary maximum" by 2,2 hours. The retardation during the rising and falling part of the effect can be derived from figures 22 and 23. In this way we obtain an idea of the development of the meteorological effect. On this meteorological effect the height of the tides must be superposed, which are derived from the tide-tables. Only then can we form an opinion of the maximum height of the sealevel. If this height will endanger the dykes, a warning is issued. For Bergen op Zoom, situated on the East-Scheldt, the windeffect on this estuary has to be taken into account. From the preceding considerations it may be derived, that many sources of errors are present in the prediction of the height of a storm surge. Especially the estimate of the windvelocity is liable to uncertainty, so that it may cause large errors in the prediction. An error of 10 cm at least must be expected.

CHAPTER VI. THE WIND EFFECT ON THE EAST-SCHELDT

After having studied the meteorological effect on the Dutch coast, it is important to study also the windeffect caused in the estuaries, which break the coastline. For the windeffect, caused in places on the banks of these estuaries, consists of two parts: the windeffect on the *coast*, and the windeffect caused in the channel, formed by the estuary *itself*. For Bergen op Zoom, situated at the end of the East-Scheldt, this has been investigated by VAN EVERDINGEN. He found, that the windeffect (the "pressure-effect" was negligible) could be represented by:

$$\triangle \zeta = a(\psi) \, . \, V^2.$$

Here again, therefore, a quadratic law. $a(\psi)$ is the coefficient which represents the angular distribution of the windeffect. The values of $a(\psi)$ are tabulated in table 23. In this table, and throughout this chapter, ψ does not denote the direction of the *isobars* but of the *wind*.

TABLE 23 *Angular distribution of the windeffect on the East-Scheldt*

Direction of the wind	SW	WSW	W	WNW	NW	NNW
$a(\psi)$	0.054	0.111	0.212	0.240	0.245	0.171

An approximate value for $a(\psi)$ can be found. The windeffect can then be represented by the equation:

$$\triangle \zeta = 0{,}26 \; V^2 \cos(\psi - 30°). \tag{1}$$

If, however, we calculate the value of the constant factor of equation (1) theoretically, we obtain a much smaller value than 0,26. Besides, it turned out in practice that formula (1) yielded results, which were far too high. This problem has therefore been investigated again. The theory is discussed in the first paragraph. Next a better formula is derived from the data at our disposal, which agrees perfectly with theory. And finally the reason, why VAN EVERDINGEN obtained such a different result, is investigated.

1. Theory

In discussing the theory of the windeffect in the East-Scheldt, we are allowed to treat this as a case of a long, narrow channel, closed at one end. In this case, according to several investigations, we have

$$\triangle \zeta = \frac{0{,}036 \; V^2 \, L \cos(\psi - \psi_0).}{H} \tag{2}$$

L = length of the channel (in km),
V = windvelocity (in m/sec),
ψ = direction of the wind,
ψ_o = direction of the channel,
H = depth of the channel.

From the theory, given in Chapter II, we can derive immediately the result, that the formula for the windeffect must have indeed the same form as equation (2). In Chapter II, however, we assumed a value of 0,032 for the constant factor, in accordance with the results of PALMÉN. But the investigations of PALMÉN are concerned with a large inland sea. For that reason the value he obtained for this coefficient cannot be simply applied to the case of a narrow channel, as here other conditions prevail. That is why we use throughout this chapter the value 0,036, which has turned out to be in good agreement with the conditions in channels.

In formula (2) we have to substitute the values of L, ψ_o and H for the East-Scheldt. Here, however, some difficulties arise. The East-Scheldt consists namely of parts with very different depths. Especially transversely the depth changes considerably: apart from one or two very deep navigable channels, very shallow parts occur. In the longitudinal direction changes in H and ψ_o occur also. All these changes in depth must be taken into account. First we shall investigate the influence of the depth changing in transverse direction.

We assume the slope γ of the waterlevel to be always directed parallel to the longitudinal axis of the part in question of the channel. And moreover, that γ is a constant everywhere in a *transverse* direction. This is not absolutely in accordance with reality, but this assumption will do in our case.

If we neglect the rotation of the earth, which is allowed in the case of a narrow channel, we can easily derive from the theory of Chapter II, that the total current in a point of a cross-section of the channel can be represented by the equation:

$$S(b) = p\gamma H^3(b) + q W H^2(b).$$

H = depth of the channel, considered as a function of the transverse coordinate b;
p, q = constants, which are independent of H;
γ = slope of the watersurface;
W = vector of the frictional force of the wind.

If the depth of the channel were constant over a cross-section, we should everywhere have $S = 0$. Hence:

$$\gamma = -\frac{q}{p} \cdot \frac{W}{H}.$$

But in our case this is no longer true. In the shallow parts there will exist a current which flows in the direction of the wind, and in the deep parts the water will flow in the opposite direction. The only condition for the stationary state is, that the total current through the *whole* cross-section shall be equal to zero, as the channel is closed and in no place a permanent accumulation of water occurs. Hence:

$$\int_0^B S(b) \, . \, db = 0.$$

B = total breadth of the channel. Substituting in the equation for S:

$$\int_0^B S(b) \, . \, db = p\gamma \int_0^B H^3(b)\, db + qW \int_0^B H^2(b)\, db = 0.$$

$$\gamma = -\frac{q}{p} \cdot \frac{\int_0^B H^2(b)\, db}{\int_0^B H^3(b)\, db} \, . \, W.$$

We can put this formula into the form:

$$\gamma = -\frac{q}{p} \cdot \frac{W}{\overline{H}},$$

if we introduce for H the formula:

$$\overline{H} = \frac{\int_0^B H^3(b)\, db}{\int_0^B H^2(b)\, db}. \qquad (3)$$

In the case of the East-Scheldt we can, therefore, avail ourselves of formula (2), provided we calculate an "average" value of H with the aid of formula (3).

If we calculate the value of $\bar{H}$ in the way just mentioned for all parts of the East-Scheldt, it appears that $\bar{H}$ changes along the channel. We put therefore:

$$\bar{H} = \bar{H}(l).$$

l = coordinate in the longitudinal direction of the channel.

It was already pointed out, that ψ_0 is also a function of l, so that the total windeffect along the channel can be represented by:

$$\triangle \zeta = 0{,}036\, V^2 . \int_0^L \frac{\cos\{\psi - \psi_o(l)\}\, dl.}{\bar{H}(l)}$$

L = total length of the channel.

Evaluating $\triangle \zeta$ by means of this formula in the case of the East-Scheldt, we finally obtain:

$$\triangle \zeta = 0{,}10\, V^2 \cos(\psi - 20°). \tag{4}$$

Comparing this formula with formula (1) it appears, that the optimum direction of the wind computed by us ($\psi_0 = 20°$) agrees rather well with the result of VAN EVERDINGEN ($\psi_0 = 30°$). The value of the coefficient we obtained, however, is much smaller (0,10) than VAN EVERDINGEN's value (0,26). And it will presently turn out, that our theoretical result is confirmed perfectly by the empirical investigation.

2. The material

Here too, as in the investigations in preceding Chapters, we have to obtain data concerning the *wind* and the *windeffect* on the East-Scheldt. They will be treated separately.

a. *Windeffect*

For the derivation of the windeffect on the East-Scheldt we have to compare the height of the waterlevel at the beginning and at the end of the channel. But in this case, records of the waterlevel are not available as in the case of Hook of Holland. At the beginning (*Burgh*) and at the end (*Bergen op Zoom*) of the channel only the height of the *high tide at day* is observed. In order to obtain the value of the windeffect in the channel, we have therefore to compare the differences between the calculated and actually observed values of these high tides. This yields the windeffect at Burgh and Bergen op Zoom. And we obtain finally the windeffect, caused in the channel itself, by taking the difference of the two windeffects. We see, therefore, that we must first of all compute the astronomical height of high tide at Burgh and Bergen op Zoom. Now only for the places Zierikzee and Wemeldinge, situated on the East-Scheldt, predictions of the height of the tides are published in the tide-tables for the Dutch coast. That is why we tried to start from *these* predictions for the computation of the heights of the corresponding tides at Burgh and Bergen op Zoom. Without going into detail we give the results of our investigation. Introducing:

Bu = height of high tide at Burgh,
Z = height of high tide at Zierikzee,
W = height of high tide at Wemeldinge,
Be = height of high tide at Bergen op Zoom,

we have:

$$Bu = Z - 3.$$

$$Be - 189 = 1{,}129\,(W - 161).$$

All values of the height of high tide are expressed in cm with reference to N.A.P. By means of these formulas we are able to calculate the height of high tide at Burgh and

Bergen op Zoom. The value of the windeffect can then be found by comparing the calculated and actually observed values of the high tides. Finally the windeffect caused in the channel itself is obtained by taking the difference between the windeffects at Burgh and Bergen op Zoom. We obtain in this way the values of table 24.

b. The wind

In order to obtain the value of the velocity and the direction of the wind on the East-Scheldt VAN EVERDINGEN used the records of the wind at Flushing. It turns out, however, that owing to the meteorological station being situated in the vicinity of the town, the recording of the windvelocity yields values, which are too low, when $\psi > 0°$. When $\psi < 0°$, the windvelocities, recorded at Flushing are in agreement with the velocities, recorded at the other stations on the coast. When $\psi > 0°$, however, the velocities at Flushing amount only to 60—65 % of the velocities recorded elsewhere. If we introduce:

V = actual velocity of the wind,
V' = recorded velocity of the wind (for $\psi > 0°$),

we have approximately:

$$V = 1{,}6\ V'.$$

Substituting in formula (4):

$$\triangle \zeta = 0{,}26\ V'^2 \cos(\psi - 20°).$$

This formula is nearly identical with formula (1), so that, in all probability, the wrong result of VAN EVERDINGEN is caused by his using wrong values of the windvelocity. For obtaining the true velocity of the wind we have therefore used:

for $\psi < 0°$: the records at Flushing, Hook of Holland and IJmuiden;
for $\psi > 0°$: the records at Hook of Holland and IJmuiden.

Moreover, it appeared from the preceding chapters, that time-lags occur in the generation of the windeffect. We assumed a time-lag of 1—2 hours for the East-Scheldt and for that reason correlated the windeffect with the average value of the wind over a period of 3 hours before the time of high tide.

Also we did not use the directions of the *isobars*, but of the *wind itself*.

The values obtained in this way, are tabulated in table 24.

TABLE 24 *Values of windeffect and wind on the East-Scheldt*

Date	V	ψ	ζ	Date	V	ψ	ζ
17 January 1921 . . .	11.5	— 85°	6	20 December 1926 . . .	17.5	90°	40
18 January 1921 . . .	14.0	— 45°	16	21 December 1926 . . .	7.0	40°	— 1
18 January 1921 . . .	20.0	0°	30	23 November 1928 . . .	8.0	— 65°	9
19 January 1921 . . .	18.5	25°	26	24 November 1928 . . .	18.5	0°	43
5 November 1921 . . .	15.5	5°	23	25 November 1928 . . .	16.0	— 20°	24
6 November 1921 . . .	22.0	30°	26	26 November 1928 . . .	17.0	30°	21
25 November 1925 . . .	16.0	40°	35	13 January 1930 . . .	12.5	— 25°	— 4
26 November 1925 . . .	4.0	90°	2	14 August 1930 . . .	16.0	15°	24
27 November 1925 . . .	14.0	30°	22	15 August 1930 . . .	15.0	20°	23
9 March 1926 . . .	13.0	— 30°	20	16 August 1930 . . .	7.0	20°	5
10 March 1926 . . .	20.5	35°	29	10 November 1930 . . .	13.5	25°	6
9 October 1926 . . .	17.0	— 25°	7	11 November 1930 . . .	16.0	50°	1
10 October 1926 . . .	20.0	15°	25	12 November 1930 . . .	11.0	0°	8
10 October 1926 . . .	9.0	— 20°	3	22 November 1930 . . .	13.0	— 60°	25
11 October 1926 . . .	12.0	— 55°	— 3	23 November 1930 . . .	21.0	50°	50
12 October 1926 . . .	7.0	— 30°	5	23 November 1930 . . .	16.0	10°	35
13 October 1926 . . .	12.0	— 20°	4	17 January 1931 . . .	19.0	25°	53

Date	V	ψ	ζ	Date	V	ψ	ζ
18 January 1931 . . .	14.0	30°	22	6 December 1936 . . .	15.0	— 5°	22
16 February 1935 . . .	19.0	— 25°	29	7 December 1936 . . .	11.0	80°	— 6
17 February 1935 . . .	9.0	— 10°	11	19 February 1937 . . .	9.0	20°	0
19 October 1935 . . .	16.0	— 55°	12	28 January 1938 . . .	16.0	20°	17
20 October 1935 . . .	12.5	30°	16	29 January 1938 . . .	17.0	— 50°	— 9
8 September 1936 . . .	18.0	— 5°	32	30 January 1938 . . .	22.0	20°	57
16 October 1936 . . .	13.0	20°	4	31 January 1938 . . .	15.0	60°	30
17 October 1936 . . .	13.0	— 10°	12	1 February 1938 . . .	10.0	— 50°	1
18 October 1936 . . .	15.0	30°	13	2 February 1938 . . .	15.0	— 30°	15
19 October 1936 . . .	13.0	20°	18	3 April 1938 . . .	11.0	20°	8
20 October 1936 . . .	12.0	65°	20	4 April 1938 . . .	17.0	45°	18
26 October 1936 . . .	11.5	— 60°	— 8	30 May 1938 . . .	9.0	10°	7
27 October 1936 . . .	20.0	0°	33	31 May 1938 . . .	19.0	— 10°	35
28 October 1936 . . .	15.0	35°	1	3 October 1938 . . .	8.5	— 70°	— 16
30 November 1936 . . .	11.0	— 5°	— 7	4 October 1938 . . .	16.5	— 55°	— 6
1 December 1936 . . .	16.5	35°	12	5 October 1938 . . .	22.0	— 20°	33
2 December 1936 . . .	12.0	20°	22	22 April 1939 . . .	18.0	— 65°	— 17
4 December 1936 . . .	11.0	— 10°	14	23 April 1939 . . .	12.0	20°	12
5 December 1936 . . .	10.0	— 70°	4		11.0	5°	11

3. Investigation of the material and results

According to theory the windeffect can be represented by formula (4):

$$\triangle \zeta = 0{,}10\ V^2 \cos(\psi - 20°). \tag{4}$$

Applying a method, analogous to those used in previous Chapters, it was first shown, that also in the present case, the windeffect was proportional to the square of the velocity of the wind.

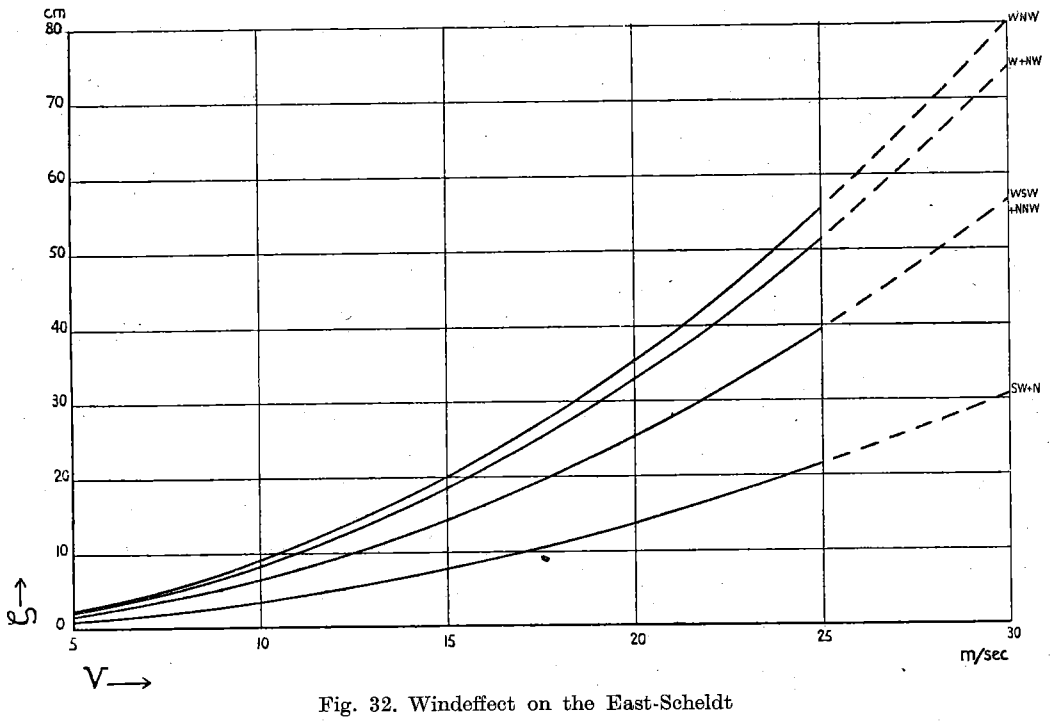

Fig. 32. Windeffect on the East-Scheldt

As this investigation offers no new points of view, we abstain from giving further details.

Having established the quadratic law, here again all values of the windeffect could be reduced to the same velocity and subsequently be compared. The cosine-law could be

shown to hold indeed. This was to be expected, because here no such effects are present, as invalidate the cosine-law on the North Sea.

Having established also the form of the angular distribution, the value of the constant in the formula could be determined by the method of least squares. We obtained:

$$\triangle \zeta = 0{,}089\ V^2 \cos(\psi - 24°). \tag{5}$$

This formula is in excellent agreement with equation (4) as well as regards the optimum direction of the wind as the value of the constant. It is hereby once more shown, that formula (1) was erroneous.

For the practical application of formula (5) it is desirable to convert it into a set of graphs, showing the value of the windeffect for different directions of the wind. This has been carried out in figure 32. The graphs refer to the directions SW, WSW, W, WNW, NW, NNW and N.

From formula (5) it appears, that the graphs for the directions W and NW are nearly identical, also for WSW and NNW, SW and N.

In order to avoid undue intricacy, we computed, therefore, "mean curves" for these "pairs of directions"; these curves, which are quite sufficient for practice, are given in figure 32. The curves are drawn as full lines only up to $V = 25$ m/sec. As this is, here again, the limiting value, to which the quadratic law has been checked. Up to 30 m/sec, however, this law has been extrapolated, which is indicated in the figure by the broken lines.

To predict the total value of the windeffect at Bergen op Zoom, we have to predict first the windeffect on the coast. To this value the windeffect has to be added, caused according to the graphs by the wind on the coast in the East-Scheldt. In practice this has been done already in a number of cases, with quite satisfactory results.

REFERENCES

(1) E. Engelenburg, Ann. Hydr. **19**, 489 (1891).

(2) E. Engelenburg, Over den invloed van windrichting en luchtdrukking op den zeespiegel. De Ingenieur, **39** (1891).

(3) F. L. Ortt, Verhandelingen Kon. Inst. v. Ingenieurs 1896—1897, p. 117—130.

(4) F. L. Ortt, Invloed van wind- en luchtdruk op de zeestand te Den Helder.

(5) F. L. Ortt, Nature **56**, 80 (1897).

(6) P. H. Gallé Stormvloeden langs de Noordzee- en de Zuiderzeekusten (Leiden, 1917).

(7) J. P. van der Stok, Elementaire theorie der getijden. Mededeelingen en verhandelingen van het K.N.M.I., **8** (1910).

(7*a*) J. P. van der Stok, Elementare Theorie der Gezeiten. Ann. d. Hydr. **39**, 227, 303, 354 (1911).

(8) Verslag van de Staatscommissie inzake buitengewoon hooge waterstanden op den Rotterdamschen Waterweg ('s-Gravenhage, 1920).

(9) G. Simpson, Professional Notes, Vol. IV, Nr. 44 (1926).

(10) E. van Everdingen, Annales de la Commission pour l'Etude des Raz de Marée, **4**, 116 (1933).

(11) C. W. Lely, Verhooging van de stormvloedstanden op de Friesche kust tengevolge van de afsluiting van de Zuiderzee (Leiden, 1918).

(12) C. W. Lely, De invloed van de Zuiderzee op de stormvloedstanden langs de Friesche kust. Diss. (1921).

(13) Verslag van de Staatscommissie inzake hoogere waterstanden tijdens storm, als gevolg van de afsluiting van de Zuiderzee (1926).

(14) J. P. Mazure, De berekening van getijden en stormvloeden op benedenrivieren. Diss. (1937).

(15) R. Witting, Finnländische hydrographisch-biologische Untersuchungen Nr. 2, (Helsingfors, 1908).

(16) O. Krümmel, Handbuch der Ozeanographie, Bd. II (1911).

(17) H. Thorade, Probleme der Wasserwellen, (Hamburg, 1931).

(18) H. Lentz, Flut und Ebbe und die Wirkungen des Windes auf dem Meeresspiegel. (Hamburg, 1879).

(19) Bubendey, Zentralblatt der Bauverwaltung **15**, 72 (1895).

(20) A. T. Doodson, Geoph. Mem. Vol. V, Nr. 47 (1929).

(21) J. S. Dines, Geoph. Mem. Vol. V, Nr. 47 (1929).

(22) A. T. Doodson, Monthly Notices of the Roy. Astr. Soc., Geoph. Suppl. I, Nr. 4, 124 (1924).

(23) B. Schulz, Archiv der Deutschen Seewarte **47**, Heft 1 (1920).

(24) Möller, Zentralblatt der Bauverwaltung **15**, No. 37 (1895).

(25) D. la Cour, Publikationer fra det danske Meteorologiska Institut, Meddelelser Nr. 4, 1—83 (1917).

(26) H. Thorade, Ann. Hydr. **46**, 234 (1918).

(27) J. Proudman and A. T. Doodson, Proc. Lond. Math. Soc., Ser. 2, **24**, part 2, 140 (1924).

(28) H. Horrocks, Proc. Roy. Soc. London, A, **115**, 170 (1927).

(29) K. Hidaka, Geophys. Mag., Tokyo, **7**, 234 (1933).

(30) K. Hidaka, Mem. Imp. Mar. Obs. Kobe, **5**, 51 (1932).

(31) K. Hidaka, Mem. Imp. Mar. Obs. Kobe, **5**, 141 (1933).

(32) K. Hidaka, Mem. Imp. Mar. Obs. Kobe, **5**, 255 (1933).

(33) T. Nomitsu, Mem. Coll. Sc. Kyoto Imp. Univ. Series A, **16**, 161 (1933).

(34) T. Nomitsu, Mem. Coll. Sc. Kyoto Imp. Univ. Series A, **16**, 275 (1933).

(35) T. Nomitsu, Mem. Coll. Sc. Kyoto Imp. Univ. Series A, **16**, 309 (1933).

(36) T. Nomitsu, Mem. Coll. Sc. Kyoto Imp. Univ. Series A, **16**, 203 (1933).

(37) T. Nomitsu, Mem. Coll. Sc. Kyoto Imp. Univ. Series A, **16**, 333 (1933).

(38) T. Nomitsu and T. Takegami, Mem. Coll. Sc. Kyoto Imp. Univ. Series A, **17**, 93 (1934).

(39) T. Nomitsu, Mem. Coll. Sc. Kyoto Imp. Univ. Series A, **17**, 249 (1934).

(40) A. Colding, Det Kong. Danske Vid Selsk. Skrifter, naturw. og math. Afd. 5, Raekke, XI: 3, 247 (1880).

(41) A. Colding, Det Kong. Danske Vid. Selsk. Skrifter, 6 Raekke, I, 243 (1881).

(42) Dr. Leverkinck, Veröff. des Kaiserlichen Obs. in Wilhelmshaven. Berlin, 1915.

(43) J. Hayford, Effects of winds and of barometric pressures on the great lakes. Publ. Carnegie Inst., Washington, 1922.

(44) E. Palmén, Commentationes Physico-mathematicae VI, No. 14 (Helsingfors, 1932).

(45) E. Palmén, Ann. Hydr. **60**, 435 (1932).

(46) E. Palmén and E. Laurila, Commentationes Physico-Mathematicae X, No. 1 (Helsingfors, 1938).

(47) E. Palmén, Commentationes Physico-Mathematicae XI, No. 7 (1941).

(48) B. Hellström, Windeffect on lakes and rivers. Diss. (Stockholm, 1940).

(49) H. Prügel, Die Sturmflutschäden an der Schleswig-Holsteinischen Westküste in ihrer meteorologischen und morphologischen Abhängigkeit. Schriften des Geographischen Instituts der Universität Kiel, Band II, Heft 3.

(50) V. W. Ekman, Ark. f. Mat., Astr. och Fys., K. Svenska Vet. Ak. Stockholm, **2**, Nr. 11 (1905/1906).

(51) V. W. Ekman, Arkiv f. Mat., Astr. och Fys. **17**, K. Svenska Vet. Ak. Stockholm, Nr. 26 (1922/1923).

(52) V. W. Ekman, Dynamische Gesetze der Meeresströmungen. Vorträge aus dem Gebiete der Hydro- und Aerodynamik (Levi-Civita and v. Kármán), 97 (1922).

(53) H. Jeffreys, Phil. Mag. **46**, 114 (1923).

(54) H. Jeffreys, Phil. Mag. **49**, 793 (1925).

(55) J. Proudman, Monthly Notices of the Roy. Astron. Soc. II, No. 4, 197 (1929).

(56) C. K. M. Douglas, Met. Mag. **64**, 187 (1929).

(57) T. Nomitsu, Mem. Coll. Sc. Kyoto Imp. Univ., Series A, **18** (No. 4), 201 (1935).

(58) T. Takegami, Mem. Coll. Sc. Kyoto Imp. Univ., Series A, **19** (No. 3), 109 (1936).

(59) T. Takegami, Mem. Coll. Sc. Kyoto Imp. Univ., Series A, **21** (No. 2, 3), pag. 55 (1938).

(60) L. Prandtl, Beiträge zur Physik der fr. Atmosphäre, **19**, 188 (1932).

(61) Th. v. Kármán and T. Levi-Civita, Vorträge aus dem Gebiete der Hydro- und Aerodynamik. (1922).

(62) J. E. Fjeldstadt, Z. Angew. Math. u. Mech. **10**, 121 (1930).

(63) T. Takegami, Mem. Coll. Sc. Kyoto Imp. Univ. Series A, **17** (No. 5), 305 (1934).

(64) F. Wolf, Z. f. angew. Math. u. Mech. **6**, 118 (1926).

(65) R. Courant, Z. f. angew. Math. u. Mech. **6**, 322 (1926).

(66) G. I. Taylor, Proc. Lond. Math. Soc., Sec. Series, **20**, 148 (1922).

(67) C. Braak, Het klimaat van Nederland. D. Wind. Mededeelingen en Verhandelingen van het K. N. M. I., **32** (1929).

(68) C. Braak, Het klimaat van Nederland. D (vervolg). Wind. Mededeelingen en Verhandelingen van het K. N. M. I., **46** (1942).

(69) E. Kuhlbrodt, Ann. Hydr., zweites Köppenheft, 14 (1936).

(70) G. Bleck, Ann. Hydr. **70**, 293 (1942).

(71) H. Seilkopf, Wind, Wetter und Wellen auf dem Weltmeere (Das Meer in volkstümlichen Darstellungen, Bd. 8, 1940).

(72) H. H. Kimball, Monthly Weather Rev. **48**, 147 (1920).

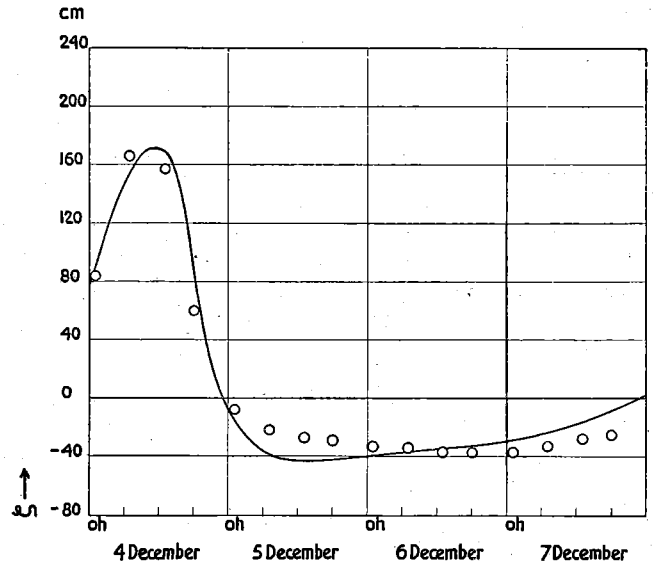

Fig. 33*a*. The storm surge of December 1920 (empirical and theoretical data)

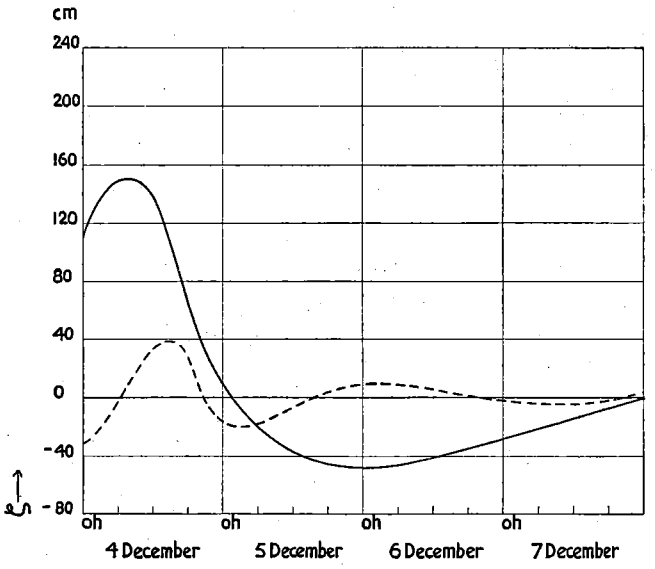

Fig. 33*b*. The storm surge of December 1920 (oscillations due to inertia separated from "stationary state")

TABLE 25 *Numerical data concerning the storm surge of December 1920*

Date	Hour	V_1	ψ_1	V_2	ψ_2	V_3	ψ_3	ζ (exp.)	ζ_0	$(\Delta\zeta)_p$	$\zeta_0-(\Delta\zeta)_p$	ζ (calc.)	ΔT
4 December	1	Depression (see table 16)						90	121	— 1	122	84	— 0.5
id.	7	Depression (see table 16)						155	150	1	149	166	— 1.2
id.	13	Depression (see table 16)						168	131	1	130	157	+ 0.5
id.	18	Depression (see table 16)						86	67	— 5	72	60	— 1.9
5 December	1	*12.5*	*90°*	*11.0*	*140°*	*4.0*	*80°*	— 16	2	— 10	12	— 8	—
id.	7	*10.0*	*135°*	*9.5*	*145°*	*4.0*	*120°*	— 38	— 23	— 12	— 11	— 22	—
id.	13	*9.5*	*150°*	*9.0*	*150°*	*4.0*	*155°*	— 43	— 39	— 12	— 27	— 27	—
id.	18	*9.5*	*153°*	*8.5*	*157°*	*4.0*	*180°*	— 42	— 46	— 12	— 34	— 29	—
6 December	1	*9.5*	*157°*	*8.0*	*164°*	*4.5*	*210°*	— 39	— 48	— 12	— 36	— 33	—
id.	7	*9.5*	*162°*	*8.0*	*170°*	*4.5*	*230°*	— 37	— 46	— 12	— 34	— 34	—
id.	13	*10.0*	*168°*	*8.0*	*177°*	*5.0*	*243°*	— 35	— 40	— 12	— 28	— 37	—
id.	18	*10.0*	*171°*	*8.0*	*182°*	*5.0*	*251°*	— 32	— 35	— 12	— 23	— 37	—
7 December	1	*9.0*	*174°*	*8.0*	*190°*	*5.5*	*261°*	— 28	— 27	— 11	— 16	— 37	—
id.	7	*7.5*	*178°*	*7.5*	*196°*	*6.0*	*266°*	— 24	— 20	— 10	— 10	— 33	—
id.	13	*5.5*	*181°*	*7.0*	*203°*	*6.0*	*268°*	— 16	— 14	— 9	— 5	— 28	—
id.	18	*3.5*	*184°*	*6.5*	*210°*	*6.0*	*270°*	— 9	— 8	— 8	0	— 25	—

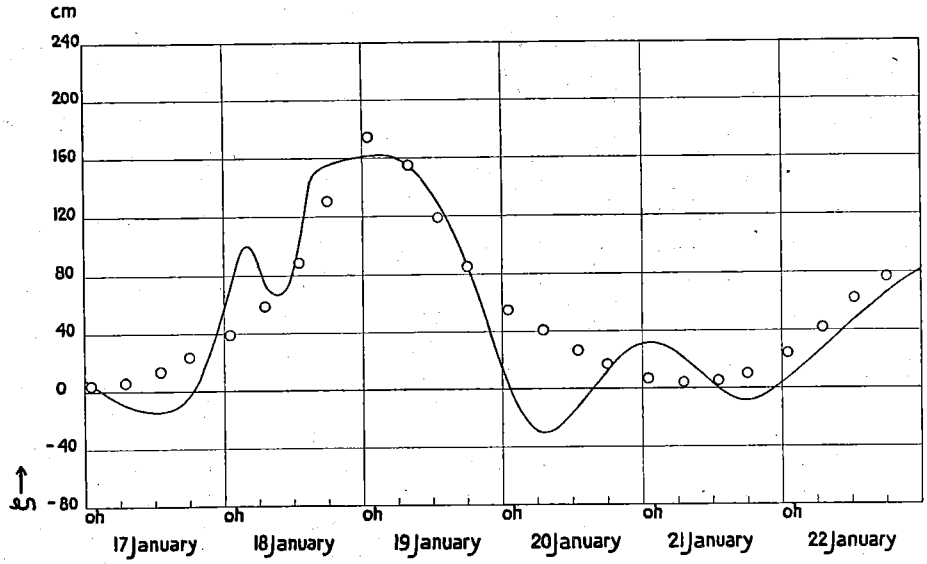

Fig. 34*a*. The storm surge of January 1921 (empirical and theoretical data)

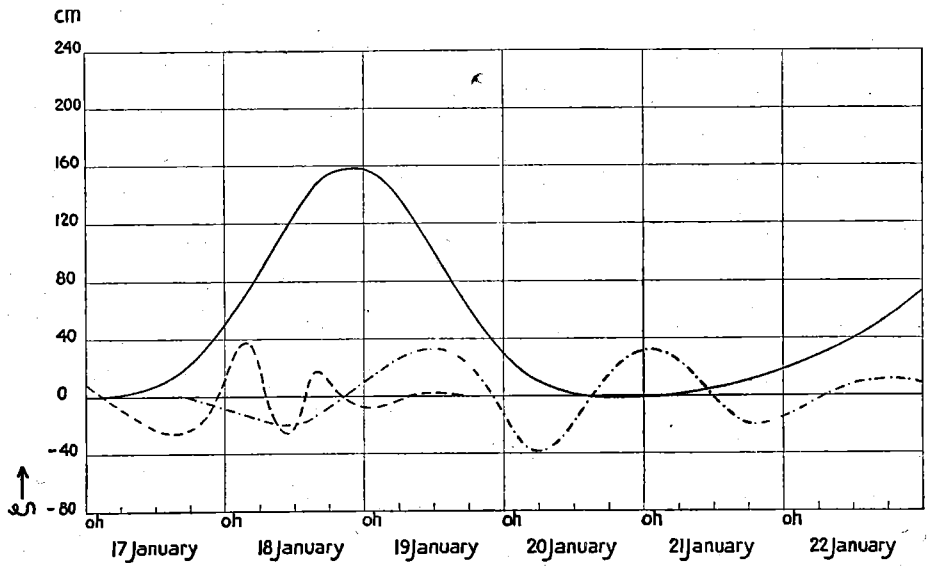

Fig. 34*b*. The storm surge of January 1921 (oscillations due to inertia separated from "stationary state")

TABLE 26 *Numerical data concerning the storm surge of January 1921*

Date	Hour	V_1	ψ_1	V_2	ψ_2	V_3	ψ_3	ζ (exp.)	ζ_0	$(\triangle\zeta)_p$	$\zeta_0-(\triangle\zeta)_p$	ζ (calc.)	$\triangle T$
17 January	1	11.7	—18°	13.2	—28°	12.8	—26°	5	0	— 13	13	4	— 1.3
id.	7	12.0	—16°	13.3	—26°	13.0	—24°	— 9	2	— 10	12	6	+ 0.3
id.	13	12.7	—13°	13.7	—22°	13.5	—19°	— 15	9	— 7	16	14	— 0.6
id.	18	13.3	— 8°	14.0	—17°	13.8	—12°	— 3	23	— 3	26	24	+ 0.9
18 January	1	14.2	0°	14.5	— 8°	14.2	0°	71	56	1	55	39	+ 1.6
id.	7	15.0	12°	15.5	5°	15.2	12°	76	94	5	89	59	+ 2.1
id.	13	17.0	24°	17.4	20°	16.9	24°	100	133	8	125	89	+ 1.0
id.	18	19.0	37°	19.9	36°	19.2	39°	155	155	6	149	131	— 1.0
19 January	1	19.5	50°	20.8	50°	19.5	56°	162	157	2	155	175	— 1.4
id.	7	17.6	55°	19.0	58°	18.0	65°	157	132	— 2	134	155	— 1.1
id.	13	15.0	57°	16.7	64°	14.8	62°	129	94	— 5	99	119	+ 0.5
id.	18	12.7	43°	14.6	55°	12.5	30°	86	62	— 8	70	85	— 0.5
20 January	1	*11.0*	*22°*	*13.0*	*22°*	*12.5*	*22°*	4	25	— 8	33	55	—
id.	7	*9.5*	*20°*	*11.5*	*22°*	*12.0*	*22°*	— 30	8	— 9	17	41	—
id.	13	*8.0*	*18°*	*10.0*	*20°*	*11.5*	*19°*	— 12	1	— 10	11	27	—
id.	18	*7.0*	*16°*	*9.0*	*18°*	*10.5*	*16°*	12	— 1	— 11	10	17	—
21 January	1	*6.0*	*9°*	*8.0*	*15°*	*9.0*	*6°*	32	— 1	— 12	11	7	—
id.	7	*6.0*	*3°*	*8.0*	*9°*	*9.0*	—4°	21	1	— 12	13	4	—
id.	13	*7.0*	*0°*	*9.0*	*2°*	*11.0*	—9°	1	6	— 11	17	5	—
id.	18	*9.0*	*0°*	*10.0*	—1°	*13.5*	—7°	— 8	11	— 9	20	10	—
22 January	1	*11.5*	—1°	*12.5*	—1°	*15.0*	*0°*	7	20	— 7	27	24	—
id.	7	*13.0*	*3°*	*14.5*	*6°*	*15.0*	*14°*	28	29	— 5	34	42	—
id.	13	*13.0*	*10°*	*16.0*	*17°*	*14.5*	*28°*	49	42	— 5	47	62	—
id.	18	*12.5*	*17°*	*16.5*	*25°*	*14.0*	*37°*	66	54	— 5	59	77	—

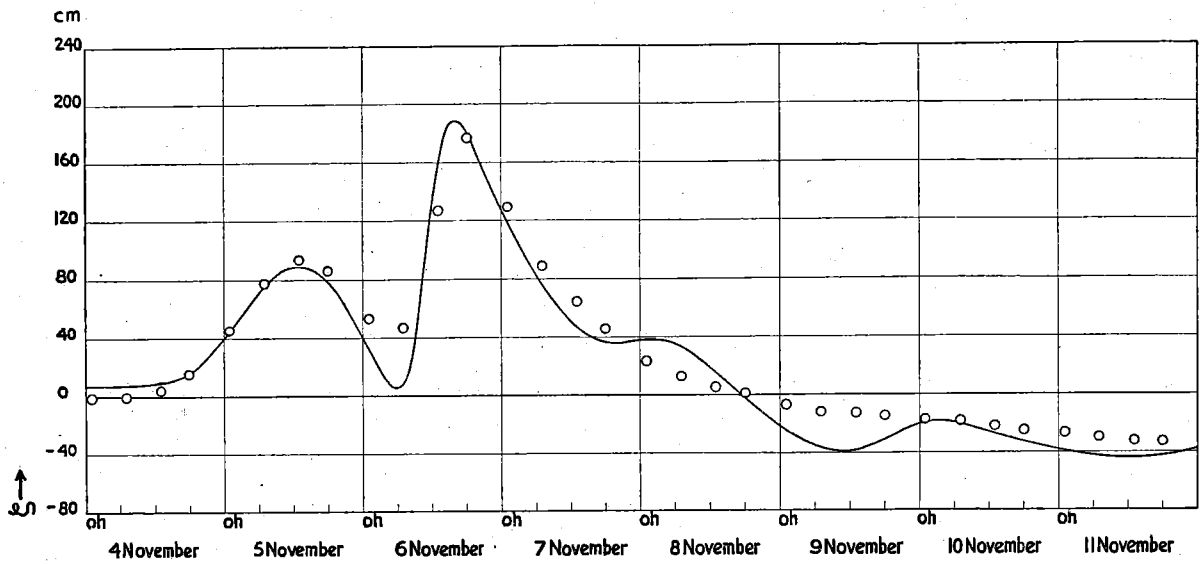

Fig. 35*a*. The storm surge of November 1921 (empirical and theoretical data)

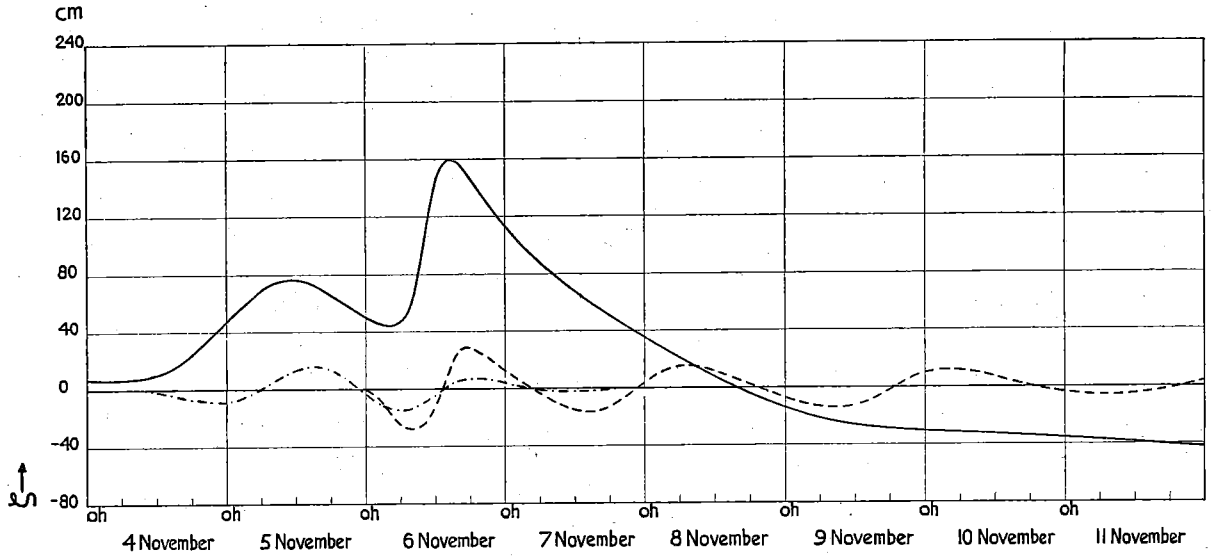

Fig. 35*b*. The storm surge of November 1921 (oscillations due to inertia separated from "stationary state")

TABLE 27 *Numerical data concerning the storm surge of November 1921*

Date	Hour	V_1	ψ_1	V_2	ψ_2	V_3	ψ_3	ζ (exp.)	ζ_0	$(\triangle\zeta)_p$	$\zeta_0-(\triangle\zeta)_p$	ζ (calc.)	$\triangle T$
4 November	1	5.6	—15°	5.3	—45°	4.3	—80°	7	7	— 3	10	— 1	— 3.5
id.	7	6.7	— 8°	6.2	—35°	5.2	—67°	7	7	— 3	10	0	0.0
id.	13	8.0	5°	8.7	—24°	7.3	—35°	9	12	— 2	14	4	+ 0.5
id.	18	10.3	16°	12.0	—11°	11.0	—13°	16	24	— 1	25	15	+ 0.5
5 November	1	12.1	27°	15.0	7°	14.0	14°	46	51	0	51	45	— 1.3
id.	7	12.7	32°	16.1	22°	14.3	32°	75	72	0	72	78	— 3.1
id.	13	12.1	30°	15.7	37°	12.2	72°	89	76	0	76	94	— 0.3
id.	18	10.8	17°	14.2	46°	7.0	98°	79	66	1	65	86	— 3.4
6 November	1	—	—	—	—	—	—	34	48	3	45	53	— 2.5
id.	7		Depression (see table 16)					8	51	5	46	47	— 2.9
id.	13		Depression (see table 16)					161	156	8	148	127	— 1.2
id.	18		Depression (see table 16)					181	146	5	141	177	— 4.4
7 November	1	—	—	—	—	—	—	117	108	1	107	129	— 4.9
id.	7	8.8	66°	14.4	66°	14.4	70°	76	84	— 2	86	89	— 4.3
id.	13	7.9	68°	12.5	68°	12.5	80°	47	64	— 4	68	64	— 2.1
id.	18	7.0	70°	10.6	70°	10.6	90°	37	50	— 5	55	46	— 4.6
8 November	1	*7.0*	*70°*	*9.0*	*80°*	*7.5*	*80°*	38	32	— 6	38	23	—
id.	7	*7.0*	*85°*	*8.0*	*100°*	*5.5*	*85°*	33	18	— 7	25	13	—
id.	13	*7.0*	*102°*	*7.5*	*108°*	*5.0*	*80°*	15	5	— 8	13	5	—
id.	18	*7.0*	*118°*	*7.0*	*106°*	*5.0*	*65°*	— 3	— 5	—10	5	1	—
9 November	1	*6.0*	*137°*	*5.0*	*85°*	*5.0*	*25°*	—25	—16	—12	— 4	— 7	—
id.	7	*5.0*	*154°*	*3.5*	*55°*	*5.0*	*—10°*	—37	—23	—13	—10	—12	—
id.	13	*4.0*	*170°*	*2.5*	*25°*	*5.0*	*—30°*	—38	—27	—14	—13	—13	—
id.	18	*4.0*	*180°*	*2.0*	*— 5°*	*5.0*	*—38°*	—32	—30	—15	—15	—15	—
10 November	1	*4.0*	*187°*	*2.5*	*—40°*	*5.0*	*—45°*	—20	—31	—15	—16	—17	—
id.	7	*4.5*	*189°*	*3.0*	*—75°*	*5.5*	*—47°*	—21	—32	—15	—17	—18	—
id.	13	*5.0*	*188°*	*4.0*	*—100°*	*6.0*	*—48°*	—28	—33	—17	—16	—22	—
id.	18	*5.5*	*186°*	*4.5*	*—125°*	*6.0*	*—49°*	—33	—34	—17	—17	—25	—
11 November	1	*6.0*	*182°*	*5.5*	*—145°*	*6.5*	*—50°*	—39	—35	—16	—19	—27	—
id.	7	*7.0*	*175°*	*6.0*	*—160°*	*6.5*	*—52°*	—43	—37	—15	—21	—30	—
id.	13	*7.5*	*170°*	*7.0*	*—175°*	*7.0*	*—55°*	—44	—39	—13	—26	—32	—
id.	18	*8.0*	*165°*	*7.5*	*—180°*	*7.5*	*—60°*	—43	—40	—11	—29	—33	—

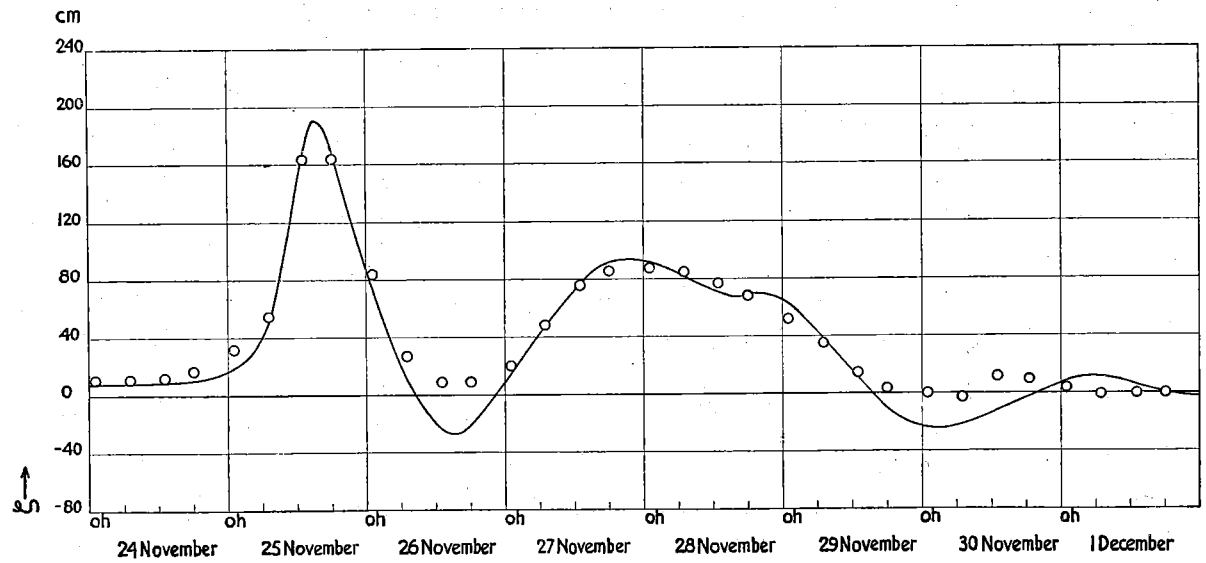

Fig. 36*a*. The storm surge of November 1925 (empirical and theoretical data)

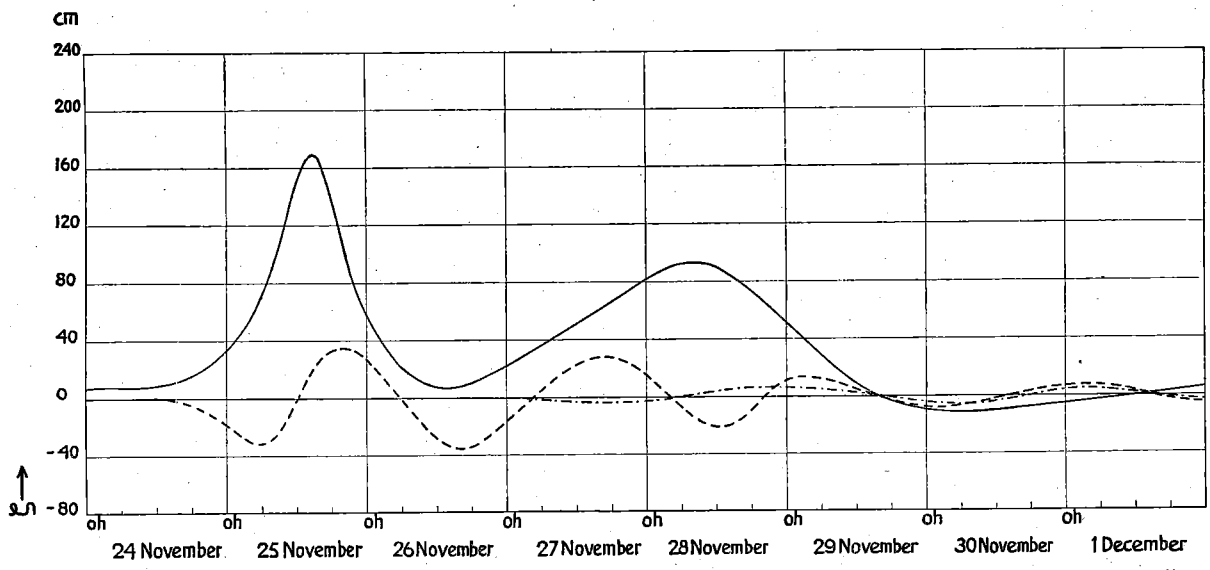

Fig. 36*b*. The storm surge of November 1925 (oscillations due to inertia separated from "stationary state")

TABLE 28 *Numerical data concerning the storm surge of November 1925*

Date	Hour	V_1	ψ_1	V_2	ψ_2	V_3	ψ_3	ζ (exp.)	ζ_0	$(\triangle\zeta)_p$	$\zeta_0-(\triangle\zeta)_p$	ζ (calc.)	$\triangle T$
24 November	1	5.7	86°	6.8	87°	6.8	85°	8	8	— 5	13	11	— 2.5
id.	7	5.6	80°	6.8	73°	6.8	78°	8	8	— 5	13	11	— 2.2
id.	13	5.7	72°	6.9	62°	6.9	75°	9	9	— 4	13	12	— 2.3
id.	18	6.3	70°	7.8	58°	7.8	73°	10	16	— 2	18	17	— 2.5
25 November	1	Depression (see table 16)						18	38	0	38	32	— 2.2
id.	7	13.0	67°	15.6	82°	15.4	115°	49	81	2	79	55	— 2.9
id.	13	16.1	84°	21.7	93°	18.0	107°	168	160	4	156	164	— 4.4
id.	18	15.8	89°	20.7	95°	17.6	101°	171	137	2	135	164	— 4.2
26 November	1	9.6	87°	13.2	92°	12.7	88°	75	51	0	51	84	— 4.7
id.	7	4.6	80°	7.5	83°	7.5	75°	11	17	— 2	19	27	— 3.9
id.	13	2.4	65°	5.8	71°	5.8	63°	— 24	7	— 4	11	9	— 2.3
id.	18	2.5	57°	5.8	56°	5.8	56°	— 21	12	— 4	16	9	— 3.9
27 November	1	5.3	35°	9.9	41°	9.9	57°	14	25	— 4	29	20	— 3.8
id.	7	8.1	40°	12.8	45°	12.8	63°	47	39	— 2	41	48	— 3.9
id.	13	10.2	58°	14.4	66°	14.4	71°	77	54	0	54	76	— 3.8
id.	18	11.2	70°	15.1	76°	15.1	77°	92	67	2	65	86	— 3.1
28 November	1	11.8	77°	15.1	80°	15.0	83°	92	85	4	81	88	— 3.9
id.	7	11.6	81°	14.7	81°	14.5	91°	82	93	4	89	85	— 4.7
id.	13	10.8	83°	14.1	84°	13.9	98°	71	88	4	84	77	— 3.0
id.	18	9.9	85°	13.0	89°	12.5	103°	69	72	3	69	69	— 3.1
29 November	1	8.7	83°	11.1	95°	10.3	107°	63	45	2	43	52	— 3.3
id.	7	7.7	70°	8.5	85°	7.8	101°	39	24	1	23	35	— 6.1
id.	13	7.5	45°	5.6	22°	6.0	− 50°	12	6	0	6	15	— 1.7
id.	18	7.7	20°	4.4	− 40°	5.5	− 80°	— 10	— 4	— 1	— 3	4	— 4.1
30 November	1	*8.0*	*0°*	*5.0*	*− 80°*	*7.5*	*−130°*	— 24	— 10	— 2	— 8	0	—
id.	7	*8.0*	*− 5°*	*8.0*	*−105°*	*6.5*	*−140°*	— 21	— 11	1	— 12	— 3	—
id.	13	*Depression (see table 16)*						— 12	— 10	5	— 15	12	—
id.	18	*Depression (see table 16)*						— 4	— 8	7	— 15	10	—
1 December	1	*Depression (see table 16)*						8	— 5	5	— 10	4	—
id.	7	*8.0*	*110°*	*9.0*	*135°*	*5.0*	*120°*	11	— 2	1	— 3	— 1	—
id.	13	*6.0*	*100°*	*6.5*	*90°*	*4.0*	*100°*	6	1	— 2	3	0	—
id.	18	*4.0*	*90°*	*4.0*	*70°*	*3.0*	*90°*	1	3	— 5	8	0	—

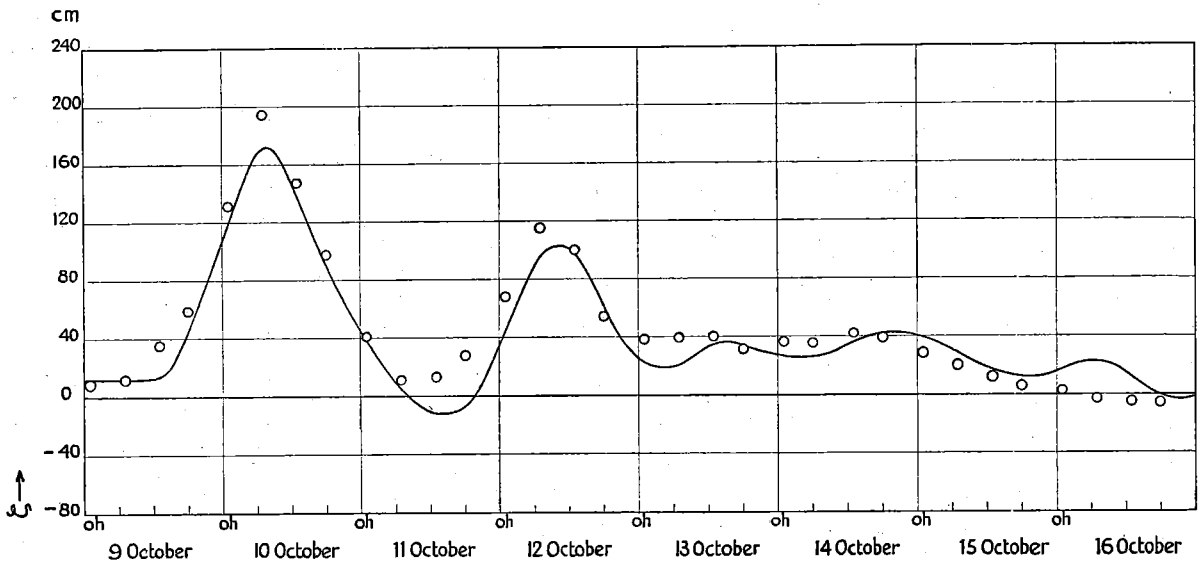

Fig. 37*a*. The storm surge of October 1926 (empirical and theoretical data)

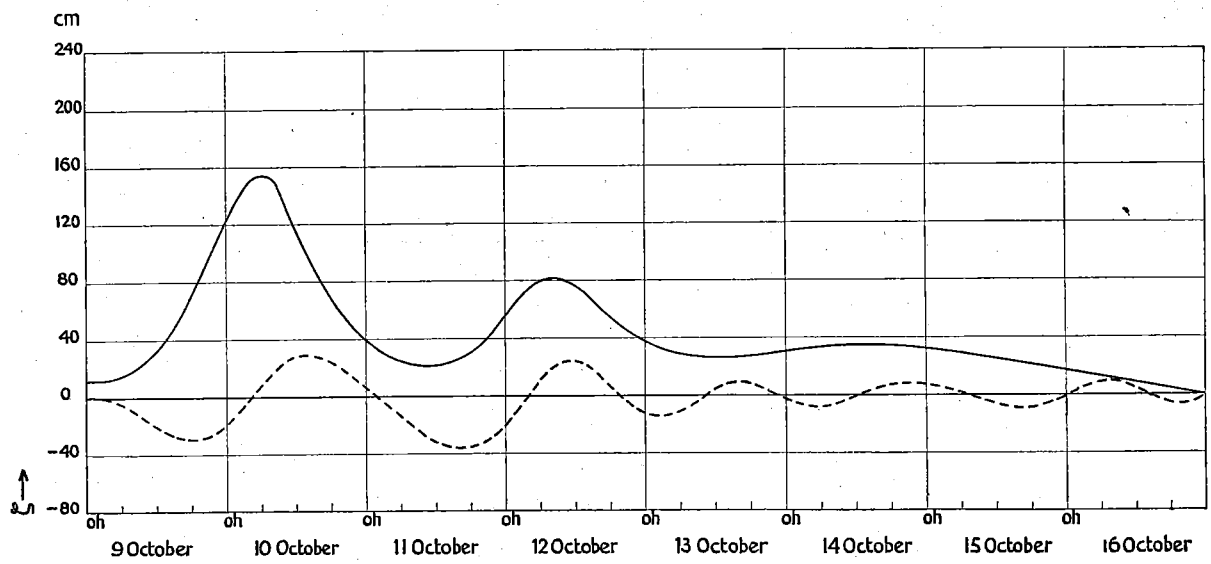

Fig. 37*b*. The storm surge of October 1926 (oscillations due to inertia separated from "stationary state")

TABLE 29 *Numerical data concerning the storm surge of October 1926*

Date	Hour	V_1	ψ_1	V_2	ψ_2	V_3	ψ_3	ζ (exp.)	ζ_0	$(\triangle\zeta)_p$	$\zeta_0-(\triangle\zeta)_p$	ζ (calc.)	$\triangle T$
9 October	1	6.0	—12°	10.7	—25°	6.5	— 40°	12	12	0	12	9	— 0.4
id.	7	14.0	—19°	15.0	—40°	11.6	—120°	12	17	3	14	12	— 1.4
id.	13	Depression (see table 16)						14	37	7	30	35	— 1.3
id.	18	Depression (see table 16)						44	72	7	65	59	— 2.7
10 October	1	17.7	27°	20.1	37°	19.0	63°	117	130	5	125	131	— 3.4
id.	7	16.3	37°	20.8	48°	19.8	76°	172	154	3	151	194	— 3.8
id.	13	14.2	37°	17.7	51°	16.5	75°	138	108	0	108	147	— 2.7
id.	18	11.8	27°	13.7	45°	11.3	64°	91	69	— 3	72	97	— 3.6
11 October	1	9.0	0°	9.7	21°	2.0	26°	38	36	— 5	41	41	— 3.6
id.	7	8.4	—11°	8.8	— 4°	4.8	— 1°	5	23	— 5	28	11	— 3.4
id.	13	11.2	— 7°	11.0	—13°	10.2	— 7°	— 12	22	— 3	25	13	— 1.7
id.	18	13.0	7°	14.3	— 9°	13.0	3°	— 7	30	0	30	28	— 1.0
12 October	1	14.2	21°	16.6	13°	15.2	50°	44	62	3	59	68	— 0.2
id.	7	13.6	18°	16.5	36°	16.0	73°	96	81	1	80	115	— 2.9
id.	13	12.0	8°	14.5	33°	14.5	76°	98	73	— 1	74	100	— 2.2
id.	18	10.5	— 4°	11.6	—16°	5.0	68°	62	55	— 3	58	54	— 3.7
13 October	1	Depression (see table 16)						22	35	— 2	37	38	— 3.9
id.	7	Depression (see table 16)						21	28	— 1	29	39	+ 0.1
id.	13	Depression (see table 16)						35	27	— 1	28	40	+ 0.1
id.	18	13.1	— 7°	12.4	— 7°	11.7	— 7°	34	27	— 2	29	31	— 0.1
14 October	1	13.2	—10°	12.8	— 3°	6.0	— 6°	27	30	— 2	32	36	+ 0.1
id.	7	Depression (see table 16)						26	33	— 2	35	35	+ 0.3
id.	13	12.3	— 7°	12.3	7°	9.1	10°	36	34	— 1	35	42	— 0.7
id.	18	11.5	—10°	11.4	9°	10.2	27°	42	34	— 1	35	39	— 1.3
15 October	1	—	—	*10.5*	*13°*	*9.0*	*40°*	39	32	— 2	34	29	—
id.	7	—	—	*9.0*	*16°*	*7.0*	*42°*	28	29	— 3	32	20	—
id.	13	—	—	*7.0*	*21°*	*5.5*	*45°*	17	25	— 4	29	12	—
id.	18	*11.0*	*—10°*	*6.0*	*25°*	*4.5*	*48°*	12	21	— 5	26	6	—
16 October	1	—	—	*4.0*	*30°*	*3.5*	*52°*	17	17	— 5	22	3	—
id.	7	*5.0*	*135°*	*3.5*	*35°*	*3.0*	*55°*	23	12	— 6	18	— 3	—
id.	13	*4.0*	*160°*	*2.5*	*41°*	*2.5*	*58°*	12	8	— 7	15	— 5	—
id.	18	*2.0*	*180°*	*2.0*	*48°*	*2.0*	*61°*	0	4	— 8	12	— 6	—

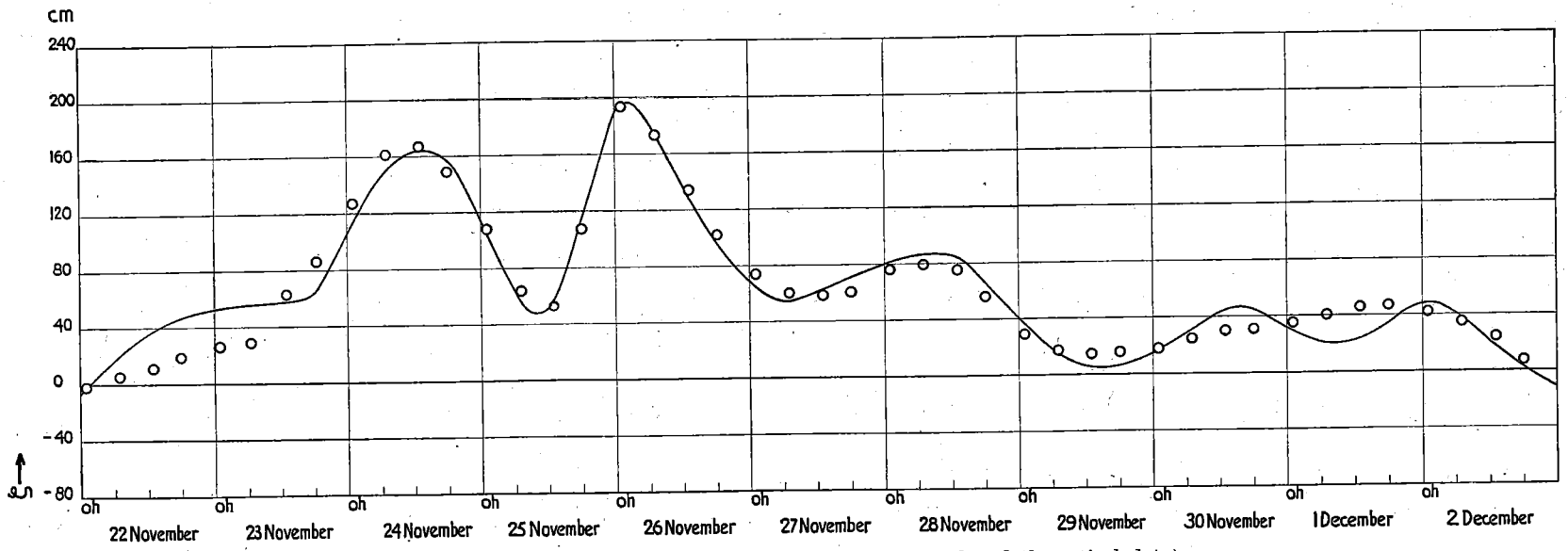

Fig. 38*a*. The storm surge of November 1928 (empirical and theoretical data)

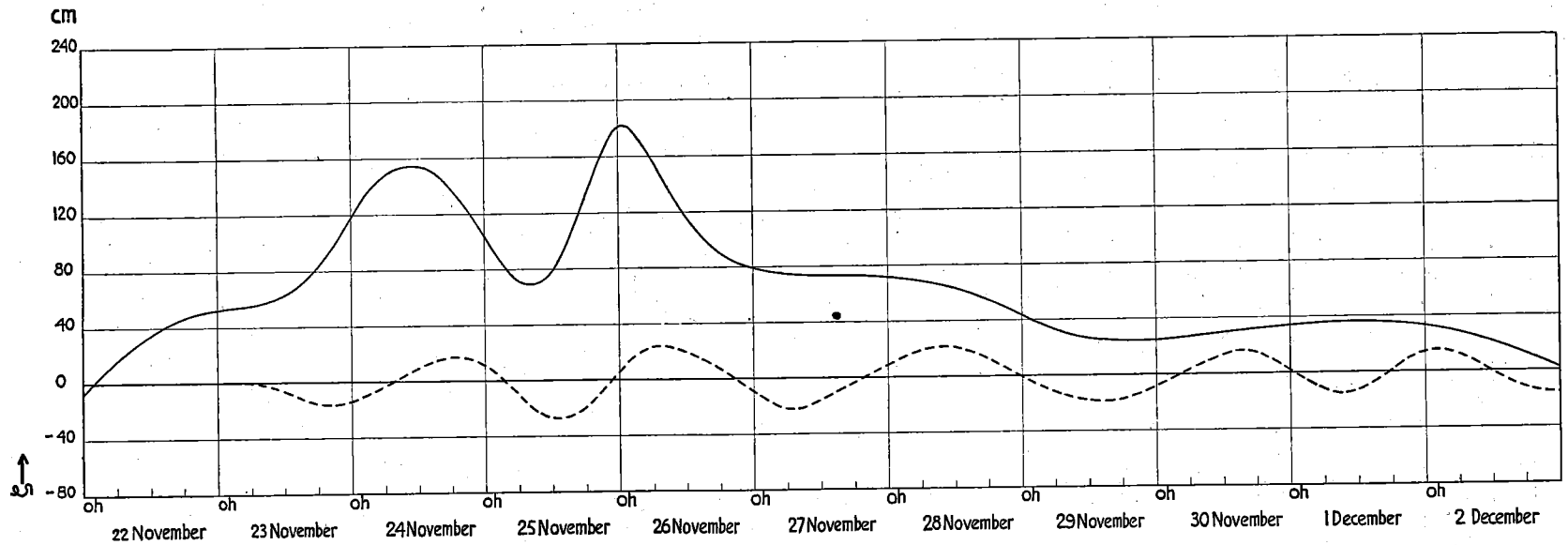

Fig. 38*b* The storm surge of November 1928 (oscillations deu to inertia separated from "stationary state")

TABLE 30 *Numerical data concerning the storm surge of November 1928*

Date	Hour	V_1	ψ_1	V_2	ψ_2	V_3	ψ_3	ζ (exp.)	ζ_0	$(\triangle\zeta)_p$	$\zeta_0-(\triangle\zeta)_p$	ζ (calc.)	$\triangle T$
22 November	1	11.7	—13°	11.6	—43°	10.8	—64°	— 2	— 3	— 5	2	— 2	+ 0.3
id.	7	12.4	—11°	12.2	—37°	11.3	—53°	20	20	— 5	25	5	+ 1.2
id.	13	13.0	—10°	12.7	—31°	11.6	—43°	37	37	— 4	41	11	+ 1.0
id.	18	13.4	— 9°	12.8	—24°	11.6	—34°	46	47	— 2	49	19	+ 0.3
23 November	1	13.2	— 7°	12.5	—18°	11.3	—25°	53	53	0	53	26	+ 0.1
id.	7	12.6	— 5°	11.8	—12°	10.7	—18°	56	56	2	54	29	— 1.2
id.	13	Depression (see table 16)						58	65	5	60	63	+ 0.4
id.	18	Depression (see table 16)						66	82	9	73	86	0.0
24 November	1	Depression (see table 16)						114	125	10	115	127	— 1.3
id.	7	Depression (see table 16)						150	151	9	142	161	— 2.1
id.	13	Depression (see table 16)						164	154	9	145	167	— 1.0
id.	18	17.8	25°	17.9	38°	17.0	70°	157	139	7	132	149	— 1.5
25 November	1	17.0	15°	16.8	13°	14.1	15°	105	97	4	93	108	— 1.4
id.	7	16.8	5°	16.1	—16°	9.7	—50°	57	70	7	63	64	— 1.9
id.	13	Depression (see table 16)						57	85	13	72	53	— 0.2
id.	18	17.7	40°	17.4	53°	15.2	72°	114	130	15	115	107	— 2.2
26 November	1	17.8	45°	20.1	59°	18.8	70°	195	182	10	172	193	— 3.1
id.	7	16.8	42°	19.3	61°	15.7	69°	174	150	8	142	173	— 2.9
id.	13	14.8	39°	17.0	60°	11.8	69°	128	111	6	105	124	— 1.5
id.	18	13.5	37°	15.0	59°	10.1	70°	96	91	5	86	102	— 2.0
27 November	1	13.0	41°	13.0	55°	9.1	71°	65	78	4	74	74	— 1.8
id.	7	13.0	48°	12.1	54°	9.3	73°	54	74	3	71	60	— 2.2
id.	13	13.2	58°	12.3	58°	10.5	75°	62	73	2	71	58	— 1.2
id.	18	13.5	66°	13.0	64°	12.6	79°	70	73	1	72	60	— 2.0
28 November	1	13.7	73°	14.7	74°	14.4	83°	81	72	— 1	73	76	— 2.4
id.	7	13.5	80°	15.1	81°	14.8	87°	87	68	— 3	71	80	— 2.1
id.	13	12.0	81°	14.4	88°	13.5	89°	84	62	— 5	67	75	— 1.7
id.	18	10.0	81°	12.6	89°	11.0	89°	66	54	— 8	62	56	— 2.5
29 November	1	*8.5*	*80°*	*11.0*	*70°*	*9.5*	*10°*	36	42	— 9	51	29	—
id.	7	*7.0*	*55°*	*9.0*	*45°*	*8.0*	*10°*	15	32	—10	42	17	—
id.	13	*7.0*	*40°*	*9.0*	*25°*	*8.0*	*10°*	5	26	—10	36	14	—
id.	18	*7.0*	*25°*	*9.0*	*25°*	*8.0*	*25°*	7	24	— 9	33	15	—
30 November	1	*7.0*	*35°*	*9.0*	*45°*	*8.0*	*48°*	17	24	— 8	32	18	—
id.	7	*7.0*	*55°*	*9.5*	*65°*	*8.5*	*65°*	31	27	— 7	34	25	—
id.	13	*7.5*	*65°*	*10.0*	*70°*	*9.0*	*70°*	45	29	— 7	36	30	—
id.	18	*8.0*	*65°*	*10.5*	*65°*	*9.5*	*65°*	45	31	— 8	39	31	—
1 December	1	*8.0*	*65°*	*11.0*	*60°*	*10.0*	*60°*	30	34	— 8	42	35	—
id.	7	*8.0*	*65°*	*12.0*	*60°*	*11.0*	*60°*	21	36	— 9	45	41	—
id.	13	*8.0*	*80°*	*12.5*	*70°*	*12.0*	*60°*	24	37	— 9	46	46	—
id.	18	*8.0*	*90°*	*12.5*	*78°*	*12.0*	*60°*	34	36	— 9	45	47	—
2 December	1	*7.0*	*100°*	*12.0*	*80°*	*11.0*	*60°*	48	32	— 9	41	42	—
id.	7	*6.5*	*95°*	*11.0*	*75°*	*10.0*	*45°*	37	26	—10	36	35	—
id.	13	*6.0*	*90°*	*10.0*	*45°*	*9.8*	*0°*	17	20	—10	30	24	—
id.	18	*5.0*	*50°*	*8.0*	*0°*	*8.0*	*—45°*	3	12	—11	23	7	—

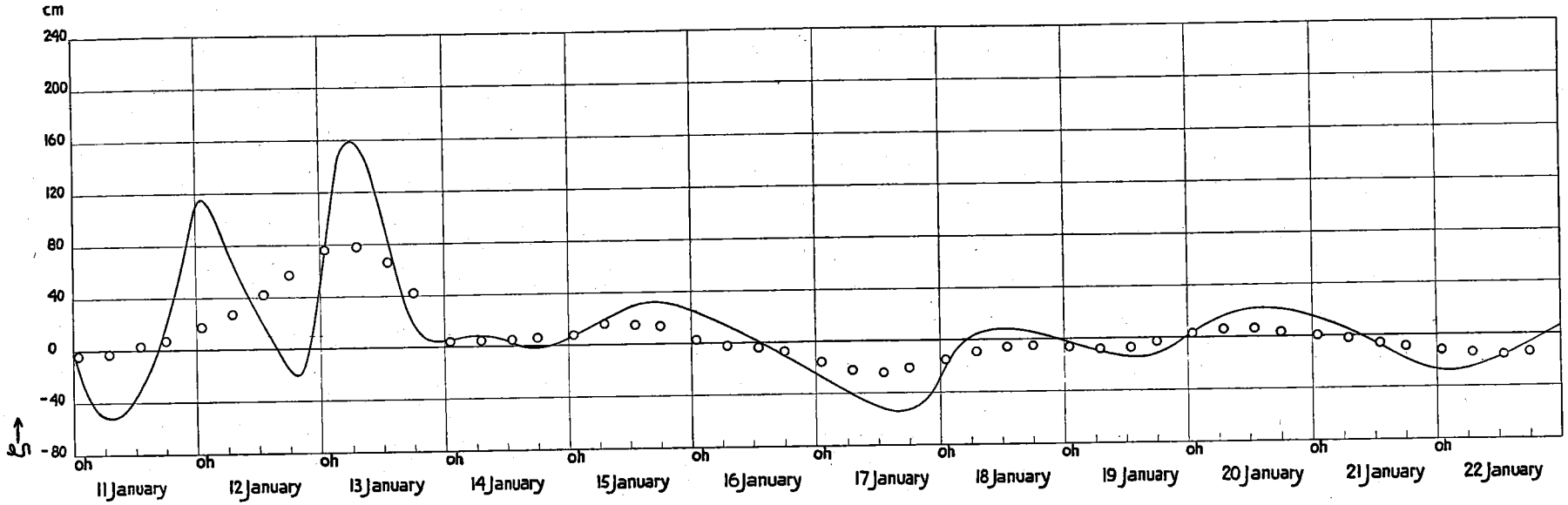

Fig. 39*a*. The storm surge of January 1930 (empirical and theoretical data)

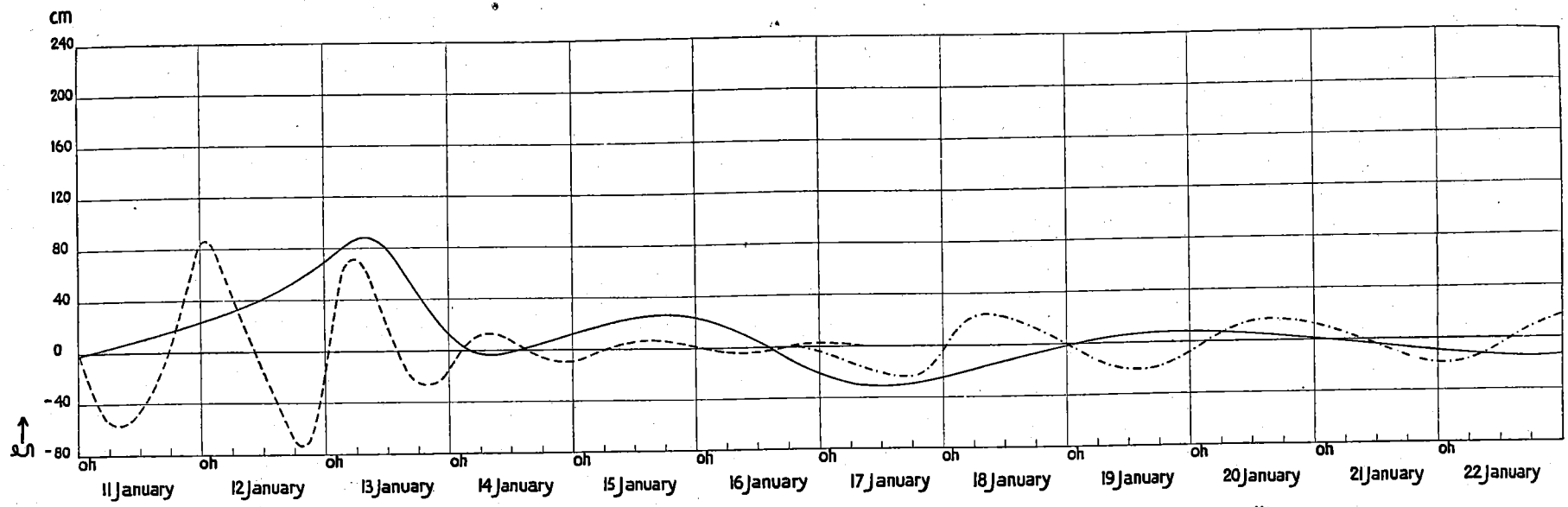

Fig. 39*b* The storm surge of January 1930 (oscillations due to inertia separated from "stationary state")

TABLE 31 *Numerical data concerning the storm surge of January 1930*

Date	Hour	V_1	ψ_1	V_2	ψ_2	V_3	ψ_3	ζ (exp.)	ζ_0	$(\triangle\zeta)_p$	$\zeta_0-(\triangle\zeta)_p$	ζ (calc.)	$\triangle T$
11 January	1	11.6	—20°	13.4	—54°	14.0	—40°	— 15	— 1	2	— 3	— 4	— 1.1
id.	7	11.8	—18°	13.8	—48°	14.3	—50°	— 52	5	4	1	— 3	— 0.9
id.	13	12.2	—17°	14.2	—43°	14.7	—42°	— 28	11	5	6	3	— 0.9
id.	18	12.6	—16°	14.5	—38°	15.1	—38°	18	16	6	10	7	— 0.8
12 January	1	13.2	—15°	15.1	—30°	15.7	—30°	115	24	7	17	17	— 4.0
id.	7	14.0	—14°	15.8	—23°	15.9	—23°	67	33	7	26	27	— 2.3
id.	13	14.8	—12°	16.7	—15°	15.5	—13°	18	43	7	36	42	— 0.7
id.	18	15.6	—10°	17.7	— 9°	13.5	— 6°	— 16	53	6	47	57	— 1.0
13 January	1	15.8	— 6°	18.4	— 1°	4.5	1°	81	72	5	67	76	+ 0.1
id.	7	14.7	— 4°	17.6	4°	3.5	0°	157	88	4	84	78	— 1.7
id.	13	12.4	—13°	15.1	— 2°	8.5	— 8°	84	75	1	74	66	— 0.3
id.	18	10.8	—27°	12.2	—22°	9.7	—25°	17	44	— 1	45	42	+ 0.5
14 January	1	*10.5*	*—35°*	*11.0*	*—43°*	*9.0*	*—43°*	6	8	— 3	11	4	—
id.	7	*10.5*	*—40°*	*10.5*	*—42°*	*7.0*	*—42°*	8	— 3	— 4	1	5	—
id.	13	*10.5*	*—55°*	*10.0*	*—41°*	*4.0*	*—41°*	3	0	— 4	4	5	—
id.	18	*10.0*	*—50°*	*10.0*	*—40°*	*2.0*	*—40°*	— 1	5	— 4	9	6	—
15 January	1	*10.0*	*—40°*	*9.5*	*—26°*	*0.0*	*—25°*	8	13	— 5	18	8	—
id.	7	*9.0*	*—25°*	*9.0*	*4°*	*0.0*	*5°*	19	20	— 5	25	16	—
id.	13	*8.0*	*—30°*	*8.0*	*20°*	*6.0*	*40°*	30	24	— 6	30	15	—
id.	18	*8.0*	*—50°*	*6.5*	*20°*	*9.0*	*30°*	32	26	— 7	33	14	—
16 January	1	*7.5*	*—62°*	*4.5*	*11°*	*9.0*	*10°*	24	23	— 8	31	3	—
id.	7	*7.5*	*—83°*	*3.5*	*—11°*	*7.0*	*—10°*	13	15	— 9	24	— 2	—
id.	13	*8.0*	*—90°*	*3.5*	*—45°*	*4.0*	*—45°*	1	2	— 10	12	— 4	—
id.	18	*8.0*	*—88°*	*5.0*	*—62°*	*5.0*	*—65°*	— 10	— 9	— 12	3	— 7	—
17 January	1	*8.5*	*—85°*	*8.0*	*—71°*	*9.0*	*—70°*	— 26	— 22	— 12	— 10	— 15	—
id.	7	*9.0*	*—78°*	*10.0*	*—71°*	*11.0*	*—70°*	— 40	— 30	— 13	— 17	— 22	—
id.	13	*9.0*	*—68°*	*11.5*	*—65°*	*12.5*	*—65°*	— 52	— 31	— 13	— 18	— 24	—
id.	18	*8.5*	*—60°*	*11.5*	*—60°*	*13.0*	*—60°*	— 53	— 30	— 12	— 18	— 21	—
18 January	1	*8.0*	*—50°*	*11.0*	*—50°*	*13.0*	*—50°*	— 20	— 24	— 11	— 13	— 15	—
id.	7	*7.5*	*—40°*	*10.0*	*—42°*	*11.5*	*—40°*	4	— 18	— 10	— 8	— 9	—
id.	13	*7.0*	*—35°*	*8.5*	*—38°*	*10.0*	*—40°*	8	— 12	— 9	— 3	— 6	—
id.	18	*7.5*	*—40°*	*8.5*	*—38°*	*10.0*	*—40°*	5	— 7	— 8	1	— 5	—
19 January	1	*8.0*	*—45°*	*10.0*	*—45°*	*12.0*	*—45°*	— 3	— 1	— 7	6	— 6	—
id.	7	*9.0*	*—50°*	*11.0*	*—48°*	*13.0*	*—50°*	— 10	3	— 6	9	— 8	—
id.	13	*8.5*	*—50°*	*11.0*	*—48°*	*13.0*	*—50°*	— 14	6	— 5	11	— 7	—
id.	18	*8.0*	*—45°*	*11.0*	*—40°*	*12.0*	*—40°*	— 12	8	— 5	13	— 3	—
20 January	1	*7.0*	*—40°*	*10.0*	*—25°*	*11.0*	*—25°*	4	8	— 5	13	3	—
id.	7	*5.5*	*—27°*	*9.5*	*—15°*	*10.0*	*—15°*	16	7	— 5	12	6	—
id.	13	*4.5*	*—16°*	*9.0*	*— 8°*	*9.0*	*—10°*	22	5	— 6	11	6	—
id.	18	*3.5*	*—14°*	*8.0*	*— 6°*	*9.0*	*— 5°*	21	3	— 7	10	3	—
21 January	1	*3.0*	*—20°*	*7.0*	*— 8°*	*7.0*	*—10°*	14	1	— 8	9	0	—
id.	7	*3.0*	*—40°*	*6.5*	*—20°*	*6.5*	*—20°*	5	— 1	— 8	7	— 2	—
id.	13	*3.5*	*—70°*	*6.0*	*—45°*	*7.0*	*—45°*	— 7	— 4	— 8	4	— 6	—
id.	18	*4.0*	*—80°*	*6.0*	*—60°*	*7.0*	*—60°*	— 18	— 6	— 8	2	— 9	—
22 January	1	*5.0*	*—90°*	*6.5*	*—72°*	*8.5*	*—70°*	— 28	— 8	— 8	0	— 12	—
id.	7	*6.0*	*—90°*	*7.0*	*—75°*	*9.5*	*—75°*	— 25	— 11	— 8	— 3	— 14	—
id.	13	*7.0*	*—85°*	*8.0*	*—72°*	*10.5*	*—70°*	— 16	— 13	— 7	— 6	— 16	—
id.	18	*8.0*	*—80°*	*9.0*	*—65°*	*11.5*	*—65°*	— 7	— 14	— 7	— 7	— 14	—

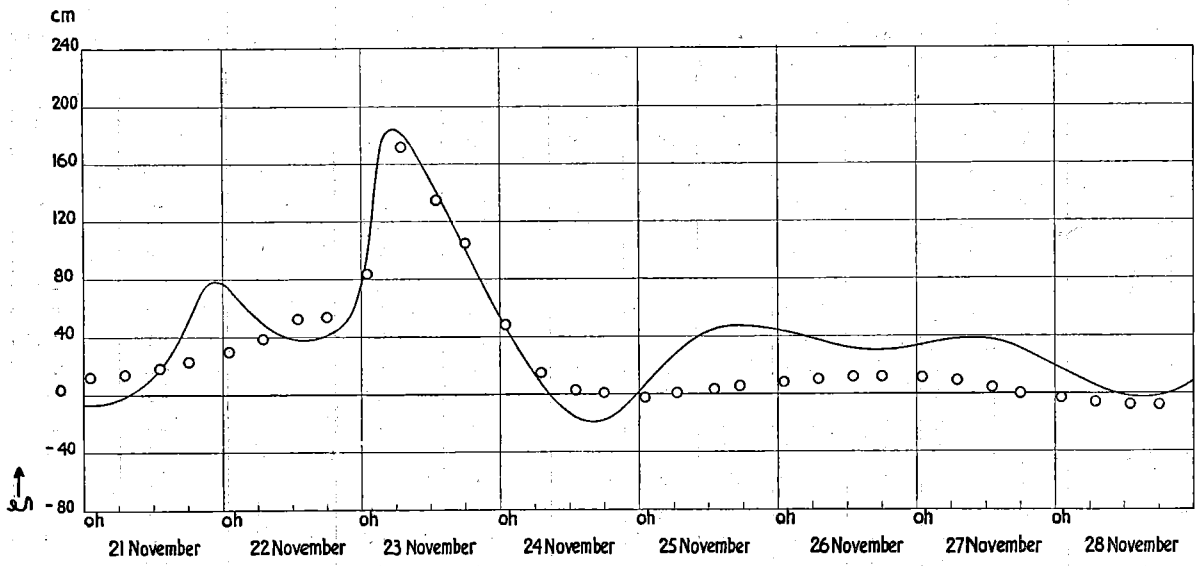

Fig. 40*a*. The storm surge of November 1930 (empirical and theoretical data)

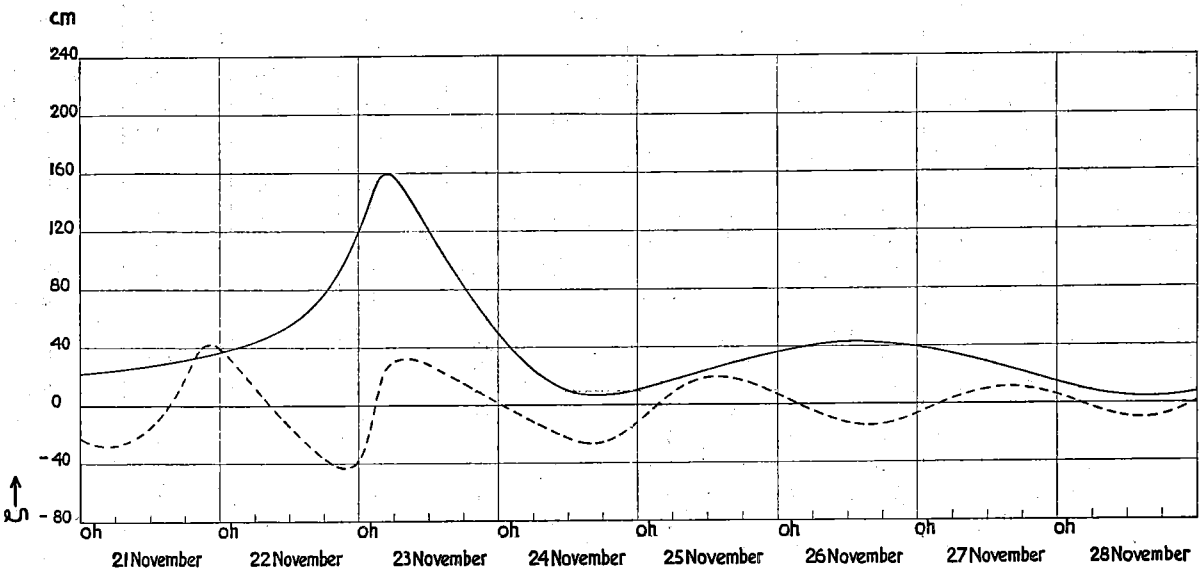

Fig. 40*b*. The storm surge of November 1930 (oscillations due to inertia separated from "stationary state")

TABLE 32 *Numerical data concerning the storm surge of November 1930*

Date	Hour	V_1	ψ_1	V_2	ψ_2	V_3	ψ_3	ζ (exp.)	ζ_0	$(\triangle\zeta)_p$	$\zeta_0-(\triangle\zeta)_p$	ζ (calc.)	$\triangle T$
21 November	1	10.0	—20°	9.0	—30°	9.0	—55°	— 6	23	3	20	12	+ 1.5
id.	7	11.1	—21°	9.3	—30°	7.7	—45°	— 2	25	3	22	14	+ 1.0
id.	13	12.1	—22°	9.8	—29°	6.5	—36°	17	28	3	25	18	+ 1.5
id.	18	13.0	—23°	10.5	—28°	5.6	—30°	51	32	5	27	23	+ 0.8
22 November	1	13.8	—22°	11.9	—25°	5.0	—23°	73	38	6	32	30	+ 0.6
id.	7	14.3	—20°	14.0	—22°	4.7	—10°	49	46	7	39	39	+ 1.6
id.	13	14.8	—18°	16.5	—10°	4.3	26°	38	58	8	50	53	+ 1.9
id.	18	Depression (see table 16)						41	76	8	68	54	+ 0.8
23 November	1	Depression (see table 16)						100	129	5	124	84	+ 0.3
id.	7	10.0	20°	19.6	45°	19.6	70°	181	153	0	153	172	— 2.2
id.	13	9.6	5°	18.1	48°	18.1	75°	139	115	— 5	120	135	— 0.9
id.	18	10.3	—18°	15.5	41°	15.5	68°	100	83	— 8	91	105	— 1.0
24 November	1	*12.0*	*— 80°*	*12.5*	*10°*	*12.5*	*0°*	45	45	— 8	53	48	—
id.	7	*13.0*	*— 70°*	*13.0*	*— 30°*	*13.0*	*— 70°*	7	22	— 6	28	15	—
id.	13	*13.0*	*— 20°*	*13.0*	*— 55°*	*13.0*	*—100°*	— 16	10	— 3	13	3	—
id.	18	*13.0*	*— 15°*	*13.0*	*— 61°*	*13.0*	*—105°*	— 18	7	0	7	1	—
25 November	1	*13.0*	*— 15°*	*13.0*	*— 63°*	*13.0*	*—105°*	6	12	2	10	— 2	—
id.	7	*13.0*	*— 15°*	*13.0*	*— 61°*	*13.0*	*—100°*	30	19	3	16	1	—
id.	13	*12.5*	*— 15°*	*12.5*	*— 58°*	*12.5*	*— 90°*	44	25	4	21	3	—
id.	18	*12.0*	*— 15°*	*12.0*	*— 54°*	*12.0*	*— 80°*	47	30	4	26	5	—
26 November	1	*11.0*	*— 15°*	*11.0*	*— 48°*	*11.0*	*— 70°*	43	37	5	32	8	—
id.	7	*10.0*	*— 15°*	*10.0*	*— 43°*	*10.0*	*— 55°*	37	42	5	37	10	—
id.	13	*9.0*	*— 15°*	*9.0*	*— 35°*	*9.0*	*— 45°*	32	43	5	38	12	—
id.	18	*8.0*	*— 17°*	*8.0*	*— 30°*	*8.0*	*— 38°*	30	42	4	38	12	—
27 November	1	*7.0*	*— 20°*	*7.0*	*— 22°*	*7.0*	*— 25°*	34	39	3	36	11	—
id.	7	*6.0*	*— 30°*	*6.0*	*— 15°*	*6.0*	*— 10°*	38	34	0	34	9	—
id.	13	*5.0*	*— 95°*	*5.0*	*— 8°*	*5.0*	*5°*	38	28	— 3	31	4	—
id.	18	*4.0*	*—180°*	*4.0*	*— 8°*	*4.0*	*10°*	31	22	— 4	26	0	—
28 November	1	*4.0*	*—190°*	*4.0*	*— 15°*	*4.0*	*10°*	17	14	— 5	19	— 3	—
id.	7	*3.0*	*—200°*	*3.0*	*—100°*	*3.0*	*— 40°*	5	9	— 5	14	— 5	—
id.	13	*3.0*	*—210°*	*3.0*	*—160°*	*3.0*	*—100°*	— 2	6	— 5	11	— 8	—
id.	18	*3.0*	*—220°*	*3.0*	*—180°*	*3.0*	*—100°*	— 2	5	— 5	10	— 8	—

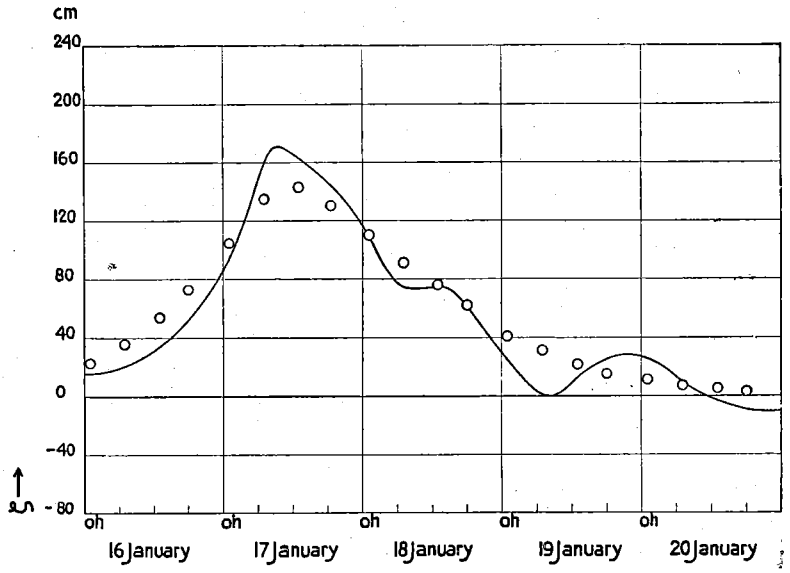

Fig. 41*a*. The storm surge of January 1931 (empirical and theoretical data)

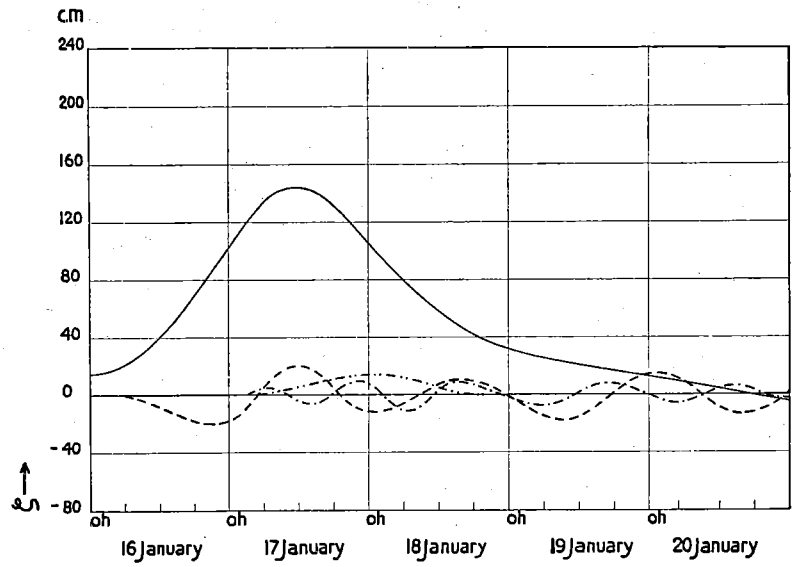

Fig. 41*b*.The storm surge of January 1931 (oscillations due to inertia separated from "stationary state")

TABLE 33 *Numerical data concerning the storm surge of January 1931*

Date	Hour	V_1	ψ_1	V_2	ψ_2	V_3	ψ_3	ζ (exp.)	ζ_0	$(\triangle\zeta)_p$	$\zeta_0-(\triangle\zeta)_p$	ζ (calc.)	$\triangle T$
16 January	1	8.3	14°	11.3	8°	11.4	8°	6	14	— 5	19	23	+ 1.0
id.	7	10.8	15°	13.2	9°	12.7	10°	11	23	— 3	26	36	+ 0.9
id.	13	13.2	19°	15.1	11°	14.0	12°	24	44	— 1	45	54	+ 1.0
id.	18	15.1	25°	16.9	15°	15.0	21°	42	69	2	67	73	+ 1.3
17 January	1	17.0	36°	18.5	27°	16.0	41°	84	110	5	105	105	+ 0.5
id.	7	17.2	44°	18.9	40°	16.6	57°	150	138	5	133	135	— 0.9
id.	13	15.9	51°	18.4	51°	16.8	66°	154	144	5	139	143	— 0.2
id.	18	13.7	53°	17.6	60°	16.5	69°	136	132	3	129	130	— 1.0
18 January	1	11.4	54°	16.0	65°	16.0	70°	100	101	1	100	110	— 1.7
id.	7	10.3	52°	14.8	62°	14.9	66°	65	76	0	76	91	— 2.1
id.	13	9.8	48°	13.5	54°	13.5	59°	65	56	— 1	57	76	— 0.9
id.	18	10.1	41°	12.5	47°	12.6	50°	51	43	— 2	45	62	— 2.5
19 January	1	*10.5*	*30°*	*10.5*	*30°*	*5.0*	*30°*	15	31	— 2	33	41	—
id.	7	*9.5*	*15°*	*9.5*	*15°*	*4.0*	*15°*	— 9	25	— 1	26	31	—
id.	13	*8.5*	*5°*	*8.5*	*5°*	*3.0*	*5°*	3	20	0	20	22	—
id.	18	*7.5*	*— 5°*	*7.5*	*— 5°*	*3.0*	*— 5°*	15	17	1	16	15	—
20 January	1	*6.5*	*—15°*	*6.5*	*—15°*	*3.0*	*—15°*	16	12	2	10	11	—
id.	7	*5.5*	*—25°*	*5.5*	*—25°*	*4.5*	*—25°*	0	8	2	6	7	—
id.	13	*4.5*	*—35°*	*4.5*	*—35°*	*6.0*	*—35°*	— 13	4	3	1	5	—
id.	18	*3.5*	*—45°*	*4.0*	*—45°*	*7.0*	*—45°*	— 19	0	3	— 3	3	—

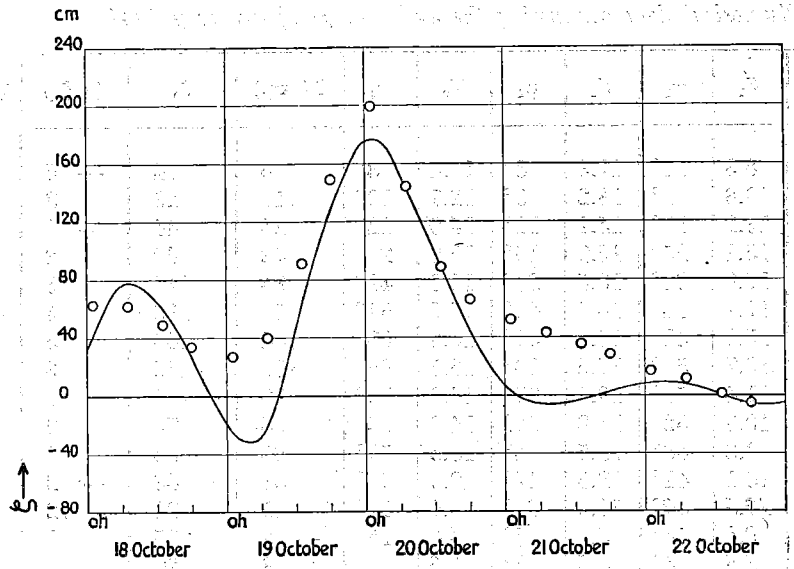

Fig. 42*a*. The storm surge of October 1935 (empirical and theoretical data)

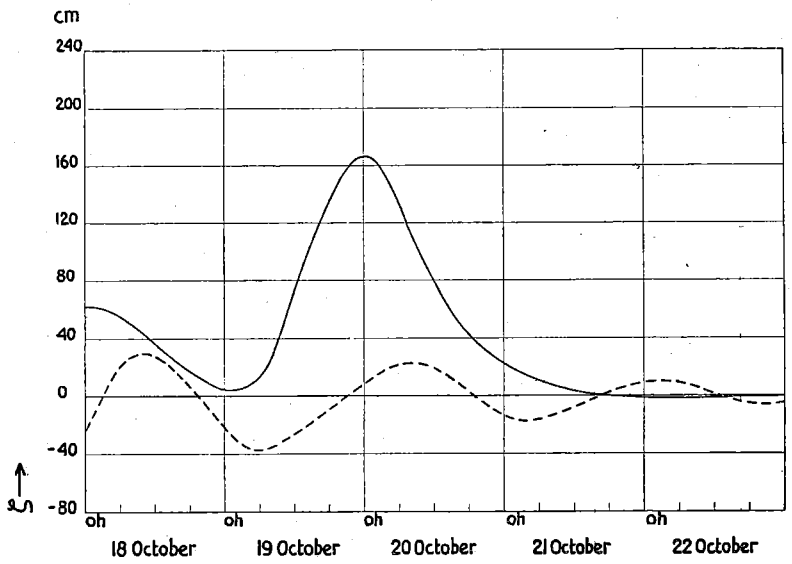

Fig. 42*b*. The storm surge of October 1935 (oscillations due to inertia separated from "stationary state")

TABLE 34 *Numerical data concerning the storm surge of October 1935*

Date	Hour	V_1	ψ_1	V_2	ψ_2	V_3	ψ_3	ζ (exp.)	ζ_0	$(\triangle\zeta)_p$	$\zeta_0-(\triangle\zeta)_p$	ζ (calc.)	$\triangle T$
18 October	1	7.2	40°	14.7	36°	14.7	43°	41	62	— 9	71	63	— 0.7
id.	7	9.3	26°	14.3	32°	14.3	26°	78	53	— 9	62	62	— 2.1
id.	13	11.1	8°	13.9	8°	14.0	0°	60	33	— 10	43	49	— 1.2
id.	18	12.6	— 4°	14.2	— 9°	14.5	—20°	27	17	— 10	27	34	— 2.0
19 October	1	14.0	—10°	16.0	—21°	16.3	—34°	— 25	4	— 5	9	27	— 0.3
id.	7	14.8	— 4°	19.4	—17°	19.2	—32°	— 21	18	0	18	40	— 2.9
id.	13	Depression (see table 16)						61	84	3	81	91	— 1.7
id.	18	Depression (see table 16)						128	135	5	130	149	— 2.5
20 October	1	Depression (see table 16)						177	165	5	160	199	— 3.2
id.	7	Depression (see table 16)						144	123	3	120	144	— 2.6
id.	13	11.7	70°	14.3	50°	14.8	70°	90	72	1	71	89	— 2.3
id.	18	11.0	68°	12.4	50°	14.3	65°	45	43	— 1	44	66	— 3.0
21 October	1	*10.0*	*60°*	*11.5*	*50°*	*13.5*	*60°*	3	20	— 2	22	52	—
id.	7	*9.5*	*45°*	*10.5*	*50°*	*12.0*	*50°*	— 6	9	— 3	12	43	—
id.	13	*8.5*	*30°*	*9.5*	*50°*	*10.5*	*50°*	— 3	2	— 4	6	35	—
id.	18	*7.5*	*20°*	*8.5*	*60°*	*9.0*	*60°*	2	0	— 4	4	28	—
22 October	1	*5.5*	*10°*	*6.5*	*70°*	*7.5*	*70°*	8	— 1	— 5	4	17	—
id.	7	*4.5*	*—10°*	*5.5*	*75°*	*6.0*	*75°*	7	— 2	— 5	3	11	—
id.	13	*4.0*	*—50°*	*4.5*	*0°*	*4.0*	*0°*	0	— 1	— 6	5	1	—
id.	18	*3.0*	*—90°*	*3.0*	*—90°*	*3.0*	*—90°*	— 6	— 1	— 6	5	— 5	—

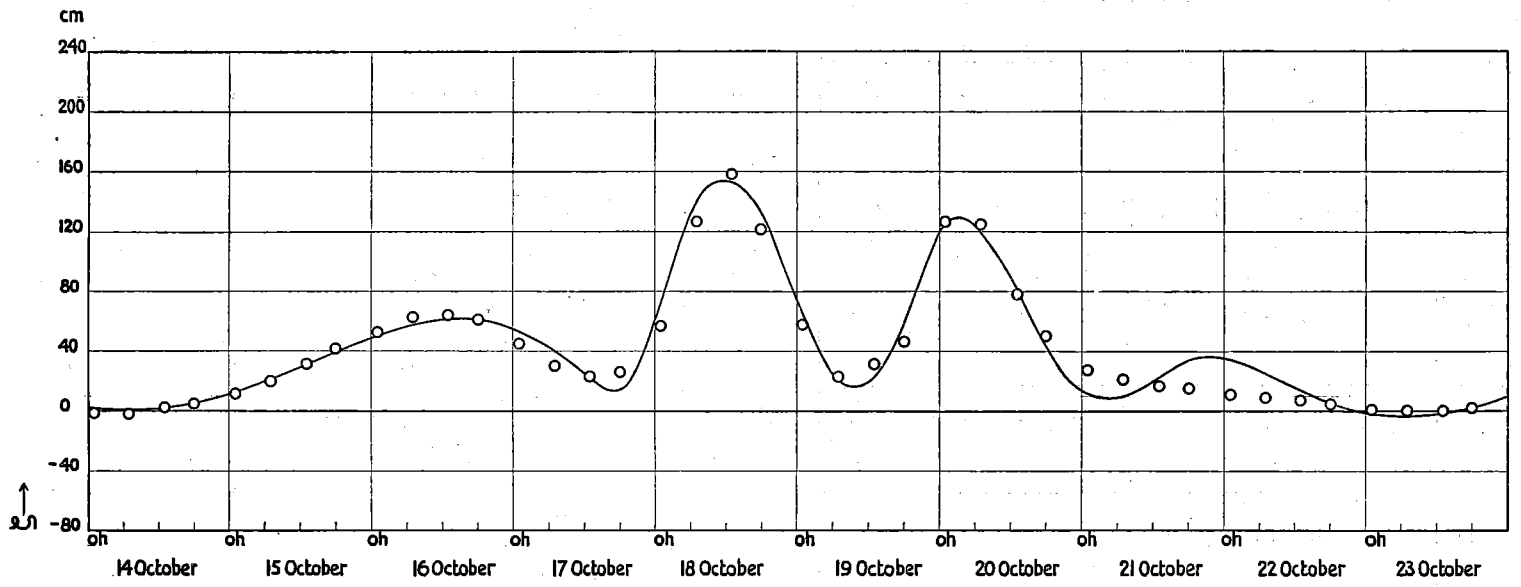

Fig. 43*a*. The first storm surge of October 1936 (empirical and theoretical data)

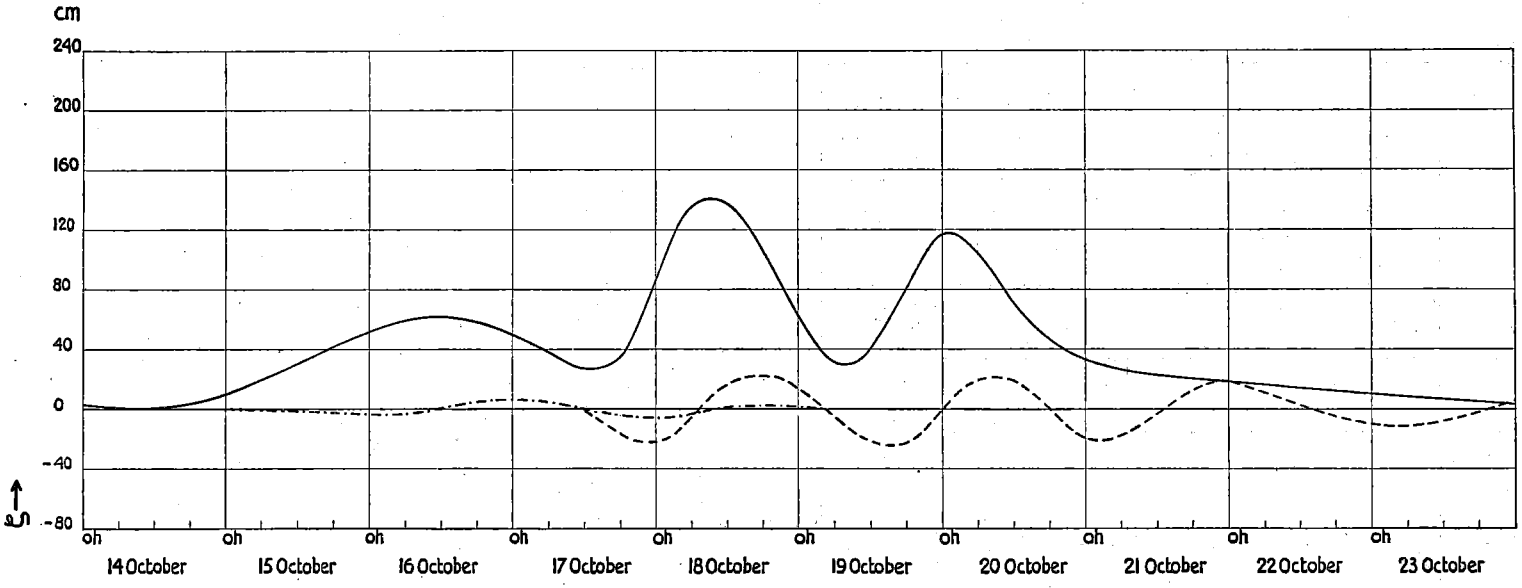

Fig. 43*b*. The first storm surge of October 1936 (oscillations due to inertia separated from "stationary state")

TABLE 35 *Numerical data concerning the first storm surge of October 1936*

Date	Hour	V_1	ψ_1	V_2	ψ_2	V_3	ψ_3	ζ (exp.)	ζ_0	$(\Delta\zeta)_p$	$\zeta_0-(\Delta\zeta)_p$	ζ (calc.)	ΔT
14 October	1	*4.0*	*0°*	*4.0*	*10°*	*3.0*	*10°*	2	2	— 6	8	— 1	—
id.	7	*4.0*	*— 5°*	*4.0*	*—50°*	*3.0*	*0°*	1	2	— 6	8	— 2	—
id.	13	*5.0*	*0°*	*5.0*	*—13°*	*4.0*	*—13°*	2	2	— 5	7	2	—
id.	18	*5.0*	*5°*	*7.0*	*—18°*	*6.0*	*—18°*	5	4	— 5	9	5	—
15 October	1	5.0	13°	8.8	5°	8.3	5°	12	12	— 5	17	12	— 0.1
id.	7	6.3	20°	10.4	15°	10.1	15°	21	22	— 5	27	20	— 0.4
id.	13	7.6	26°	11.7	24°	11.7	24°	31	32	— 6	38	31	+ 0.3
id.	18	8.7	29°	12.9	28°	13.4	28°	40	42	— 7	49	42	+ 0.4
16 October	1	10.0	31°	14.1	30°	15.1	30°	50	54	— 8	62	53	— 0.5
id.	7	11.0	30°	15.0	28°	16.4	28°	57	60	— 8	68	63	— 0.6
id.	13	11.4	26°	15.3	23°	16.8	22°	62	62	— 8	70	64	— 0.4
id.	18	11.0	16°	15.3	14°	16.5	10°	61	58	— 8	66	61	— 0.5
17 October	1	9.8	4°	14.5	4°	14.5	—12°	54	48	— 7	55	45	— 0.5
id.	7	9.7	— 5°	13.6	— 5°	13.0	—45°	40	36	— 6	42	30	+ 0.3
id.	13	10.5	— 4°	13.7	—10°	13.0	—40°	22	27	— 5	32	23	+ 0.5
id.	18	12.0	1°	15.0	— 9°	14.5	—21°	15	36	— 4	40	26	+ 0.5
18 October	1	14.5	15°	19.3	1°	19.4	12°	75	98	— 3	101	57	+ 0.3
id.	7	15.4	27°	20.9	20°	21.1	38°	141	138	— 4	142	127	— 1.8
id.	13	13.9	31°	19.7	36°	19.8	50°	152	134	— 5	139	158	— 0.8
id.	18	11.7	27°	16.5	37°	14.8	50°	132	106	— 6	112	122	— 1.8
19 October	1	11.0	12°	12.3	11°	8.6	25°	66	55	— 6	61	58	— 1.8
id.	7	11.5	— 5°	10.2	—14°	4.3	—18°	20	30	— 4	34	23	— 3.0
id.	13	Depression (see table 16)						24	47	— 1	48	31	— 2.4
id.	18	Depression (see table 16)						60	80	3	77	46	— 2.0
20 October	1	14.5	72°	17.8	80°	17.9	80°	125	118	0	118	127	— 2.6
id.	7	12.5	69°	16.2	77°	16.1	77°	120	101	— 3	104	125	— 2.8
id.	13	10.3	60°	13.3	66°	13.0	66°	82	66	— 6	72	78	— 2.0
id.	18	9.8	48°	11.0	46°	10.8	46°	44	46	— 8	54	50	— 2.2
21 October	1	*10.0*	*13°*	*10.0*	*13°*	*10.0*	*13°*	12	32	— 6	38	27	—
id.	7	*9.0*	*8°*	*9.0*	*8°*	*9.0*	*8°*	10	26	— 4	30	21	—
id.	13	*8.0*	*14°*	*8.0*	*14°*	*8.0*	*14°*	22	23	— 3	26	17	—
id.	18	*7.0*	*19°*	*7.0*	*19°*	*7.0*	*19°*	34	20	— 3	23	15	—
22 October	1	*6.5*	*18°*	*6.5*	*18°*	*6.5*	*18°*	35	18	— 3	21	11	—
id.	7	*6.0*	*14°*	*6.0*	*14°*	*6.0*	*14°*	25	16	— 3	19	9	—
id.	13	*6.0*	*3°*	*6.0*	*3°*	*6.0*	*3°*	14	14	— 3	17	7	—
id.	18	*6.0*	*—10°*	*6.0*	*—10°*	*6.0*	*—10°*	5	12	— 3	15	5	—
23 October	1	*6.0*	*—30°*	*6.0*	*—30°*	*6.0*	*—30°*	— 2	10	— 3	13	1	—
id.	7	*6.0*	*—40°*	*6.0*	*—40°*	*6.0*	*—40°*	— 3	8	— 3	11	0	—
id.	13	*6.5*	*—42°*	*6.5*	*—42°*	*6.5*	*—42°*	— 1	6	— 2	8	0	—
id.	18	*7.5*	*—40°*	*7.5*	*—40°*	*7.5*	*—48°*	3	5	— 2	7	2	—

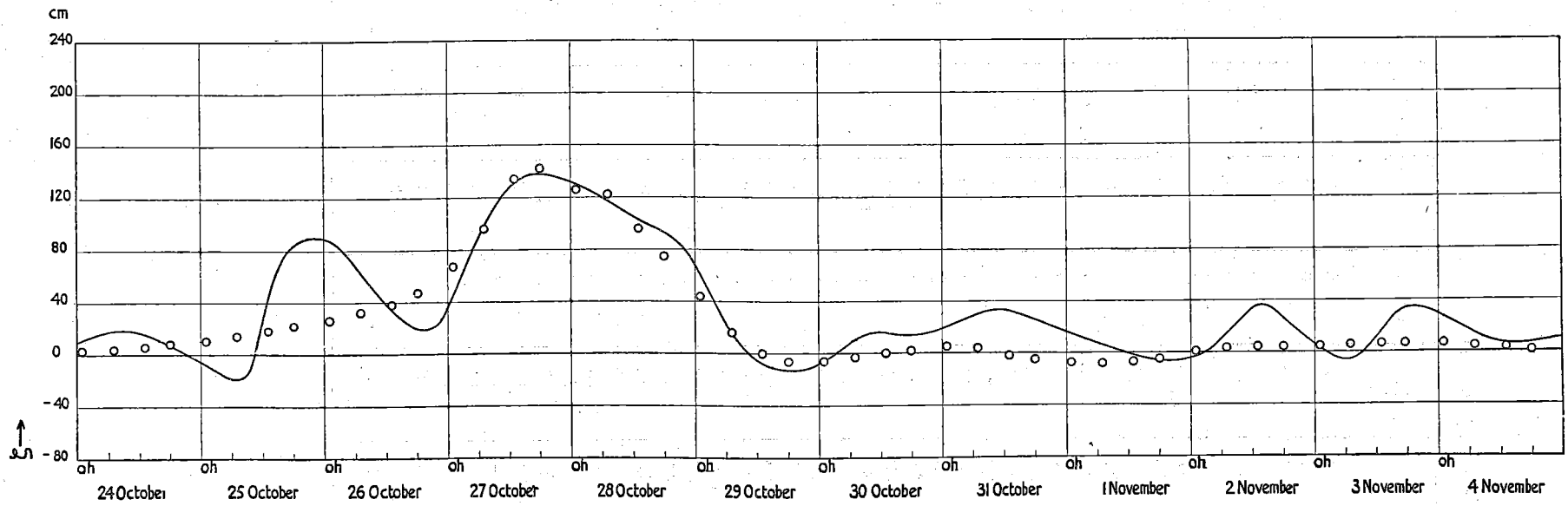

Fig. 44*a*. The second storm surge of October 1936 (empirical and theoretical data)

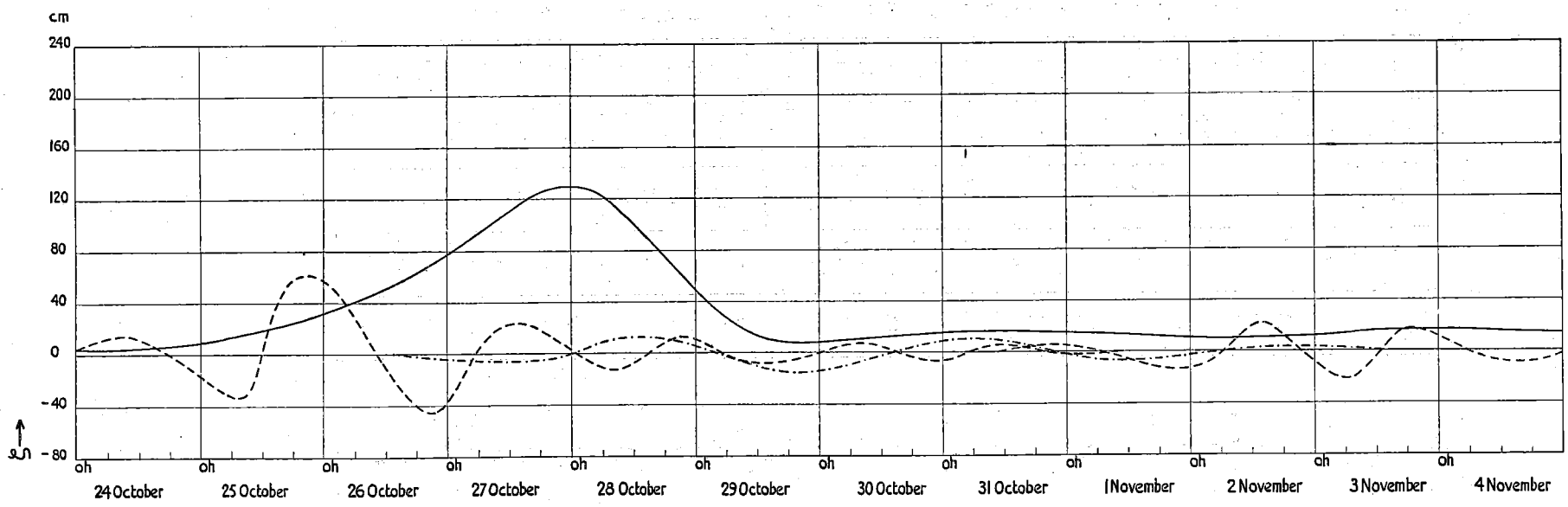

Fig. 44*b*. The second storm surge of October 1936 (oscillations due to inertia separated from "stationary state")

TABLE 36 *Numerical data concerning the second storm surge of October 1936*

Date	Hour	V_1	ψ_1	V_2	ψ_2	V_3	ψ_3	ζ (exp.)	ζ_0	$(\triangle\zeta)_p$	$\zeta_0-(\triangle\zeta)_p$	ζ (calc.)	$\triangle T$
24 October	1	*9.0*	*—38°*	*9.0*	*—38°*	*9.0*	*—38°*	11	4	— 1	5	3	—
id.	7	*10.0*	*—35°*	*10.0*	*—35°*	*10.0*	*—35°*	18	4	— 1	5	4	—
id.	13	*11.0*	*—30°*	*11.0*	*—30°*	*11.0*	*—30°*	15	5	— 2	7	6	—
id.	18	*12.5*	*—27°*	*12.5*	*—27°*	*12.5*	*—27°*	7	6	— 4	10	8	—
25 October	1	13.2	12°	12.7	—28°	14.1	—30°	— 8	10	— 5	15	10	— 0.7
id.	7	13.3	7°	12.9	—27°	13.4	—29°	— 19	14	— 4	18	14	— 0.7
id.	13	13.4	1°	13.1	—26°	12.6	—28°	43	20	— 3	23	18	— 2.1
id.	18	13.7	— 3°	13.3	—24°	12.2	—27°	84	26	— 2	28	22	— 2.3
26 October	1	14.2	— 5°	13.6	—21°	12.1	—24°	88	34	— 1	35	26	— 2.8
id.	7	14.7	— 3°	14.0	—17°	12.5	—19°	63	42	0	42	32	— 2.6
id.	13	15.4	0°	14.6	—14°	13.4	—11°	35	53	1	52	38	— 2.1
id.	18	15.8	4°	15.9	—11°	14.2	— 2°	20	63	2	61	47	+ 0.1
27 October	1	16.3	8°	18.7	— 6°	15.7	15°	46	80	3	77	67	— 0.2
id.	7	16.1	12°	21.5	0°	16.8	30°	98	96	2	94	96	— 3.7
id.	13	15.5	18°	22.7	7°	17.5	44°	131	114	1	113	134	— 3.0
id.	18	15.0	24°	21.7	15°	17.6	53°	138	124	0	124	142	— 3.2
28 October	1	14.1	32°	19.3	28°	16.8	62°	131	130	— 1	131	126	— 3.9
id.	7	13.0	38°	17.2	41°	15.6	66°	118	120	— 2	122	122	— 2.3
id.	13	11.6	40°	15.0	51°	14.0	70°	103	98	— 3	101	96	+ 0.5
id.	18	9.4	35°	13.2	50°	11.8	65°	93	75	— 5	80	75	— 1.6
29 October	1	*4.0*	*5°*	*11.0*	*40°*	*7.0*	*40°*	60	44	— 7	51	44	—
id.	7	*4.5*	*— 5°*	*10.0*	*5°*	*7.0*	*5°*	16	24	— 9	33	16	—
id.	13	*5.5*	*—10°*	*9.5*	*—25°*	*8.0*	*—25°*	— 7	12	— 10	22	0	—
id.	18	*6.0*	*—15°*	*9.0*	*—35°*	*10.0*	*—35°*	— 13	8	— 10	18	— 6	—
30 October	1	*7.0*	*—15°*	*8.0*	*—40°*	*8.0*	*—40°*	— 6	8	— 9	17	— 6	—
id.	7	*7.0*	*—20°*	*7.5*	*—35°*	*7.0*	*—35°*	10	10	— 8	18	— 3	—
id.	13	*8.0*	*—17°*	*6.5*	*—25°*	*6.5*	*—25°*	16	12	— 7	19	0	—
id.	18	*8.0*	*—13°*	*5.5*	*—15°*	*5.5*	*—15°*	14	13	— 6	19	2	—
31 October	1	*8.0*	*2°*	*4.5*	*15°*	*4.5*	*15°*	20	15	— 5	20	5	—
id.	7	*8.5*	*35°*	*4.0*	*50°*	*4.0*	*50°*	30	16	— 5	21	4	—
id.	13	*8.5*	*75°*	*3.5*	*65°*	*3.5*	*70°*	32	16	— 6	22	— 2	—
id.	18	*8.5*	*95°*	*3.5*	*70°*	*3.5*	*70°*	26	16	— 7	23	— 5	—
1 November	1	*8.5*	*100°*	*3.0*	*70°*	*3.0*	*60°*	15	15	— 8	23	— 7	—
id.	7	*8.0*	*95°*	*3.0*	*65°*	*5.0*	*0°*	6	14	— 8	22	— 8	—
id.	13	*8.0*	*75°*	*3.0*	*60°*	*7.0*	*—40°*	— 2	13	— 8	21	— 7	—
id.	18	*7.5*	*40°*	*3.0*	*55°*	*7.0*	*—40°*	— 6	12	— 7	19	— 5	—
2 November	1	*7.0*	*0°*	*3.5*	*50°*	*5.0*	*30°*	— 3	11	— 6	17	1	—
id.	7	*6.5*	*—10°*	*3.5*	*42°*	*4.0*	*70°*	14	10	— 6	16	3	—
id.	13	*6.0*	*— 5°*	*4.0*	*35°*	*4.0*	*90°*	36	11	— 5	16	4	—
id.	18	*5.5*	*0°*	*4.5*	*30°*	*5.0*	*90°*	27	12	— 5	17	4	—
3 November	1	*5.0*	*5°*	*5.0*	*23°*	*5.0*	*35°*	4	13	— 4	17	5	—
id.	7	*4.5*	*10°*	*5.5*	*18°*	*6.0*	*25°*	— 6	14	— 4	18	6	—
id.	13	*4.0*	*10°*	*6.5*	*10°*	*7.5*	*10°*	16	15	— 4	19	6	—
id.	18	*4.0*	*10°*	*7.0*	*4°*	*8.0*	*4°*	34	16	— 4	20	6	—
4 November	1	*4.0*	*7°*	*7.5*	*— 4°*	*9.0*	*— 4°*	26	17	— 4	21	6	—
id.	7	*3.5*	*5°*	*8.0*	*—10°*	*10.0*	*—10°*	14	16	— 4	20	4	—
id.	13	*3.5*	*0°*	*8.5*	*—16°*	*10.5*	*—16°*	6	15	— 5	20	3	—
id.	18	*3.0*	*— 5°*	*9.0*	*—22°*	*10.0*	*—22°*	6	14	— 6	20	1	—

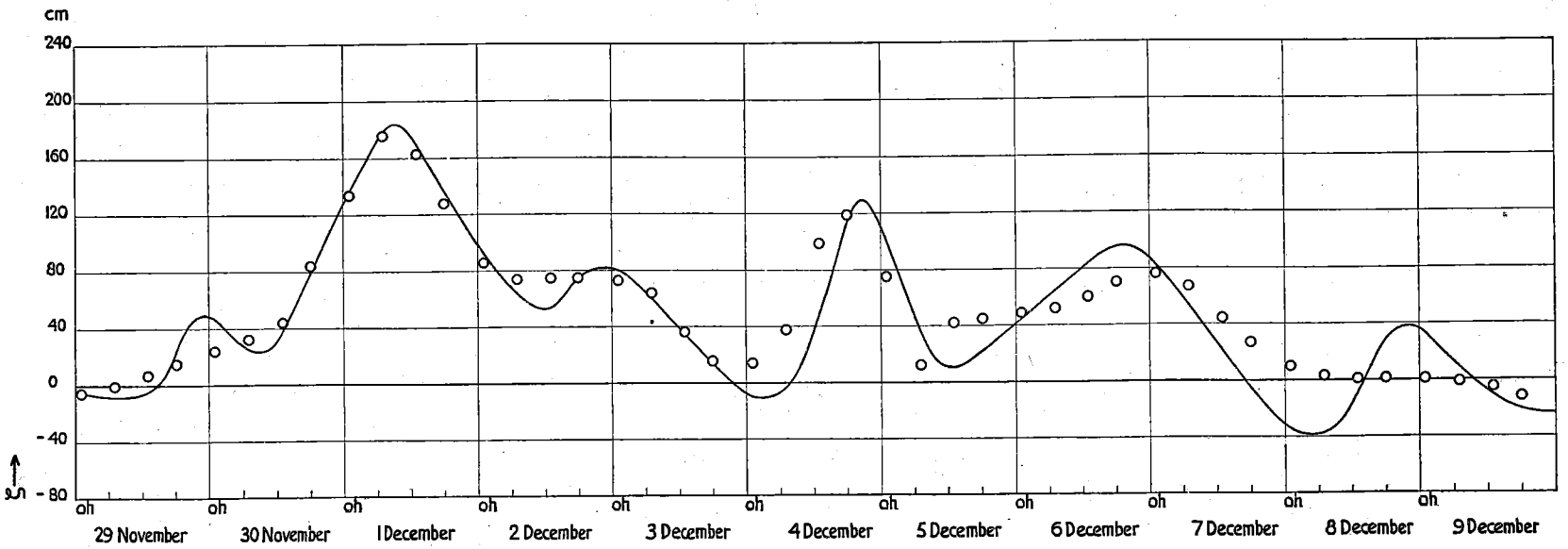

Fig. 45*a*. The storm surge of December 1936 (empirical and theoretical data)

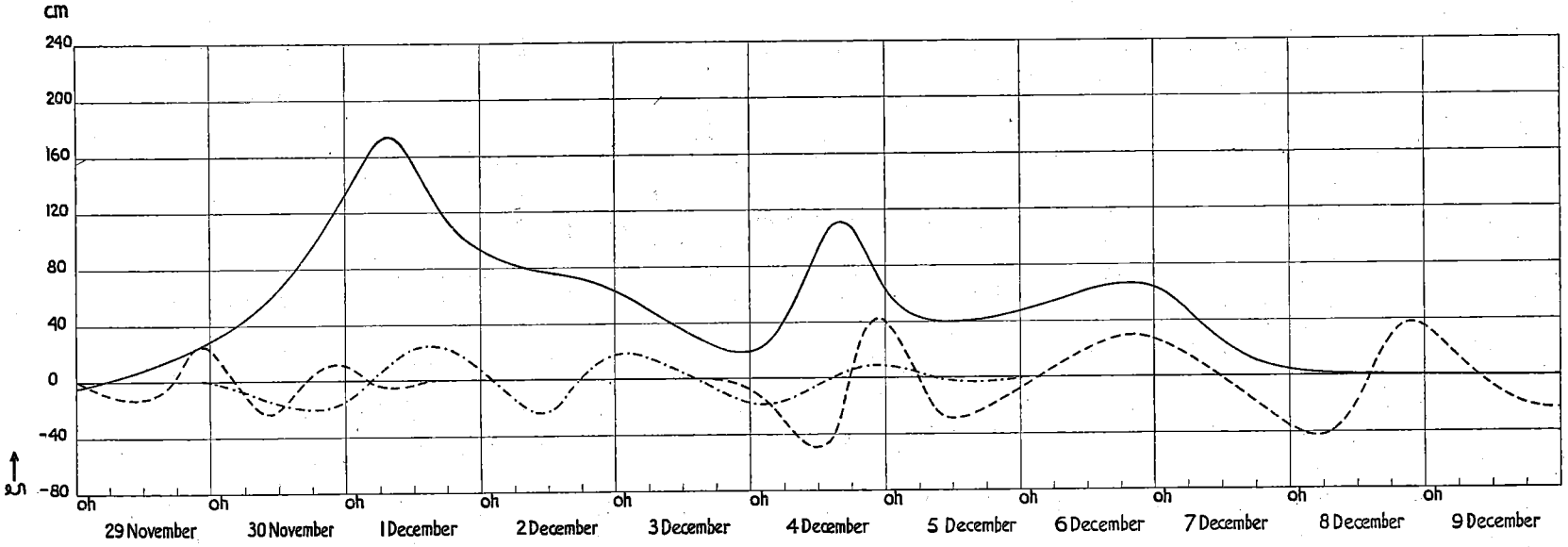

Fig. 45*b*. The storm surge of December 1936 (oscillations due to inertia separated from "stationary state")

TABLE 37 *Numerical data concerning the storm surge of December 1936*

Date	Hour	V_1	ψ_1	V_2	ψ_2	V_3	ψ_3	ζ (exp.)	ζ_0	$(\triangle\zeta)_p$	$\zeta_0-(\triangle\zeta)_p$	ζ (calc.)	$\triangle T$
29 November	1	*3.5*	*90°*	*6.0*	*— 7°*	*15.0*	*—25°*	— 5	— 3	— 6	3	— 7	—
id.	7	*5.5*	*50°*	*7.0*	*— 1°*	*14.0*	*—12°*	— 8	2	— 5	7	0	—
id.	13	*8.0*	*20°*	*8.0*	*5°*	*12.5*	*5°*	— 5	9	— 5	14	7	—
id.	18	*10.0*	*5°*	*9.0*	*10°*	*11.0*	*10°*	— 23	17	— 5	22	15	—
30 November	1	10.0	12°	10.2	16°	10.3	12°	47	31	— 5	36	24	+ 0.2
id.	7	10.6	20°	11.3	19°	11.4	16°	25	47	— 4	51	32	+ 1.2
id.	13	12.2	30°	14.2	24°	15.2	26°	38	69	— 3	72	44	+ 1.8
id.	18	14.8	38°	17.9	31°	18.6	38°	79	96	— 2	98	84	+ 0.5
1 December	1	18.3	43°	20.1	42°	20.2	51°	137	140	— 1	141	124	— 1.1
id.	7	18.2	44°	20.8	49°	20.7	58°	178	174	— 2	176	176	— 2.8
id.	13	15.0	43°	19.7	50°	18.8	58°	170	148	— 3	151	163	— 2.3
id.	18	12.2	38°	17.2	46°	16.6	54°	137	114	— 3	117	128	— 2.5
2 December	1	11.5	30°	15.0	41°	14.6	48°	93	90	— 2	92	86	— 2.7
id.	7	12.8	28°	13.9	40°	13.8	48°	64	81	0	81	74	— 0.9
id.	13	13.9	31°	13.5	42°	13.5	58°	54	75	3	72	75	— 0.6
id.	18	14.1	36°	13.6	47°	13.6	64°	75	72	1	71	75	— 1.5
3 December	1	13.5	34°	13.4	52°	13.4	63°	81	61	— 1	62	73	— 2.8
id.	7	11.9	26°	11.8	40°	12.0	45°	60	48	— 3	51	64	— 2.0
id.	13	10.8	15°	9.6	7°	10.8	0°	35	33	— 5	38	36	— 2.3
id.	18	10.8	9°	10.0	—11°	11.5	—40°	14	23	— 5	28	16	0.0
4 December	1	11.7	9°	13.4	—15°	14.2	—45°	— 10	20	— 4	24	14	+ 0.7
id.	7	12.3	14°	16.3	0°	17.3	— 5°	— 3	48	— 3	51	38	+ 0.9
id.	13	12.2	17°	18.3	20°	19.2	35°	49	99	— 3	102	99	+ 1.6
id.	18	11.4	11°	18.2	21°	19.2	35°	114	107	— 4	111	119	— 1.2
5 December	1	10.0	— 5°	15.2	— 5°	14.0	5°	102	58	— 4	62	75	— 2.1
id.	7	8.6	—18°	11.8	—43°	10.0	—65°	37	42	— 4	46	12	— 0.7
id.	13	Depression (see table 16)						11	40	— 4	44	42	— 2.1
id.	18	Depression (see table 16)						22	42	— 4	46	45	— 2.2
6 December	1	Depression (see table 16)						44	48	— 4	52	49	— 3.3
id.	7	Depression (see table 16)						64	55	— 5	60	52	— 3.6
id.	13	Depression (see table 16)						83	62	— 6	68	60	— 2.5
id.	18	Depression (see table 16)						96	66	— 7	73	70	— 2.3
7 December	1	Depression (see table 16)						84	62	— 8	80	76	— 2.8
id.	7	Depression (see table 16)						53	43	— 9	52	67	— 2.6
id.	13	7.5	80°	11.0	80°	11.0	80°	21	22	— 10	32	44	— 2.1
id.	18	6.2	50°	9.4	50°	9.8	50°	— 5	4	— 10	14	27	— 2.5
8 December	1	*6.0*	*— 5°*	*8.0*	*— 5°*	*10.0*	*—20°*	— 34	2	— 11	13	10	—
id.	7	*5.5*	*— 3°*	*7.5*	*0°*	*9.0*	*—10°*	— 37	0	— 11	11	3	—
id.	13	*5.0*	*0°*	*7.0*	*7°*	*8.0*	*0°*	— 9	0	— 12	12	1	—
id.	18	*4.5*	*3°*	*6.5*	*25°*	*8.0*	*15°*	29	0	— 12	12	1	—
9 December	1	*4.0*	*5°*	*6.0*	*20°*	*8.5*	*30°*	32	0	— 12	12	1	—
id.	7	*4.0*	*0°*	*6.0*	*10°*	*9.5*	*30°*	9	0	— 12	12	— 1	—
id.	13	*4.0*	*—25°*	*6.5*	*—15°*	*11.0*	*0°*	— 11	0	— 13	13	— 5	—
id.	18	*4.5*	*—180°*	*7.0*	*—25°*	*12.0*	*—20°*	— 21	0	— 14	14	— 12	—

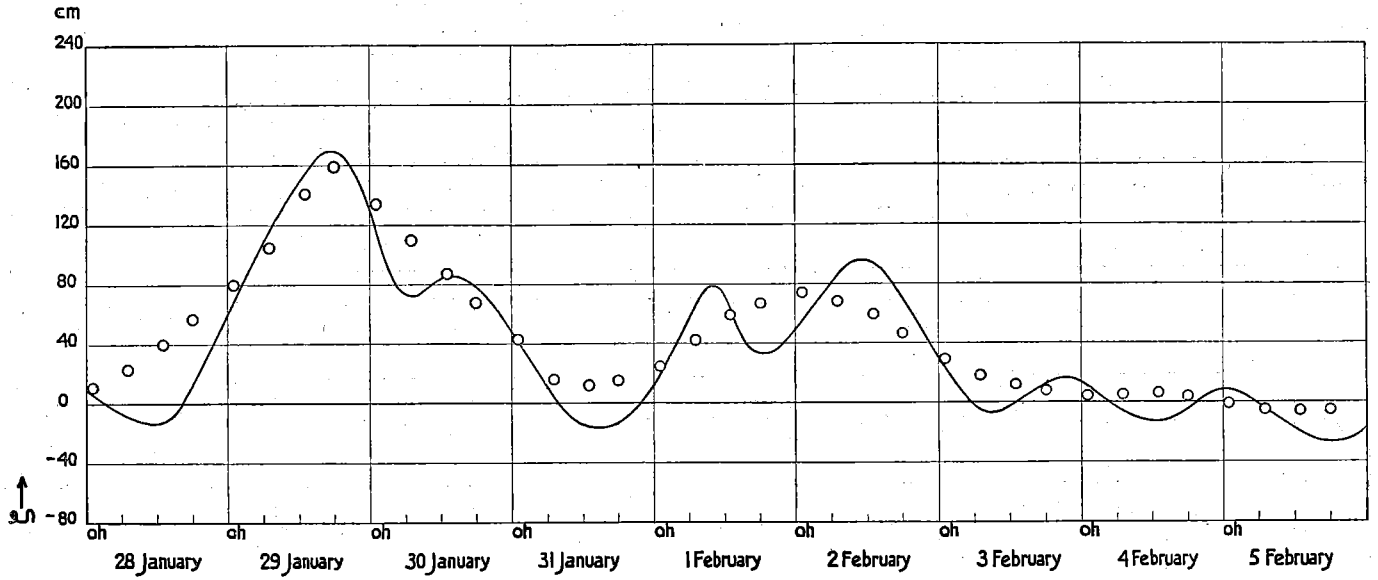

Fig. 46*a*. The storm surge of January 1938 (empirical and theoretical data)

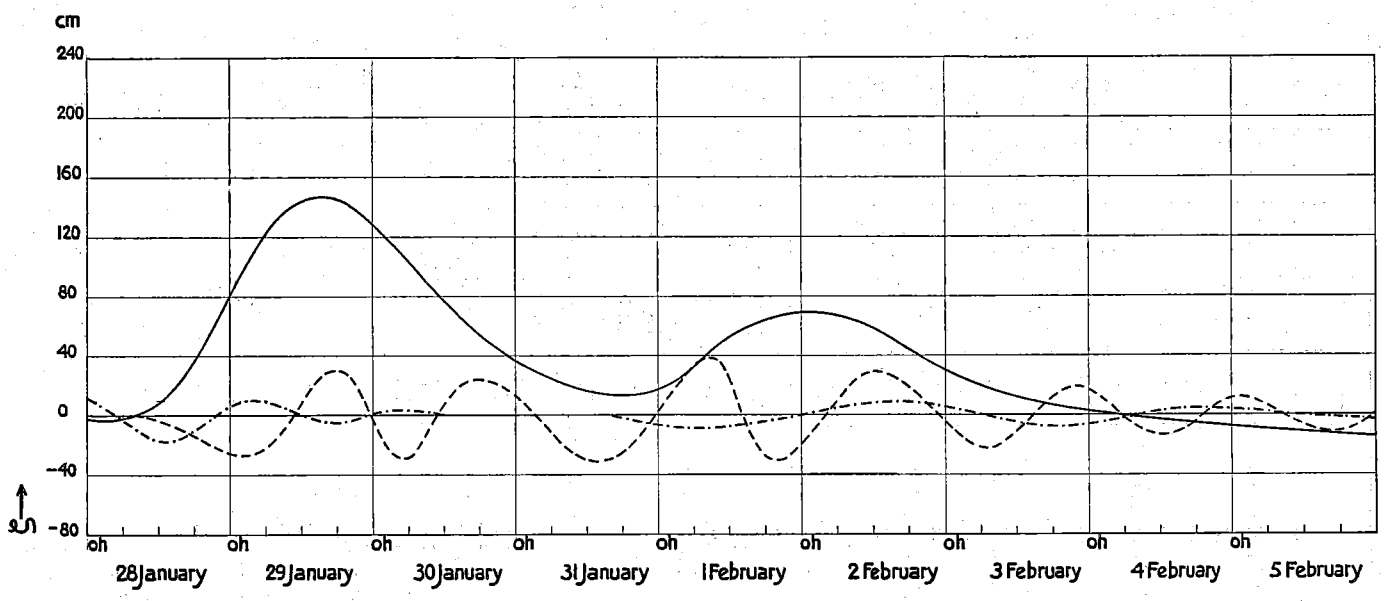

Fig. 46*b*. The storm surge of January 1938 (oscillations due to inertia separated from "stationary state")

TABLE 38 *Numerical data concerning the storm surge of January 1938*

Date	Hour	V_1	ψ_1	V_2	ψ_2	V_3	ψ_3	ζ (exp.)	ζ_0	$(\triangle\zeta)_p$	$\zeta_0-(\triangle\zeta)_p$	ζ (calc.)	$\triangle T$
28 January	1	12.0	0°	13.1	—22°	13.1	—22°	6	— 3	— 5	2	11	— 1.3
id.	7	13.2	5°	13.8	—14°	13.6	—14°	— 8	— 2	— 3	1	23	— 0.5
id.	13	14.3	10°	14.8	— 5°	14.5	— 5°	— 12	12	0	12	40	— 0.3
id.	18	15.5	16°	15.8	2°	15.6	2°	12	36	4	32	57	+ 2.0
29 January	1	17.2	22°	17.5	9°	17.5	9°	68	88	9	79	80	+ 2.3
id.	7	18.8	28°	19.2	17°	19.2	17°	115	127	10	117	105	— 0.5
id.	13	19.5	32°	20.2	25°	20.2	25°	155	146	8	138	141	+ 0.5
id.	18	19.2	37°	19.8	32°	19.8	33°	170	145	7	138	159	— 0.7
30 January	1	17.8	39°	17.7	42°	17.7	45°	118	125	6	119	134	— 1.1
id.	7	15.8	38°	15.4	50°	15.4	53°	72	99	5	94	110	— 1.5
id.	13	13.9	36°	13.5	52°	13.5	56°	86	73	3	70	87	— 1.3
id.	18	12.4	29°	12.0	47°	12.0	45°	79	54	0	54	68	— 1.8
31 January	1	10.9	14°	10.8	16°	10.8	0°	42	34	— 3	37	43	— 1.6
id.	7	10.7	2°	10.7	—13°	10.7	—45°	5	22	— 5	27	16	— 1.2
id.	13	11.9	— 8°	11.5	—27°	11.5	—50°	— 16	16	— 3	19	12	+ 0.5
id.	18	13.9	—12°	13.2	—29°	13.2	—45°	— 13	13	0	13	15	+ 1.5
1 February	1	16.1	—14°	15.4	—27°	15.2	—40°	19	20	2	18	25	+ 1.7
id.	7	17.7	—13°	17.7	—22°	16.4	—30°	65	36	3	33	42	— 0.9
id.	13	17.8	— 5°	18.6	—15°	16.7	—16°	64	55	3	52	59	+ 0.7
id.	18	17.0	4°	18.3	— 8°	16.3	0°	33	64	2	62	67	+ 0.1
2 February	1	15.4	15°	16.8	5°	15.2	21°	55	69	0	69	74	— 0.5
id.	7	13.6	22°	15.0	13°	14.2	36°	86	66	— 2	68	68	— 0.7
id.	13	11.6	27°	13.5	18°	13.0	38°	94	56	— 3	59	59	+ 1.2
id.	18	9.8	23°	12.1	18°	11.8	30°	70	44	— 5	49	46	— 0.1
3 February	1	*8.5*	*15°*	*10.0*	*15°*	*11.0*	*15°*	23	28	— 6	34	29	—
id.	7	*8.0*	*10°*	*9.0*	*10°*	*10.0*	*10°*	— 5	18	— 7	25	18	—
id.	13	*7.0*	*5°*	*8.5*	*5°*	*9.0*	*5°*	0	11	— 8	19	12	—
id.	18	*6.5*	*0°*	*8.5*	*0°*	*9.0*	*0°*	12	6	— 9	15	8	—
4 February	1	*6.5*	*— 5°*	*9.0*	*— 4°*	*10.0*	*— 4°*	10	2	— 11	13	4	—
id.	7	*7.0*	*—10°*	*10.0*	*— 8°*	*11.0*	*— 8°*	— 6	— 1	— 12	11	5	—
id.	13	*7.5*	*—15°*	*11.0*	*—11°*	*12.0*	*—10°*	— 13	— 3	— 12	9	6	—
id.	18	*7.0*	*—25°*	*10.0*	*—13°*	*11.0*	*—11°*	— 5	— 5	— 13	8	4	—
5 February	1	*6.5*	*—35°*	*9.0*	*—18°*	*10.0*	*—12°*	8	— 7	— 14	7	— 1	—
id.	7	*6.0*	*—45°*	*8.5*	*—22°*	*9.0*	*—13°*	— 4	— 9	— 14	5	— 5	—
id.	13	*5.5*	*—55°*	*8.5*	*—28°*	*8.5*	*—14°*	— 20	— 11	— 12	1	— 6	—
id.	18	*5.0*	*—70°*	*8.5*	*—33°*	*8.5*	*—14°*	— 27	— 13	— 11	— 2	— 5	—